Spatial and Temporal Controls on the Solute behavior of Rivers in Arid environments: The Okavango River, NW Botswana

By

GOABAONE JAQUELINE RAMATLAPENG

DISSERTATION

Submitted in partial satisfaction of the requirements for the degree of

DOCTOR OF PHILOSOPHY

in

Earth and Planetary Sciences

in the

OFFICE OF GRADUATE STUDIES

of the

UNIVERSITY OF CALIFORNIA

DAVIS

Approved:

Eliot A. Atekwana, Chair

Dawn Sumner

Alyssa Griffin

Committee in Charge

2024

Acknowledgements

I thank my advisor, Dr. Eliot Atekwana, for his great mentorship and unwavering support. His advice and guidance went a long way in the completion of this work. A huge thank you to Dean Estella Atekwana for being a role model and a constant source of support and inspiration. I thank my committee members, Dr. Dawn Sumner and Dr. Alyssa Griffin, for their support and contributions that expanded my understanding. I thank Dr. Loago Molwalefhe for his valuable contributions to this work. Special thanks to Ms. Vanita Tjitunga and Mr. Tshepo Keatshaba from Maun, Botswana for collecting rain and river water samples used in this work.

To my family, I cannot thank you enough for your warm love and support, it literally carried me through my studies. To my mom, Kelebogile Ramatlapeng and my dad, Motlamedi Ramatlapeng, thank you for being a solid source of strength and hope in challenging times of this journey. Thank you for believing in me. To my siblings, Tshepiso Ramatlapeng and Karabo Ramatlapeng, thank you for constantly cheering up on me. I drew strength in your love and confidence in me. To all my relatives and friends, I appreciate your support and prayers. I am because you are!

Special thanks to the Atekwana Lab group members from the University of Delaware (UD) to University of California, Davis (UC Davis); Kopo Oromeng, Desire Piphus, Kesego Letshele, Joy Foluso, and Claris Sunjo, and all my fellow graduate students and friends, your constant academic and moral support helped in the completion of my studies. Karen Carlson, thank you for your mentorship at UD and your moral support during my transition from UD to UC Davis, I truly appreciate it.

This work wouldn't have been possible without the financial support from the National Science Foundation (NSF), Department of Earth Sciences at UD, Department of Earth and Planetary Sciences at UC Davis, Schlumberger Foundation Faculty for the Future Fellowship and the American Association for University Women (AAUW) International Doctoral Fellowship. The financial support ensured the successful completion of this work and development of new ideas to pursue beyond this PhD. For that, I am forever grateful. I thank my friends and colleagues from the Schlumberger Foundation Faculty for the Future Fellowship and my fellow National Geographic Society Explorers for their encouragement and amazing support.

This dissertation is dedicated to the loving memory of my grandfather, Mosiiwa Tanana Ramatlapeng. He was my source of inspiration to keep doing my best in life and that sustained me through my PhD journey. His words, *"You will achieve all that we couldn't achieve"* were a constant beautiful affirmation that cheered me up in challenging times. Thank you, grandpa, you remain my moral compass and a guiding star!

Abstract

Solute cycling models for rivers in arid environments must consider water and solute sources, river connectivity to solute sources, and solute transformation across watersheds to better constrain the processes that control the solute behavior in these rivers. Here, we employ water source partitioning techniques using solutes (e.g., total dissolved ions (TDI), silica and major ions) and stable water isotopes (δD and $\delta^{18}O$), and high frequency time series hydrochemical (TDI, water levels and water temperatures) data to decipher the fundamental processes that govern the spatial and temporal variability in the behavior of solutes in the Okavango River flowing through the Okavango Delta (Delta) in the middle Kalahari Desert, Botswana. We measured solute concentrations and stable water isotopes at sub-weekly and daily intervals for 5 years in the Okavango River at the outlet of the Delta. The high frequency time series hydrochemical data were collected at hourly intervals over a 2-year period at four stations distributed longitudinally along the Okavango River. The combined results from our studies reveal anomalously high solute concentrations in the river during the beginning of seasonal rains and flooding in the Delta. The anomalous increases in the solute concentrations are due to evapoconcentration during the hot rainy season, the transfer of dissolved salt precipitates stored in the floodplains and on hundreds of thousands of tree islands scattered across the Delta wetlands, and 'flushing' of remnant evaporated flood water of higher salinity trapped in isolated wetland pools. Overland flow generated by seasonal rains and flooding connect the river to the solute stores in the watershed. The temporally activated overland flow transfer solutes to the river that then flushes them out of the Delta. We note that this mass transfer of solutes from the watershed into the river become enhanced following a drought due to the interception and mobilization of solutes that accumulated during the drought period. The transfer of solutes from the watershed to the river and solute export

from the Delta during pulse flooding and the rainy season are important mechanisms that keep the Delta's surface water resources fresh. Spatially, we observed progressive downriver enrichment in the solute concentrations associated with evapotranspiration of river water as the river transits across the Delta over a 5-month period. Our findings highlight the importance of hydrologically driven river connectivity to solute stores in the local watershed and evapotranspiration in controlling the solute behavior at variable spatial and temporal scales in rivers in arid watersheds. We anticipate that our findings will inform solute transport and solute cycling models for rivers in arid watersheds.

Dissertation Introduction

Rivers act as conduits for water and solutes (dissolved ions in water) out of the basin in exorheic basins typically found in humid environments, and to the terminus of endorheic (closed) basins in arid environments. The transport of solutes and solute transformation in rivers constitute an important component of the global solute cycle. Hydrology plays an important role in facilitating the transport of solutes in rivers by establishing flow pathways (e.g., overland flow, shallow subsurface flow and groundwater flow) that connect rivers to source(s) of solutes in the watershed (Gooseff et al., 2008; Liu et al., 2008; Covino, 2017; Geeraert et al., 2017; Fovet et al., 2018; Duvert et al., 2020; Ramatlapeng et al., 2021; 2023; Oromeng et al., 2021). This hydrologic connectivity of rivers to solute source(s) in watersheds determines the timing and magnitude of solutes delivered from watersheds to rivers (Gooseff et al., 2008; Covino, 2017; Geeraert et al., 2017; Fovet et al., 2018; Duvert et al., 2020; Ramatlapeng et al., 2021; 2023; Oromeng et al., 2021). Solute transfer from watersheds to rivers in exorheic basins in humid environments has been investigated extensively (e.g., Fovet et al., 2018; Herndon et al., 2018; Rose et al., 2018; Wymore et al., 2020; Liu et al., 2020) because these rivers contribute solutes to oceans and are therefore considered important in the global solute cycle. Although studies in rivers in humid environments have advanced our knowledge and understanding of river connectivity to watershed-derived solutes, solute transfer to rivers and solute export from watersheds, similar studies in rivers in arid watersheds, particularly in endorheic basins, still lag behind, perhaps because endorheic basins are disconnected from the ocean, are therefore regarded as unimportant in the global cycling of solutes. Nevertheless, endorheic basins occupy 20-23% of the Earth's surface (Nichols, 2007), which we use as the basis for the inference that substantial amounts of solutes transferred from the upper watershed are transformed in the rivers and stored at the terminus of endorheic basins (Li,

2014). The solute transport and cycling within endorheic basins have implications for the salinity status and sustainability of wetland ecosystems often found near or at the terminus of endorheic basins in arid environments. Yet, the processes that control solute transformation and cycling of solutes in endorheic basins in arid environments are not well understood due to limited studies (Oromeng et al., 2021; Letshele et al., 2021). Knowledge on the controls of the behavior of solutes in rivers in endorheic basins is essential for quantifying solute load and solute export from the basins, and for developing representative solute cycling models.

Unlike rivers in exorheic basins in humid environments, the hydrology of rivers in endorheic basins arid environments is characterized by highly variable river flow and downriver decrease in river discharge from water transmission losses to groundwater and the high evapotranspiration rates (Parsons et al., 1999; Tooth, 2000; Costa et al., 2012; Nanson et al., 2002). The highly variable flow and downriver decrease in the river discharge enhance the spatial and temporal heterogeneity in the river connectivity to solute source(s) and solute transport in arid watersheds. Yet, little is known on how the variable flow and downriver modifications in the flow modulate solute transfer to rivers and solute behavior at various temporal scales across arid river basins. Understanding the processes controlling the spatial and temporal variability in river solute behavior requires assessments of temporal water sources and flow pathways for solute transfer into rivers, and variations in the river solute concentrations across basins. Long-term hydrochemical studies utilizing multispecies chemical constituents allow for water and solute source apportionment and provide insights on specific biogeochemical processes and solute transformation in rivers (Koeniger et al., 2009; Ala-Aho et al., 2018; Horgby et al., 2019; Duvert et al., 2020). However, the highly variable river hydrology in arid environments necessitates high frequency time series hydrochemical data collection using automated sensors in addition to the

long-term multispecies studies to adequately characterize the controls on the river solute behavior. Yet, the application of both multispecies chemical tracers and high frequency hydrochemical data in understanding water source partitioning to rivers and tracing solute exchange between rivers and their watersheds in arid settings is not common.

We investigated the processes controlling the spatial and temporal solute behavior in the Okavango River in northwestern Botswana (Fig. 1). The Okavango River flows through the Okavango Delta (hereafter referred to as the Delta; Fig. 1) in Botswana which is the largest freshwater wetland in southern Africa (McCarthy and Ellery, 1998) and is a Ramsar World Heritage site (Secretariat of the Convention on Wetlands, 2017). The Okavango Delta lies in the middle Kalahari Desert near the terminus of the endorheic Okavango River Basin (ORB). The ORB is a transboundary basin covering Angola in its headwaters to the north, and Namibia and Botswana in its lower drainage area to the south. The ORB transcends climatic gradients from a higher rainfall temperate climate in Angola to a semi-arid climate in Botswana (Peel et al., 2007). Near the terminus of the ORB in Botswana where the Okavango Delta is located, the Okavango River meanders extensively through a narrow valley of the Panhandle region of the Delta before it spreads into numerous distributary channels on a large alluvial fan forming the lower delta region (Fig. 1). In the lower delta region, the Okavango River is mostly characterized by braided flow through the Okavango Delta wetlands. The hydrology of the Delta is highly intermittent and primarily controlled by annual flood pulses initiated by rains from the upper ORB in Angola and by local rains (Wolski et al., 2005). The Delta is also characterized by high evapotranspiration (ET) rates which cause salt precipitation on floodplains and on the numerous tree islands in the Delta wetlands (e.g., McCarthy et al., 1991, 1998; Gumbricht and McCarthy, 2003; Gumbricht et al., 2004). Evapotranspiration also causes enrichment of solutes in isolated wetland pools scattered

across the Delta (e.g., Dincer et al., 1979). The role that these solute stores (i.e., floodplains, salt islands and isolated wetland pools) which are distributed differentially across the Delta have on the Okavango River solute behavior and solute cycling needs to be investigated and constrained. A study of the behavior of solutes in the Okavango River in the Delta conducted at the inlet to the Delta in Mohembo and outlet from the Delta in Maun (Oromeng et al., 2021) suggested that hydrologic connectivity between the Okavango River and solute stores in the local Delta watershed and ET control the spatial and temporal variability in the river solute behavior. However, there was still lack of understanding of the how the highly intermittent flow in the Delta modulates the temporal river connectivity to solute stores in the local watershed. In addition, the processes driving changes in the solute concentrations in the Okavango River across the ~450 km river distance between the Delta inlet and outlet were not well understood. The Delta serves as an important source of potable water for drinking and domestic use, and food (fish, water lily) to the riparian communities (Mosepele et al., 2006, 2009; Kgathi et al., 2006) and thus, understating the processes that may affect the solute behavior in the Delta is crucial for water quality monitoring and ecological sustainability.

In this dissertation, I utilize water source partitioning techniques using solutes (e.g., total dissolved solids, major ions, silica) and stable water isotopes (δD and $\delta^{18}O$), as well as high frequency (hourly) investigation of river solutes, water levels and water temperatures to investigate the role of hydrology in facilitating solute transfer from the watershed to the river, and to decipher the processes driving the spatial and temporal variability in the river solute concentrations across the Delta.

In chapter 1, I investigate the processes controlling the temporal variability of the solute concentrations in the Okavango River. I use solute (total dissolved ions (TDI), dissolved silica,

major cations) concentrations and the stable water isotopes (δD and $\delta^{18}O$) measured at sub-weekly intervals for one year to trace temporal water and solute sources and quantify solute export in the Okavango River at the outlet of the Delta. I conducted this temporal investigation at the outlet of the Delta in order to capture the integration of the processes controlling solute behavior that affect the Okavango Delta and its wetlands. The primary finding of this chapter is that temporally activated overland flow from seasonal rains and flooding connect the Okavango River to the salt precipitates on the floodplains and on hundreds of thousands of islands scattered across the Delta wetlands, as well as remnant evaporated flood water of higher salinity trapped in isolated wetland pools in the Delta. This river connectivity to solutes in the watershed by overland flow facilitates the transfer of solutes from the watershed into the river that then flushes the solutes out of the Delta. I estimated that 17,838 Mg/y of dissolved solutes were exported from the Delta during this study, with 67% of the solutes removed during flooding (6 months) and 30% during the rainy season (4 months). Solute transfer from the watershed to the river during pulse flooding and the rainy season, and the subsequent export of the solutes from the Delta is an important mechanism that keeps the Delta's surface water resources fresh. Our findings underscore the importance of hydrologic perturbations in controlling solute behavior and solute cycling in this and other arid watersheds.

In chapter 2, I employ a high frequency time series investigation of the processes that control the spatial and temporal solute behavior in the Okavango River. I collected hourly time series of total dissolved ions (TDI) concentrations, water levels, water temperatures and air temperatures at four stations distributed longitudinally along the Okavango River. I also proposed and adapted a novel approach that utilizes normalized water levels (NWL) instead of river discharge to constrain hydrologic controls on the river solute behavior in ungauged and braided river systems where

measuring river discharge is challenging due to difficulties in defining river channel cross-sectional area and measuring flow velocity. The high resolution hydrochemical data and the concentration-normalized water levels (C-NWL) relationships reveal spatial and temporal heterogeneity in the behavior of solutes controlled by seasonal climate driven evapotranspiration (ET) and hydrologically driven differential solute transfer from the local wetlands into the Okavango River. Spatially, ET causes progressive downriver enrichment in TDI concentrations at 0.1 mg/L per km of river flow. Temporally, the TDI concentrations are enriched from evapoconcentration during the hot rainy season and decrease from addition of "fresh" floodwaters during flooding. In addition, superimposed on the seasonal solute behavior are sub-seasonal solute transfer from the floodplains, salt islands and isolated evaporated wetland pools initiated by the flood front during rising flood and wetland drainage into the river during flood recession. These findings indicate that intermittent hydrology, river connectivity to solute stores in the local watershed and evapotranspiration jointly control the solute behavior at variable spatial and temporal scales in rivers in arid watersheds.

In chapter 3, I investigate the role of flow intermittency driven by intermittent and variable seasonal rains, annual pulse flooding (rising and receding flood), and drought in controlling the long-term (5-years) behavior of solutes in the Okavango River. I measured solutes (total dissolved ions (TDI), dissolved silica, major cations and anions), and the stable water isotopes (δD and $\delta^{18}O$) at sub-weekly to daily intervals for 5 years (Nov 2017-July 2022) in the Okavango River at the outlet of the Delta. This investigation was conducted at the outlet of the Delta near the terminus of the Okavango River Basin to allow for the assessment of catchment-wide processes affecting the hydrochemical behavior of the river and to capture the response of the river chemistry to seasonal and drought-driven flow intermittency. This long-term study reveals that at the seasonal scale, the

TDI and major ion concentrations in the river were enriched during the beginning of the hot rainy season and during the start of flooding due to the transfer of dissolved salts stored in the local Delta watershed, as well as from the 'flushing' of solute enriched evaporated water in isolated wetland pools into the river. Local rains in the Delta and the annual flood pulse connect the river to the solute stores in the watershed and facilitate solute transfer into the river. The 2019-2020 drought punctuated the annual flood pulse and rain induced overland transport of solutes to the river which allowed for solute accumulation in the Delta watershed. Post drought rewetting re-established river connectivity to solute stores in the watershed which resulted in higher magnitude of solute transfer into the river, particularly during the 2021-2022 flood post drought. Of the total estimated solute load (143,565 tons) exported during this study, ~64% was exported during the 2021-2022 flood. The 2021-22 flood is the largest flood during this study, and it appears to have been sufficiently high to access more solutes including salt precipitates stored on the elevated tree islands in the Delta watershed. The interception of salts on the tree islands might not have occurred if the flood magnitude had been lower due to the higher elevation of tree islands as most of the islands are formed around and on termite mounts. Our findings demonstrate that intermittent and variable flow from rains and flooding drives river connectivity to watershed-derived solutes, and that drought plays a crucial role in ceasing this river connectivity to solutes in the watershed, and thereby allowing for solute accumulation in the watershed. The solutes are then accessed and transferred into the river during flooding post drought and the amount of solutes transferred into the river depends on the flood magnitude. These findings highlight the significance of both seasonal and drought-driven flow intermittency in controlling solute transport in the Okavango Delta and other rivers in arid watersheds.

Overall, the studies presented in this dissertation represent a significant advancement in our understanding of the processes that control the spatial and temporal variability in the solute behavior of rivers in arid watersheds. The new knowledge and insights generated in the studies presented in this dissertation will open new frontiers to investigate solute behavior of rivers in other arid watersheds which will further our scientific understanding of solute cycling in these rivers.

Citations

Akondi, R.N., Atekwana, E.A. and Molwalefhe, L., 2019. Origin and chemical and isotopic evolution of dissolved inorganic carbon (DIC) in groundwater of the Okavango Delta, Botswana. Hydrological sciences journal, 64(1), pp.105-120.

Ala-Aho, P., Soulsby, C., Pokrovsky, O.S., Kirpotin, S.N., Karlsson, J., Serikova, S., Vorobyev, S.N., Manasypov, R.M., Loiko, S. and Tetzlaff, D., 2018. Using stable isotopes to assess surface water source dynamics and hydrological connectivity in a high-latitude wetland and permafrost influenced landscape. Journal of Hydrology, 556, pp.279-293.

Costa, A.C., Bronstert, A. and De Araújo, J.C., 2012. A channel transmission losses model for different dryland rivers. Hydrology and Earth System Sciences, 16(4), pp.1111-1135.

Covino, T., 2017. Hydrologic connectivity as a framework for understanding biogeochemical flux through watersheds and along fluvial networks. Geomorphology 277, 133–144.

Dincer, T., Hutton, L.G. and Kupee, B.B.J., 1979. Study, using stable isotopes, of flow distribution, surface-groundwater relations and evapotranspiration in the Okavango Swamp, Botswana. In Isotope hydrology 1978.

Duvert, C., Hutley, L.B., Birkel, C., Rudge, M., Munksgaard, N.C., Wynn, J.G., Setterfield, S.A., Cendón, D.I. and Bird, M.I., 2020. Seasonal shift from biogenic to geogenic fluvial carbon caused by changing water sources in the wet-dry tropics. Journal of Geophysical Research: Biogeosciences, 125(2), p.e2019JG005384.

Fovet, O., Humbert, G., Dupas, R., Gascuel-Odoux, C., Gruau, G., Jaffrézic, A., Thelusma, G., Faucheux, M., Gilliet, N., Hamon, Y. and Grimaldi, C., 2018. Seasonal variability of stream water quality response to storm events captured using high-frequency and multi-parameter data. Journal of Hydrology, 559, pp.282-293.

Geeraert, N., Omengo, F.O., Borges, A.V., Govers, G., Bouillon, S., 2017. Shifts in the carbon dynamics in a tropical lowland river system (Tana River, Kenya) during flooded and non-flooded conditions. Biogeochemistry 132 (1–2), 141–163.

Gooseff, M.N., Bencala, K.E. and Wondzell, S.M., 2008. Solute transport along stream and river networks. River confluences, tributaries and the fluvial network, pp.395–417.

Gumbricht, T. and McCarthy, T.S., 2003. Spatial patterns of islands and salt crusts in the Okavango Delta, Botswana. South African Geographical Journal, 85(2), pp.164-169.

Gumbricht, T., McCarthy, J. and McCarthy, T.S., 2004. Channels, wetlands and islands in the Okavango Delta, Botswana, and their relation to hydrological and sedimentological processes. Earth Surface Processes and Landforms: The Journal of the British Geomorphological Research Group, 29(1), pp.15-29.

Herndon, E.M., Steinhoefel, G., Dere, A.L. and Sullivan, P.L., 2018. Perennial flow through convergent hillslopes explains chemodynamic solute behavior in a shale headwater catchment. Chemical Geology, 493, pp.413-425.

Horgby, Å., Boix Canadell, M., Ulseth, A.J., Vennemann, T.W. and Battin, T.J., 2019. High-resolution spatial sampling identifies groundwater as driver of CO2 dynamics in an Alpine stream network. Journal of Geophysical Research: Biogeosciences, 124(7), pp.1961-1976.

Kgathi, D.L., Kniveton, D., Ringrose, S., Turton, A.R., Vanderpost, C.H., Lundqvist, J. and Seely, M., 2006. The Okavango; a river supporting its people, environment and economic development. Journal of Hydrology, 331(1-2), pp.3-17.

Koeniger, P., Leibundgut, C. and Stichler, W., 2009. Spatial and temporal characterisation of stable isotopes in river water as indicators of groundwater contribution and confirmation of modelling results; a study of the Weser river, Germany. Isotopes in Environmental and Health Studies, 45(4), pp.289-302.

Li, J., 2014. Terminal fluvial systems in a semi-arid endorheic basin. Salar de Uyuni (Bolivia).

Liu, F., Parmenter, R., Brooks, P.D., Conklin, M.H. and Bales, R.C., 2008. Seasonal and interannual variation of streamflow pathways and biogeochemical implications in semi-arid, forested catchments in Valles Caldera, New Mexico. Ecohydrology: Ecosystems, Land and Water Process Interactions, Ecohydrogeomorphology, 1(3), pp.239–252.

Liu, J., Chen, B., Xu, Z.Y., Wei, Y., Su, Z.H., Yang, R., Ji, Y.X., Wang, X.D., Zhang, L.L., An, N., Yang, F., 2020. Tracing solute sources and carbon dynamics under various hydrological conditions in a karst river in southwestern China. Environ. Sci. Pollut. Res. 1–12.

McCarthy, T.S. and Ellery, W.N., 1998. The Okavango Delta. Transactions of the Royal Society of South Africa, 53(2), pp.157-182.

McCarthy, T.S., Bloem, A. and Larkin, P.A., 1998. Observations on the hydrology and geohydrology of the Okavango Delta. South African Journal of Geology, 101(2), pp.101-117.

McCarthy, T.S., McIver, J.R. and Verhagen, B.T., 1991. Groundwater evolution, chemical sedimentation and carbonate brine formation on an island in the Okavango Delta swamp, Botswana. Applied Geochemistry, 6(6), pp.577-595.

Mosepele, K., Moyle, P.B., Merron, G.S., Purkey, D.R., Mosepele, B., 2009. Fish, floods, and ecosystem engineers: aquatic conservation in the Okavango Delta, Botswana. Bioscience 59 (1), 53–64.

Mosepele, K., Ngwenya, B.N. and Bernard, T., 2006. Artisanal fishing and food security in the Okavango Delta, Botswana. World Sustainable Development Outlook: Global and Local Resources in Achieving Sustainable Development, Inderscience, Geneva, pp.159–168.

Nanson, G.C., Tooth, S., Knighton, A.D., Bull, L.J. and Kirkby, M.J., 2002. A global perspective on dryland rivers: perceptions, misconceptions and distinctions. Dryland rivers: hydrology and geomorphology of semi-arid channels, 388.

Nichols, G., 2007. Fluvial systems in desiccating endorheic basins. Sedimentary processes, environments and basins: a tribute to peter friend, pp.569-589.

Oromeng, K.V., Atekwana, E.A., Molwalefhe, L. and Ramatlapeng, G.J., 2021. Time-series variability of solute transport and processes in rivers in semi-arid endorheic basins: The Okavango Delta, Botswana. Science of the Total Environment, 759, p.143574.

Parsons, A.J., Wainwright, J., Stone, P.M. and Abrahams, A.D., 1999. Transmission losses in rills on dryland hillslopes. Hydrological Processes, 13(17), pp.2897-2905.

Peel, M.C., Finlayson, B.L. and McMahon, T.A., 2007. Updated world map of the Ko¨ppen-Geiger climate classification.

Ramatlapeng, G.J., Atekwana, E.A. and Molwalefhe, L., 2023. Spatial and temporal controls on the solute behavior of rivers in arid watersheds: The Okavango River, NW Botswana. Journal of Hydrology, 618, p.129141.

Ramatlapeng, G.J., Atekwana, E.A., Molwalefhe, L. and Oromeng, K.V., 2021. Intermittent hydrologic perturbations control solute cycling and export in the Okavango Delta. Journal of Hydrology, 594, p.125968.

Rose, L.A., Karwan, D.L. and Godsey, S.E., 2018. Concentration–discharge relationships describe solute and sediment mobilization, reaction, and transport at event and longer timescales. Hydrological processes, 32(18), pp.2829-2844.

Tooth, S., 2000. Process, form and change in dryland rivers: a review of recent research. Earth-Science Reviews, 51(1-4), pp.67-107.

Wolski, P., Murray-Hudson, M., Savenije, H. and Gumbricht, T., 2005. Modeling of the hydrology of the Okavango Delta. Publication of the Water and Ecosystem Resources for Regional Development (WERRD) project, HOORC, Maun, Botswana.

Wymore, A.S., Leon, M.C., Shanley, J.B. and McDowell, W.H., 2019. Hysteretic response of solutes and turbidity at the event scale across forested tropical montane watersheds. Frontiers in Earth Science, 7, p.126.

Chapter 1: Intermittent hydrologic perturbations control solute cycling and export in the Okavango Delta

This chapter is reproduced from the original publication: Ramatlapeng, G.J., Atekwana, E.A., Molwalefhe, L. and Oromeng, K.V., 2021. Intermittent hydrologic perturbations control solute cycling and export in the Okavango Delta. Journal of Hydrology, 594, p.125968.

Abstract

We measured the concentrations of the total dissolved ions (TDI), dissolved silica, major cations and the δD and δ18O at sub-weekly intervals for one year in the Okavango River at the outlet of the Okavango Delta (Delta). Our objectives were to (1) document the temporal variations in the concentrations of solutes in the Okavango River, (2) determine the processes controlling the transfer of solutes to the river and (3) assess the temporal solute load and outflux from the Delta. We found that the TDI and major cation concentrations in the river were anomalously high during the rainy season and before the arrival of the annual flood pulse. The anomalous increases in the solute concentrations are due to dissolution and mobilization of precipitated salts stored in the floodplains and on hundreds of thousands of islands scattered across the Delta wetlands, as well as from 'flushing' of remnant evaporated flood water of higher salinity trapped in isolated wetland pools. Overland flow generated by local rains and flooding connect the river to the solute stores in the watershed. The temporally activated hydrologic flow pathways transfer solutes to the river that flushes them out of the Delta. The solute load in the river was higher during the rainy season and during pulse flooding, and mimicked the discharge hydrograph. We estimate that 17,838 Mg/y of dissolved solutes was flushed out of the Delta, with 67% removed during pulse flooding (6 months) and 30% during the rainy season (4 months). The transfer of solutes from the watershed to the river during pulse flooding and the rainy season, and solute export from the Delta is an important

mechanism that keeps the Delta's surface water resources fresh, which is critical for supporting a freshwater wetland ecosystem. Our results highlight the importance of intermittent activation of hydrologic flow pathways in controlling solute cycling in this and other arid watersheds.

1. Introduction

Hydrologic connectivity between rivers and solute stores in water- sheds is established by hydrologic flow pathways (e.g., overland flow, shallow subsurface flow and groundwater) through which solutes can be transported to rivers. The intermittent hydrologic connectivity between rivers and solute stores in watersheds is a major determinant of the types and amount of solutes delivered to rivers, and controls the timing of when solutes from different solute stores are delivered to rivers (Boyer et al., 1997; Dalzell et al., 2007; Gooseff et al., 2008; Liu et al., 2008; Covino, 2017; Geeraert et al., 2017; Fovet et al., 2018; Duvert et al., 2020). Solute transfer to rivers and their transport in rivers in humid regions have been investigated extensively (e.g., Fovet et al., 2018; Herndon et al., 2018; Rose et al., 2018; Wymore et al., 2020; Liu et al., 2020) because these rivers contribute to the ocean solute budget, and are therefore considered important in the global cycling of solutes (Hope et al., 1994; Kanduˇc et al., 2007). For instance, a study by Liu et al. (2020) in the Beipan River (SW China) revealed that during high discharge, carbonate weathering becomes one of the dominant processes controlling river dissolved inorganic carbon (DIC) concentrations and this provided insights into the role of hydrological variability on solute sources and river DIC dynamics in a wet monsoonal climate. Although studies in humid regions have advanced our knowledge and under- standing of solute sources, solute mobilization and their transfer to rivers, as well as solute export from watersheds, similar studies in watersheds in arid environments, particularly in endorheic basins (Seely et al., 2003) still lag behind.

Endorheic basins constitute 20–23% of the Earth's surface (Nyberg et al., 2018) and are characterized by solute cycling occurring entirely within the terrestrial system (Yapiyev et al., 2017). Despite the decoupling of solute cycling processes in endorheic basins from global oceanic solute cycle (Yapiyev et al., 2017), the percentage of the land surface occupied by endorheic basins is the basis for the inference that significant amounts of solutes are transferred to and processed at the terminus of endorheic basins (Li, 2014; Sheng, 2014). The solutes cycled within endorheic basins are a major determinant of the salinity status and ecological sustainability of wetland ecosystems often found at or near the terminus of endorheic basins (Sheng, 2014). Yet, little is known about the delivery of solutes to rivers, transportation of solutes and their storage at or near the basin terminus, hence, solute cycling in endorheic basins remains enigmatic. Knowledge on solute cycling in endorheic basins is pivotal for informing water management decision making in these basins where water scarcity is a major challenge.

Understanding the role of rivers in solute cycling requires the assessments of the hydrologic transience controlled by water sources and the hydrologic flow pathways traveled by water to the river. Water source partitioning techniques using solutes (e.g., total dissolved solids, cations, silica) and stable water isotopes (δD and $\delta^{18}O$) have proven useful in deciphering the role of different hydrological flow pathways in delivering solutes to rivers (Koeniger et al., 2009; Ala-Aho et al., 2018; Horgby et al., 2019; Duvert et al., 2020). The use of tracers to determine the origin of solutes and the timing of solute delivery to rivers is critical in refining our understanding of the processes controlling solute transport in rivers (e.g., Runkel and Bencala, 1995; Oromeng et al., 2020) and provides insights on catchment-scale solute cycling (e.g., Darracq et al., 2010, Liu et al., 2020). Yet the application of solutes and isotopic tracers in understanding water source

partitioning to rivers and tracing how solutes are exchanged between rivers and their watersheds in arid settings is not common (Oromeng et al., 2020).

We investigated the processes controlling solute transfer and transport of solutes in the Okavango Delta near the terminus of the endorheic Okavango River Basin (ORB). The ORB spans 530,000 km2 and overlaps climatic gradients from a higher rainfall temperate region in Angola to the steppe middle Kalahari Desert in Botswana (e.g., Ellery et al., 2003; Peel et al., 2007). Near the terminus of the ORB in the middle Kalahari Desert, the Okavango River divides into several distributaries forming the Okavango Delta (Delta). The Delta is the largest freshwater wetland in southern Africa (McCarthy and Ellery, 1998) and is a Ramsar world heritage site (Secretariat of the Convention on Wetlands, 2017). The Delta is unique because it is pristine and its hydrology is controlled by annual pulse flooding initiated by rains from the upper watershed in Angola and by local rains (e.g., Wolski et al., 2005). The Delta is also characterized by high evapotranspiration rates (McCarthy and Ellery, 1998; Bauer, 2004; Bauer et al., 2006; Bauer-Gottwein et al., 2007) which induce precipitation of salts on floodplains and on the numerous tree islands in the Delta wetlands and concentrates solutes in isolated wetland pools scattered across the Delta (Dincer et al., 1979; McCarthy et al., 1991, 1998; Gumbricht and McCarthy, 2003; Gumbricht et al., 2004). Yet, the Okavango River and the surface water in the Delta wetlands remain fresh. Currently, there is a lack of understanding of how and when the Okavango River is connected to solute stores in the local Delta watershed, and how the river connectivity to the solute stores affects solute cycling and solute export from the Delta. As a freshwater riverine-wetland ecosystem serving as an important source of potable water to the nearby communities (Mosepele et al., 2006, 2009; Kgathi et al., 2006), documenting the processes that may affect the solute behavior and consequently water

quality in the Delta is crucial. Additionally, assessing the Delta's temporal solute outflux provides insights on the processes that regulate the salinity of the Delta surface water resources.

In this study, we made sub-weekly measurements of discharge, total dissolved ions (TDI), major cations (Ca2+, Mg2+, Na+, K+), dissolved silica and δD and δ18O in the Okavango River at the outlet of the Okavango Delta. Our objectives were to (1) document the temporal variations in the concentrations of solutes in the Okavango River, (2) determine the processes controlling the transfer of solutes to the river and (3) assess the temporal solute load and outflux from the Delta. We conducted our temporal investigation at the outlet of the Delta in order to capture the integration of the processes controlling solute dynamics that affect the Okavango Delta and its wetlands. Our findings provide a baseline from which to monitor future temporal solute dynamics in the Okavango Delta and insights on solute cycling near the terminus of endorheic basins.

2. The Okavango Delta

2.1. Location

The study site is located at the outlet of the Okavango Delta near the terminus of the ORB. The Okavango Delta consists of a panhandle region and a delta region (Fig. 1). The Panhandle is a narrow valley with a gradient of 1:5500 through which the Okavango River meanders extensively (McCarthy et al., 1997). When the Okavango River crosses the Gumare Fault at the end of the Panhandle, the river divides into distributary channels that form the delta region. The delta region is a gently sloping (1:3400) alluvial fan with a surface area of more than 22,000 km2 (McCarthy et al., 1992) formed within the half-graben of the Okavango Rift Zone (McCarthy et al., 1993, 1997; Modisi et al., 2000; Kinabo et al., 2007, 2008; Bufford et al., 2012; Leseane et al., 2015). The topography of the Okavango Delta has been shaped by neotectonics, river sedimentation,

channel formation and avulsion (McCarthy and Ellery, 1994; McCarthy et al., 1998). Tectonism in the delta region caused overall regional tilting, evidenced by varying elevations from 1025 m where Okavango River flows into the Delta at Mohembo to 920 m in the Mababe Depression (Gumbricht et al., 2001). The delta region is characterized by relatively flat topography (McCarthy et al., 1998; McCarthy, 2006) with gentle undulations where the local relief rarely exceeds 2 m, except for areas with termite mounds (McCarthy et al., 1998; Gumbricht et al., 2001; McCarthy, 2006).

2.2. Geology

The upper ORB watershed (Cuito and Cubango basins) in Angola lies on the Precambrian Congo Craton. The metamorphic rocks of the upper watershed formed during the Precambrian include gneisses, quartzites and migmatite (Bereslawski, 1997; Steudel et al., 2013). Large parts of the Cuito basin and southern parts of the Cubango basin are covered by sedimentary rocks of the Karoo Supergroup, and overlain by thick layers of unconsolidated sands, clays, lime rock and lateritic layers of the Kalahari Superior Formation (Bereslawski, 1997; Catuneanu et al., 2005; Jones, 2010). The headwater region of the Cubango River is characterized by crystalline bedrock comprising granite, dolerite and porphyrite (Bereslawski, 1997).

In the region surrounding the Okavango Delta, the bedrock geology consists of Precambrian crystalline rocks of the Damara and Ghanzi-Chobe orogenic belt (Modie, 2000; Milzow et al., 2009). The superficial geology consists of Quaternary Kalahari alluvium and recent swamp sediments (Ringrose et al., 2009) overlying ~40 m of sands and 105–175 m of lacustrine and fluvio-deltaic sediments (Kalscheuer et al., 2015). The lacustrine and deltaic sediments are remnants of the Paleo Lake Makgadikgadi and Paleo Okavango Megafan sedimentary units (Podgorski et al., 2013, 2015; Kalscheuer et al., 2015).

2.3. Climate and hydrology

The ORB‘s climatic regimes transition from a temperate climate in the Angolan highlands to the steppe arid middle Kalahari Desert in Botswana (Peel et al., 2007). The climate of the upper watershed in Angola and lower watershed in the Delta is characterized by wet and dry seasons (McCarthy and Ellery, 1994; Milzow et al., 2009; Steudel et al., 2013). The wet season spans from November to March and the dry season lasts from April to October. The mean annual rainfall in the upper watershed is ~1100 mm (Pombo et al., 2015). The maximum daily temperatures vary between 22 and 24 ℃ during the rainy season and decrease to 15–17 ℃ during the dry season (Steudel et al., 2013). The Delta receives an average annual rainfall of 450 mm (Milzow et al., 2009). The highest mean monthly maximum temperatures during the rainy season range between 32 and 35 ℃ and the lowest mean monthly minimum temperatures during the dry season range between 2 and 7 ℃ (Moses and Gondwe, 2019). The estimated potential evapotranspiration is 2172 mm/y, which is 4 times greater than the rainfall received in the Delta (Wilson and Dincer, 1976).

The hydrology of the Delta is driven by an annual flood pulse derived from the upper watershed in Angola and by local rains. The precipitation that falls around October in the Angolan highlands flows through the Cubango River and Cuito Rivers and reach the northern part of Botswana via the Okavango River around February-May (McCarthy and Ellery, 1998; McCarthy et al., 2003; Wolski et al., 2008; Mackay et al., 2011). After reaching the Delta, the flood pulse takes approximately 4–6 months to travel a river distance of ~400 km from the proximal portion in Mohembo to the distal portion at Maun (McCarthy and Ellery, 1998).

As the flood advances across the Delta, the area inundated gradually increases from an annual low of 4500–6000 km2 to an annual high of 9000–12,000 km2 depending on the flood magnitude

(Ramberg and Wolski, 2008). Due to the relatively high hydraulic conductivity (10–30 m/day) and porosity (30%) of the sandy soils in the Delta (Obakeng and Gieske, 1997), as well as the slow propagation of the flood wave across the Delta, the flood inundation is accompanied by recharge of the shallow unconfined aquifer (McCarthy, 2006). Thus, the Okavango River is influent, as evidenced by the deepening of the groundwater table away from the Delta wetlands (McCarthy et al., 1997; Ellery et al., 2003; McCarthy, 2006; Milzow et al., 2009; Akondi et al., 2019).

There are ~150,000 islands complexes scattered across the Delta. These islands vary in shape and size from a few square meters to ~700,000 m^2 and cover 5% of the area of the permanent swamp, 25% of the seasonal swamp and 50% of the occasionally flooded swamps (McCarthy and Metcalfe, 1990; Gumbricht et al., 2004; Humphries et al., 2014). The trees and halophytic grasses which dominate the islands facilitate evapotranspiration-driven flow of water from Okavango River towards the islands (Gumbricht and McCarthy, 2003; Ramberg and Wolski, 2008). This evaporation, as well as transpiration by vegetation on island fringes enhances the accumulation of salts in island fringes and centers (Gumbricht and McCarthy, 2003; Ramberg and Wolski, 2008). The island complexes are inundated by the annual flood pulse and periodically trap water which is then subjected to ET and precipitate salts in the island centers.

During the rainy season when there is no flooding, the seasonally and occasionally inundated wetland ecotones of the Okavango Delta are dominated by isolated surface water pools (McCarthy et al., 1998) caused by the accumulation of summer rains and previous year's floods. These isolated wetland pools show enriched $\delta^{18}O$ (0.1–7.5‰) induced by evaporation (Dincer et al., 1979; McCarthy et al., 1991, 1998).

3. Methodology

3.1. Sample collection and analyses

This study was conducted between November 2017 and December 2018, during which we sampled the Okavango River (23º28′ 48.99″ E, 19º57′ 16.77″ S) and rain (23º27′ 7.07″ E, 19º57′ 19.49″ S) in Maun. We collected 98 river samples and 51 rain samples. The river samples were collected by the grab technique into 20 ml glass scintillation vials at sub- weekly intervals. Rain samples were collected in a static collector and aliquots were transferred into 20 ml glass scintillation vials as soon as the rain event was over.

All the samples were protected from sunlight and kept in a cool storage. The samples were transported to the University of Delaware (USA), where they were filtered through 0.45 μm nylon syringe filters and refrigerated until analyses. Aliquots of the river samples were acidified with trace metal grade nitric acid and analyzed for cations by Inductively Coupled Plasma Mass Spectrometer (Agilent Tech. ICP- MS:7500cX series). Total dissolved ions (TDI) was measured using an Orion Star A212 benchtop conductivity/TDS meter calibrated according to the manufacturer's instructions. Silica concentrations were measured by spectrophotometry on a CHEMetrics (V-3000 series) photometer. The $\delta^{18}O$ and δD of river and rain samples were measured using a Los Gatos Research (LGR) Liquid Water Isotope Analyzer (LWIA). The LGR LWIA performed 6 injections per sample and the last 4 injections were averaged for the sample's isotope value. Each batch run was calibrated with Standard Light Antarctic Precipitation (SLAP2) and Vienna Standard Mean Ocean Water (VSMOW) standards and machine drift was verified by running a test sample and a select standard every 5th sample. The isotope ratios are reported in delta notation (δ) in per mil (‰):

$$\delta\ (‰) = ((R_{sample} - R_{standard}) / R_{standard}) \times 1000$$

where R is the ratio of D/H, or $^{18}O/^{16}O$ in the sample and standard. The δD and $\delta^{18}O$ are reported relative to VSMOW. The precision (1σ standard deviation) of the LGR LWIA isotopic measurement is better than ± 0.3‰ for δD and ± 0.07‰ for $\delta^{18}O$.

3.2. River discharge and solute load estimates

River discharge (Q) and water level measured at the Maun (Thamalakane) station (23º25′35.09″E, 20º0′17.04″S) were obtained from the Botswana Department of Water and Sanitation. We developed a discharge rating curve from Log water level (m) vs. Log discharge (m3/s) and obtained the least squares regression equation (R2 =0.74; n =17):

$$\text{Log Q } (m^3/s) = 3.9\text{Log water level (m)} - 0.11 \quad (1)$$

where Q and the water level are the instantaneous measured discharge and water levels, respectively. The least squares regression equation was used to estimate instantaneous discharge during each sampling episode. The total dissolved solids (TDS) (in mg/L) used in determining the solute load was obtained by adding the total dissolved ions (TDI) (mg/L) and dissolved silica (mg/L) (e.g., Gondwe et al., 2017). We determined the instantaneous solute load (ISL_i) by multiplying the instantaneous TDS concentration (C_i) in mg/L with the corresponding instantaneous discharge (Q_i) in l/s (e.g., Aulenbach et al., 2016) and assumed that the TDS concentrations represent all the dissolved solutes in the river (e.g., Hem, 1985).

$$ISL_i = C_i \times Q_i \quad (2)$$

We estimated the daily solute loads (DSL) by summing the instantaneous solute load for each day. The monthly solute loads (MSL) were estimated by summing the instantaneous solute load for each month:

$$(DSL_i) \text{ or } (MSL_i) = \sum ISL_i \times \Delta t \quad (3)$$

In making the daily and monthly solute load estimates, we assumed constant C_i and Q_i between our temporal measurements. Our assumption will be less valid if the TDS concentrations or river discharge change at frequencies higher than our sampling interval.

3.3. Rainfall and air temperature

Daily rainfall data measured at the Sexaxa weather station (23º31′42.05″E, 19º54′7.89″S) were obtained from the archives of the Okavango Research Institute (http://www.okavangodata.ub.bw/ori/monitoring/rainfall/). The mean monthly air temperature values for Maun were downloaded from the World Weather Online website (https ://www.worldweatheronline.com; accessed January 1, 2020).

4. Results

The descriptive statistics (mean, minimum, maximum and the standard deviations) of the solute concentrations (TDI, silica, TDS and cations), mean monthly air temperature, river discharge, δD of river water, $\delta^{18}O$ of river water, rainfall, δD of rain, $\delta^{18}O$ of rainfall, the instantaneous solute load and monthly solute load are shown in Table 1. The temporal δD, $\delta^{18}O$, TDI, silica, Na^+, K^+, Mg^{2+}, Ca^{2+} and daily solute load measured in the Okavango River is presented in Table 2. The temporal δD and $\delta^{18}O$ composition of Maun rain is presented in Table 3. The temporal river discharge and water level measured in the Okavango River in Maun is presented in Table 4.

4.1. Temporal variations in solute concentrations (TDI, cations and silica)

On a temporal basis, the concentrations of TDI (Fig. 2a) showed similar temporal behavior to that of Na^+ (Fig. 2b), Mg^{2+}, Ca^{2+}, K^+ and silica (Fig. 2c). The solute concentrations (TDI, Na^+ and silica) increased from November 2017 to February 2018 (Fig. 2a–c). In February 2018, the solute concentrations decreased precipitously and stayed low until the end of the rainy season in mid-April 2018. Near the start of the dry season in mid-April, there was a rapid increase in the solute concentrations which remained high until June 2018, after which the solute concentrations decreased to low values and fluctuated within a narrow range past the end of the dry season and into the rainy season in December 2018.

The order of cation abundance measured in the Okavango River in Maun is: $Na^+ > K^+ > Mg^{2+} > Ca^{2+}$. The temporal behavior of the ratio of Na^+/Ca^{2+} show higher ratios between late February 2018 and late April 2018, increasing from 7 to 19 (Fig. 2d). During other times, the Na^+/Ca^{2+} ratio remained low, fluctuating between 5 and 10.

4.2. Temporal variations in river discharge and rainfall

The hydrograph constructed from the least squares regression equation developed from discharge and water level data (Table 4) is shown in Fig. 2e. On an annual basis, the hydrograph shows two main peaks. The hydrograph is asymmetric with steep rising limbs and more gentle falling limbs. During the beginning of the rainy season, the hydrograph was receding as river discharge decreased from 13 m^3/s to 0.8 m^3/s between November 2017 and early February 2018. A smaller discharge rise in February 2018, peaked at 3.5 m^3/s in early March 2018, before slowly receding to 0.2 m^3/s in June 2018. The discharge began to rise in June 2018 and peaked at 12.6

m^3/s in August 2018 (Fig. 2e). The peak discharge was followed by a gradual recession from late August through December 2018.

Temporal rainfall distribution in the distal portion of the Okavango Delta in Maun shows that between the 2017 and 2018 rainy season, more rain fell during the second half of the rainy season between late- January to April 2018, with about 80% of the season's rain falling during January to March (Fig. 2f).

4.3. Temporal variations in air temperature

During the rainy season between November 2017 and March 2018, the mean monthly air temperature fluctuated around 29 ± 3 ℃ (Fig. 2g). During the dry season in 2018, the mean monthly air temperature decreased from 24 ℃ in April to the lowest temperature of 18 ℃ in July. After July 2018, the average monthly air temperature increased from near the end of the dry season continuously to a high of 34 ℃ in December 2018 during the rainy season.

4.4. Temporal variations in the stable isotopic composition of river water and rain

The δD and $\delta^{18}O$ of river water co-vary and we show the temporal δD variations in river water in Fig. 2h. The δD was enriched during the first half of the rainy season from November 2017 to February 2018, with the highest value of 23‰ observed in December 2017. The δD decreased precipitously in mid-February to about 43‰ and stayed low at 18 ± 5‰ to the end of the rainy season in April 2018. The start of the dry season was marked by a sudden increase in the δD to a high of 4‰, which lasted from April to late May 2018. From June through December 2018, the δD increased continuously to a high of 26‰.

The temporal variations of δD of rain shown in Fig. 2i indicates enrichment during the beginning of the rainy season in December 2017, with the highest δD value of 37‰. Between

January and March 2018, the δD varied around -60 ± 30‰. The wide ranges in the isotopic composition of rain measured in this study have been reported in previous studies (e.g., Akondi et al., 2019; Verhagen, 1992; Mazor et al., 1977; Foster et al., 1982).

5. Discussion

5.1. Temporal shifts in solute concentrations in the Okavango River

Our temporal assessment of the solute chemistry of the Okavango River at the outlet of the Okavango Delta documents seasonal and sub-seasonal variations in the concentrations of TDI, cations and silica (Fig. 2a–c). Generally, the concentrations of the different solutes increased continuously from the early rainy season in November 2017 to peak concentrations in the mid-rainy season in February 2018, before decreasing markedly and staying nearly constant through the end of the rainy season in March 2018. The solute concentrations increased sharply in April 2018 and stayed nearly constant at higher concentrations until June 2018, after which the concentrations decreased sharply and then remained nearly constant through December 2018. The temporal variations in solute concentrations in the Okavango River can be driven by (1) water column processes that enrich solutes (e.g., ET and weathering) or reactions which remove solutes (precipitation), (2) addition of water with higher (enrichment) or lower (dilution) solute concentrations during river recharge, and/or (3) episodic transfer of solutes from solute stores in the watershed to the river.

5.2. Water column addition or removal of solutes in the Okavango River

5.2.1. Evapotranspiration (ET*)*

Previous studies of the solute chemistry in the Okavango River in the Delta have suggested that ET is the major process controlling the spatio-temporal evolution of solutes (e.g., Sawula and Martins, 1991; McCarthy et al., 1993; Cronberg et al., 1996; Mladenov et al., 2005; Mackay et al., 2011; Akoko et al., 2013; Atekwana et al., 2016; Gondwe and Masamba, 2016). Potential ET in the Delta exceeds precipitation by a factor of ~4 (Wilson and Dincer, 1976; Dincer et al., 1979) and ET is responsible for downriver enrichment in solutes from the proximal portion of the Delta in Mohembo to the distal portion in Maun (e.g., Akoko et al., 2013; Gondwe et al., 2017). Increases in the TDI or ionic concentrations induced by ET at a fixed river station should correspond to seasons, such that high rates of ET and higher solute concentrations are observed during the rainy season when temperatures are high and lower rates of ET and lower solute concentrations are observed during the dry season when temperatures are cooler. The anomalously higher TDI, cations and silica concentrations during the mid-rainy season (Fig. 2a–c) occur when the air temperatures are high (Fig. 2g). However, the high TDI, cations and silica concentration anomalies at the beginning of the dry season in May 2018 (Fig. 2a–c) occur when the air temperatures are lower (Fig. 2g), and are therefore inconsistent with evapoconcentration of solutes.

To determine the effect of evaporation in increasing the solute concentrations in the Okavango River, we first demonstrate evidence of its occurrence in river water. During the evaporation of surface water, isotopic fractionation causes enrichment in the δD and $\delta^{18}O$ (Craig, 1961; Ehhalt et al., 1963; Dansgaard, 1964; Clark and Fritz, 1997; Govender et al., 2013; Good et al., 2014). The δD and $\delta^{18}O$ composition of Okavango River samples co-vary (Fig. 3). Also shown in Fig. 3 is the global meteoric water line (GMWL, Craig, 1961) and the local meteoric water line (LMWL). The LMWL is constructed from the data published by Akondi et al. (2019) and data collected for rain in this study. The δD and $\delta^{18}O$ of samples from the Okavango River lie below the GMWL and

LMWL, and along the Okavango Delta Evaporation Line (ODEL), consistent with previous studies which suggest that the Okavango River undergoes evaporation during transit through the Delta (Dincer et al., 1979; Atekwana et al., 2016; Akondi et al., 2019).

Evidence for evapoconcentration in increasing solute concentrations in the river water was assessed from the relationship between TDI concentrations and d-excess. We use the d-excess to characterize the effects of evaporation on river solute concentrations because lower d-excess values indicate greater extent of evaporation (e.g., Dansgaard, 1964; Fröhlich et al., 2002; Huang and Pang, 2012; Krishan et al., 2020). We divided the discharge hydrograph (Fig. 2e) into major changing discharge regimes (Fig. 4a): flood pulse recession (November 2017-February 2018 and September 2018-December 2018; Fig. 4b); rainy season–dry season recession (March 2018-June 2018; Fig. 4c); flood pulse rise (June 2018-August 2018; Fig. 4d) and rainy season rise (February 2018-March 2018; Fig. 4e). In Fig. 4b-e, we show the Log TDI concentrations vs. d-excess. The model line (black solid line: d-excess = 93.2 (Log TDI) + 158.1, R^2 = 0.99) and the upper and lower limits of the 95% confidence interval along the model line (pink-shaded region bounded by dashed lines) were derived from Okavango River water collected in Maun and evaporated over time (Atekwana et al., 2016). In principle, there should be a negative relationship between Log TDI concentrations vs. d-excess during evaporation (e.g., Huang and Pang, 2012) as shown by the model line, with the data falling within 95% confidence interval (pink-shaded region). Data plotting outside to the right or the left of the 95% confidence interval indicate river water with TDI concentrations affected by other factors in addition to evapoconcentration. The Log TDI concentrations-d-excess modelling allows us to determine when additional factors affect the solute concentrations as the Okavango River changes from one flow regime to another (Fig. 4). During discharge recession (November 2017-February 2018, September 2018-December 2018; Fig. 4b

and March-June 2018; Fig. 4c), there are three solute regimes: (1) a baseline solute regime dominated by evapoconcentration and characterized by data which lie along the model line within the 95% confidence interval region, (2) a solute regime of highly evaporated water with low TDI concentrations characterized by data plotting to the left beyond the 95% confidence interval and (3) a solute regime with higher d-excess where the data plot to the right and parallel to the 95% confidence interval. For the rising discharge regime during annual flooding (June-August 2018; Fig. 4d) >90% of the data lie within the 95% confidence interval, indicating river baseline condition dominated by evaporative enrichment. In contrast, during the rising discharge in the rainy season (February-March 2018; Fig. 4e), all the data plot in a cluster to the right of the 95% confidence interval, signifying a different river solute regime. From the model analysis, we deduce that in addition to the baseline evapoconcentration of river water, there are two other major processes that affect the solute regime of the Okavango River: one characterized by highly evaporated water with low TDI concentrations and another characterized by less evaporated water with low to high TDI concentrations. Since d-excess indicates the extent of evaporation, we posit that the same extent of evaporation should not result in wide ranges in TDI concentrations, unless other river solute enrichment processes are at play.

Transpiration, which can change the TDI concentrations of river water, will not affect the δD and $\delta^{18}O$ composition, because unlike evaporation, transpiration does not cause isotopic fractionation (e.g., Walker and Richardson, 1991). Thus, although transpiration affects the solute concentrations which we are unable to quantify from our data, we assumed that its effect on the river solutes is constant over space and time in the Okavango Delta, and does not adversely affect river water differentially or episodically.

Although studies of the solute chemistry in the Okavango River in the Delta have suggested that ET is the major process controlling the spatio-temporal evolution of solutes (e.g., Sawula and Martins, 1991; McCarthy et al., 1993; Masamba and Muzila, 2005; Mladenov et al., 2005; Akoko et al., 2013; Mosimane et al., 2017; Mogobe et al., 2018), the results of this study indicate that ET is not solely responsible for the temporal solute perturbations observed in the Okavango River at the exit of the Delta. We use the results of this study to suggest that the lower and nearly uniform solute concentrations observed between February 2018 and April 2018 and between June 2018 and November 2018 (Fig. 2a–c) represent the baseline solute concentrations of the river at Maun. We make this suggestion because the concentration changes from this baseline occur slowly, while perturbations from this baseline occur by sharp concentration increases. For example, TDI has a baseline con centration of 70 ± 5 (mg/L), and is nearly constant between January and mid-April, and decreases slowly from June through December (Fig. 2a). Additionally, if we assume that the transit time for river water to travel the ~400 km from the entrance of the Delta in Mohembo to the exit at Maun is constant, ET acting alone on the river water will result in similar temporary baseline concentration that will change in a relatively slow manner.

5.2.2. Weathering and precipitation reactions

The addition or removal of solutes in the water column through dissolution or precipitation reactions can alter TDI, cation and silica concentrations, and depend on the saturation state with respect to mineral phases (Drever, 1971; Miller and Drever, 1977; Hodson et al., 2010). Thermodynamic equilibrium models indicate that the Okavango River is undersaturated with respect to solid mineral phases such as calcite, aragonite and dolomite (Sawula and Martins, 1991). The undersaturated state of the Okavango River favors mineral dissolution over precipitation, and therefore we infer that the chemical removal of solutes from the water column through

precipitation is unlikely to be one of the factors affecting the observed temporal solute behavior. Although the Okavango River is undersaturated with respect to calcite, aragonite and dolomite, weathering of these mineral phases is not important because of their low abundance in sediments of the Delta (McCarthy and Metcalfe, 1990; Huntsman-Mapila et al., 2005). While there is certainly potential for mineral weathering in the water column because the Delta receives 170,000 Mg/y of bed load and 39,000 Mg/y of suspended load (McCarthy and Ellery, 1998), episodic weathering occurring only during the beginning of the rainy season and before the initiation of pulse flooding when solute concentrations are high (Fig. 2a–c) is not a viable explanation for the periodic solute enrichment. For instance, silica is generated from quartz dissolution, which is a thermodynamically slow process. The quartz solubility at the temperatures and pH of Okavango River water (25 °C; ~6.3) is about 100 μM (Frings et al., 2014), which is lower than dissolved silica concentrations measured during this study. Thus, quartz dissolution is unlikely to occur episodically within the water column. Therefore, we discount chemical weathering or precipitation in the Okavango River water column to the observed seasonal and sub-seasonal variations in river solute behavior.

5.3. Hydrologically driven episodic transport of solutes to the Okavango River

Since the solute concentrations in the Okavango River increase markedly during hydrologic perturbations, we assess the role of hydrologic connectivity between the river and the watershed solute stores in the mobilization and transfer of solutes to the river. We developed a conceptual model to illustrate how solutes at the surface can be transferred from the adjacent watershed consisting of floodplains, wetlands and islands to the river and from groundwater (Fig. 5). This conceptual model considers the role of the river in the accumulation of solutes in solute stores beyond the river channel and in groundwater and in the transfer of solutes from the solute stores

to the river. The solute stores (Fig. 5a) beyond the Okavango River channel consist of (1) salt precipitates on floodplains and on island fringes and island centers that result from ET (Gumbricht and McCarthy, 2003; Gumbricht et al., 2004; Ramberg and Wolski, 2008), (2) post flood recession isolated wetland pools and wetland water subjected to ET (Dincer et al., 1979; McCarthy et al., 1991, 1998) and (3) saline groundwater (Ramberg and Wolski, 2008; McCarthy et al., 2012). River access to the solute stores and the transfer of solutes to the river is established by temporal activation of hydrologic flow pathways connecting the river to the solute stores. Hydrologic connectivity between the river and the solute stores is via overland flow initiated during the rainy season (Fig. 5b), by flooding and return flow of flood waters following the annual pulse flooding and from groundwater influx (Fig. 5c).

Groundwater discharge to rivers in humid watersheds is an important source of solutes to rivers (Godsey et al., 2009; Liu et al., 2020; Rose et al., 2018). In arid watersheds, groundwater is an important source of solutes if groundwater supports rivers (Baskaran et al., 2009; Batlle- Aguilar et al., 2014; Imes and Wood, 2007). Surface water-groundwater interaction in the Okavango Delta has not been investigated extensively. However, on a regional basis, the hydraulic gradient of the groundwater table steepens away from the river and floodplains (McCarthy et al., 1993, 1998; Ellery et al., 2003; Milzow et al., 2009) making the Okavango River and wetlands a potential source of groundwater recharge (Fig. 6a). Studies conducted in the Okavango Delta wetlands indicate river recharge of local groundwater during periods of flooding (Dincer et al., 1979; Gieske, 1996; McCarthy, 2006). Groundwater recharge by the river appears to be prominent from an evaluation of the hydro-stratigraphy from the lower Okavango Delta where our sampling station is located (Fig. 6b). Groundwater levels near the sampling station are 5 m or more below the ground surface and groundwater flows towards the northeast and away from the middle of the delta

(Fig. 6b), indicating river recharge of groundwater (Thangarajan et al., 1999; Mangisi, 2004). Furthermore, the stable hydrogen and oxygen isotopic composition of groundwater shows enrichment and lie on the trend of the Okavango Delta Evaporation Line (Akondi et al., 2019) which is consistent with evaporated river recharge of groundwater. Although this notion of the absence of groundwater influence on the river chemistry is consistent with previous studies (McCarthy et al., 1993; Ellery et al., 2003; Milzow et al., 2009; Akondi et al., 2019), it is also possible to have input of groundwater with similar chemistry and isotopic composition to the river water spatially across the Delta, which complicates surface water-groundwater interaction dynamics. Thus, the groundwater behavior in the Delta during hydrologic events and the dry season still need to be explored and constrained. Our study is unable to constrain the temporal groundwater response during different hydrologic regimes.

We tested our conceptual model using the relationship between total dissolved solids (TDI + Silica) in river water and river discharge (C-Q relationship), which provides insights into the mobilization and transfer of solutes from watersheds to rivers (Godsey et al., 2009; Chorover et al., 2017; Rose et al., 2018; Wymore et al., 2020). In our evaluation, we use the discharge regimes described in Section 5.2.1. (Fig. 7a) to model flow regime-based C-Q relationships (Fig. 7b-e). The C-Q relationship for the Okavango River during the flood pulse recession for November 2017-February 2018 show solute enrichment with decreasing river discharge, followed by dilution, while river samples for the September 2018-December 2018 mostly cluster at lower solute concentrations (Fig. 7b). For the November 2017-February 2018 recession, the continuous solute enrichment with decrease in the river discharge, evident on the temporal plots of TDI, cations and silica concentrations (Fig. 2a-c) corresponds to highly enriched δD in river water (Fig. 2h). We interpret the concomitant shift to higher solute concentrations with decreasing discharge to mass

transfer of solute enriched evaporated water from the wetlands into the river (e.g., Diamond and Cohen, 2018; Herndon et al., 2018), following the pulse flooding and dilution (Fig. 7d). This mixture of pulse floodwater and wetland water during return flow is characterized by a negative relationship between Log TDI concentrations and d-excess (Fig. 4b). Previous studies have noted the existence of isolated saline wetland pools, which are isotopically enriched within the seasonally and occasionally flooded wetland ecotones of the Okavango Delta (Dincer et al., 1979; McCarthy et al., 1991, 1998) which serve as locations for solutes transported via return flow. We note that during the September 2018-December 2018, the peak discharge from the flood pulse was 62% lower than in 2017, and the solute concentrations (Fig. 2a-c) show only small variations, while the δD slowly increased (Fig. 2h). The C-Q relationship shows scatter, and low Log C with decreasing Log Q (Fig. 7b), indicating that the flood pulse was of such a low magnitude that it was likely confined within the river channels. The floodwater was subjected only to evaporation and was unmixed with higher solute concentration water from the wetlands as the flood receded, consistent with the low d-excess and TDI concentrations (Fig. 4b).

The C-Q relationship of the Okavango River during hydrograph recession in the late rainy season and early dry season (March-June 2018; Fig. 7a) is characterized by a marked increase in solute concentrations in the middle of the recession, followed by nearly constant so lute concentrations, and subsequent dilution (Fig. 7c). During the first half of the recession when the solute concentrations are low, the Na^+/Ca^{2+} ratios indicate a shift in the type of solutes in the river because river water was getting progressively enriched in Na^+ relative to Ca^{2+} (Fig. 2d). We suggest that there is a hydrologic connection between the solute sources in floodplains and islands, and the Okavango River, which provides solutes enriched in Na^+. McCarthy and Metcalfe (1990), McCarthy et al. (1991) and Gumbricht and McCarthy (2003) indicate that chemical sedimentation

caused by ET of river and wetland water on the thousands of islands in the Okavango Delta include sodium carbonate salts (trona, thermonatrite). Thus, although the overall river solute concentrations decrease from the dilution effect of rain (Fig. 2a–c; Fig. 7c), rain-induced overland flow dissolves sodium salts from the floodplains and island, which is then transferred to the river (Fig. 2d; Fig. 5b).

The C-Q relationship of the Okavango River during increasing discharge from the pulse flooding in June-August 2018 (Fig. 7a) is characterized by solute enrichment with increasing river discharge, followed by solute dilution near peak flooding (Fig. 7d). During the period of slow solute concentration increases, the Log TDI concentrations vs. d-excess show data that cluster around the model line (Fig. 4d). Additionally, during the discharge increases, Na^{+}/Ca^{2+} was flat and consistent with the baseline concentrations, indicating the addition of evaporated river water with a similar proportion of ions to river water, although the solute concentrations were slightly higher. Such enriched evaporated river water can come from the adjacent isolated wetland pools hosting isotopically enriched water (Dincer et al., 1979; McCarthy et al., 1991, 1998). The water from the evaporated wetland pools is delivered to the river by the arriving flood pulse via the 'Hydrologic Piston model' (Glover and Johnson, 1974) where "old", highly evaporated water enriched in solutes is pushed by the flood front during the arrival of new flood pulse (Fig. 5c). Near the peak discharge, "fresh" floodwaters arrive in Maun, causing a slight decrease in solute concentrations (Fig. 7d). We suggest hydrologic connection between the river and adjacent evaporated water in the wetlands. Since the flood magnitude was low in 2018, floodwaters were not sufficient to overtop the wetlands to flood the salt islands.

During the rainy season when river discharge increased in February 2018-March 2018, the C-Q relationship of the Okavango River is characterized by a slight increase in solute concentrations,

followed by slight dilution near peak discharge (Fig. 7e). During this period of slow solute concentrations increases, the data for the Log TDI concentrations vs. d-excess are off to the right of the model line, and clustered at low TDI concentrations and higher d-excess (Fig. 4e). The low TDI concentrations are consistent with rain dilution, and the higher d-excess indicates lower evaporation effects. Nevertheless, the Na^+/Ca^{2+} increased above baseline (Fig. 2d), indicating the mobilization of solutes rich in Na^+ from solute stores to the river by overland flow initiated by rain (Fig. 5b).

5.4. Temporal solute load and solute flux from the Okavango Delta

The instantaneous dissolved solute load estimated from TDS concentrations (TDI + Silica) and discharge shows a bi-annual distribution (Fig. 8a). Higher dissolved solute loads in the river are observed between July and November and between February and May, although the solute load magnitudes are different. The temporal variations in the instantaneous dissolved solute loads behave similar to river discharge (Fig. 2e) and are higher during high river discharge and lower during low river discharge. This temporal behavior in solute load can be used to infer that increased discharge is associated with increase in solute concentrations, yet increased discharge is from the annual pulse flooding and seasonal rains, which are more dilute compared to the baseline chemistry of river water at Maun. This behavior in the temporal dissolved solute load is consistent with solute transfer from the floodplains, island and evaporated isolated wetland pools discussed in Section 5.3.

During this study, an annual dissolved solute flux of 17,838 Mg was removed from the Delta (Table 1). When examined on a monthly basis, the solute flux mirrors the daily solute load (Fig. 8b). Higher amounts of solutes leave the Delta during the annual pulse flooding between July and November and during the rainy season in February through May. For dissolved solute outflux from

the Okavango Delta, 67% leaves during pulse flooding (6 months), 30% during the rainy season (4 months) and 3% during the rest of the time (2 months). The results of this study show that river discharge perturbations associated with the annual pulse flooding and rain are responsible for transferring 97% of the annual solute load removed from the Delta via the Okavango River.

5.5. Solute transport and cycling in the Okavango Delta

The Okavango Delta is a solute store and sink and there is ample evidence of salt accumulation on the island edges and centers (Gumbricht and McCarthy, 2003; Zimmermann et al., 2006; Ramberg and Wolski, 2008), and in isolated evaporated saline wetland pools (Dincer et al., 1979; McCarthy et al., 1991, 1998), yet the surface waters of the Delta remain relatively fresh. The pristine conditions of the Delta have been attributed to the "island salt sinking model" which is a salt removal process controlled by density-driven sinking of saline waters (McCarthy and Ellery, 1994; Bauer, 2004; Bauer-Gottwein et al., 2007; Ramberg and Wolski, 2008). In the "island salt sinking" model, ET concentrates salts in thousands of islands in the Delta and then the saline water beneath islands sinks to greater depths due to density driven flow. The island sinking salt model does not address the salt precipitates left as crust on the surface of the islands and floodplains. We propose a "hydrological flushing" model as an additional mechanism that contributes to maintaining the pristine water quality condition of the Okavango Delta. In the hydrologic flushing model, the annual pulse flooding and seasonal rains dissolve salt precipitates on the floodplains and islands and transfer the solutes along with evaporated wetland water to the Okavango River which is then transported out of the Delta (Oromeng et al., 2020). The solutes exported from the Delta accumulate at the ORB's terminus in the Makgadikgadi Pans, a source for the salt mining sector in Botswana (Molwalefhe, 2003).

6. Conclusions and implications

Total dissolved ions, major cations (Ca^{2+}, Mg^{2+}, Na^{+}, K^{+}) dissolved silica concentrations and the δD and $\delta^{18}O$ of river water were used to investigate the processes controlling temporal solute behavior in the Okavango River at the distal portion of the Delta in the semi-arid Botswana. Our investigation showed that the temporal variability of solute concentrations in the Delta is primarily controlled by the temporally changing hydrology (pulse flood and rains) and that these hydrological perturbations complement evapotranspiration during solute cycling. Solutes in the Delta are cycled between the riverine solute pool and the islands, floodplains and wetland pools. Enhanced solute transfer to the river occurs during hydrologic perturbations when hydrologic connectivity is established between the river and solute stores in floodplains, islands and wetlands.

The results of this study also showed that 97% of the dissolved solutes export from the Delta occur during the rainy season and during the annual pulse flooding. The enhanced solute outflux from the Delta during hydrologic perturbations indicate the significance of hydrologic events in "flushing" out solutes from the Delta as a mechanism for maintaining the Delta's pristine condition. The periodic interception of river solutes by stores beyond the river act as 'transient solute storage' and gives us insights into the existence of hydro-geochemical "hotspots" and "hot moments" (McClain et al., 2003) in the Okavango Delta. Floodplains, salt islands and isolated wetland pools that accumulated solutes are "hotspots" compared to their surroundings. The periods when solutes are transferred from the solutes stores to the river characterized by anomalously high solute concentrations in the river indicate "hot moments" of dissolved solute flux and export. The hotspots and hot moments in the Okavango Delta have implications for the Delta's ecological and water quality status.

Due to the highly dynamic annual flooding regime in the Okavango Delta (Wolski et al., 2008; Wolski and Murray-Hudson, 2008; Murray-Hudson et al., 2014), the inter-annual variability in solute concentrations and solute load in the Okavango Delta needs to be constrained. We recognize that the river's chemical response will vary depending on flow magnitude, and that our study may not capture "the typical" annual hydrochemical response or cover the range in the inter-annual changes in river solute chemistry. Future work designed and conducted to investigate long term annual cycles will capture the extent to which the inter-annual variability persists over the longer term. Additionally, water samples collected at a frequency higher than in this study may provide greater constraints on the Delta's hydrochemical processes (Oromeng et al., 2020).

7. Figures

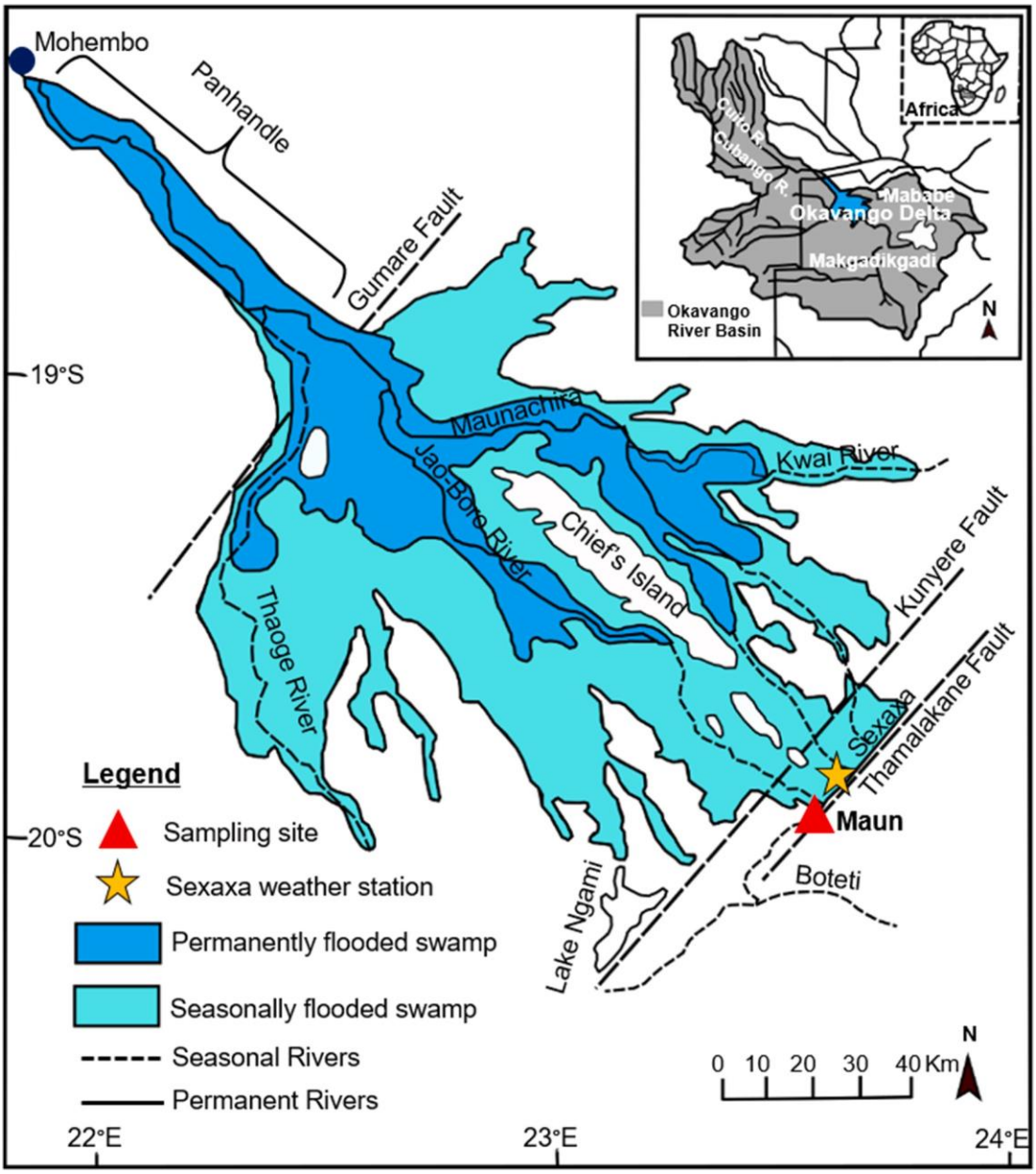

Figure 1: Map of the Okavango Delta, showing the Panhandle, the Delta region, seasonal and permanent rivers and select islands (Modified from Ellery et al., 2003). The river and rainwater sampling locations used in this study are shown as a filled red triangle and an orange star, respectively. The insert shows the location of the Okavango Delta in Africa and the Okavango River catchment (Modified from Kgathi et al., 2006).

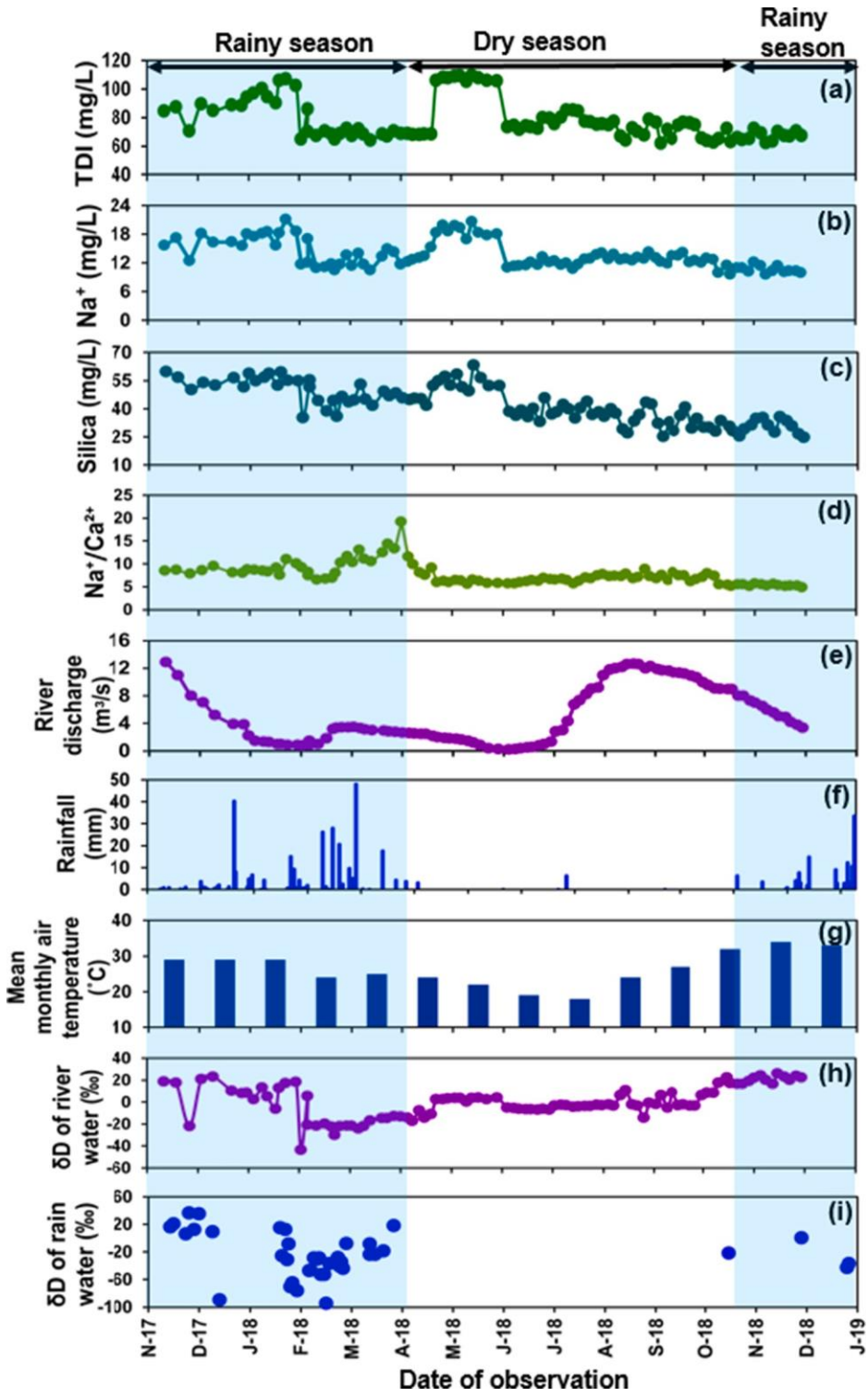

Figure 2: Temporal plots of (a) total dissolved ions (TDI), (b) Na^+, (c) silica, (d) Na^+/Ca^{2+} in river samples, (e) river discharge, (f) daily rainfall, (g) mean monthly air temperature, (h) deuterium

isotope (δD) in river samples and (i) δD in rain samples measured at the distal portion of the Okavango Delta in Maun. The blue shade represents the rainy season and the unshaded portion is the dry season.

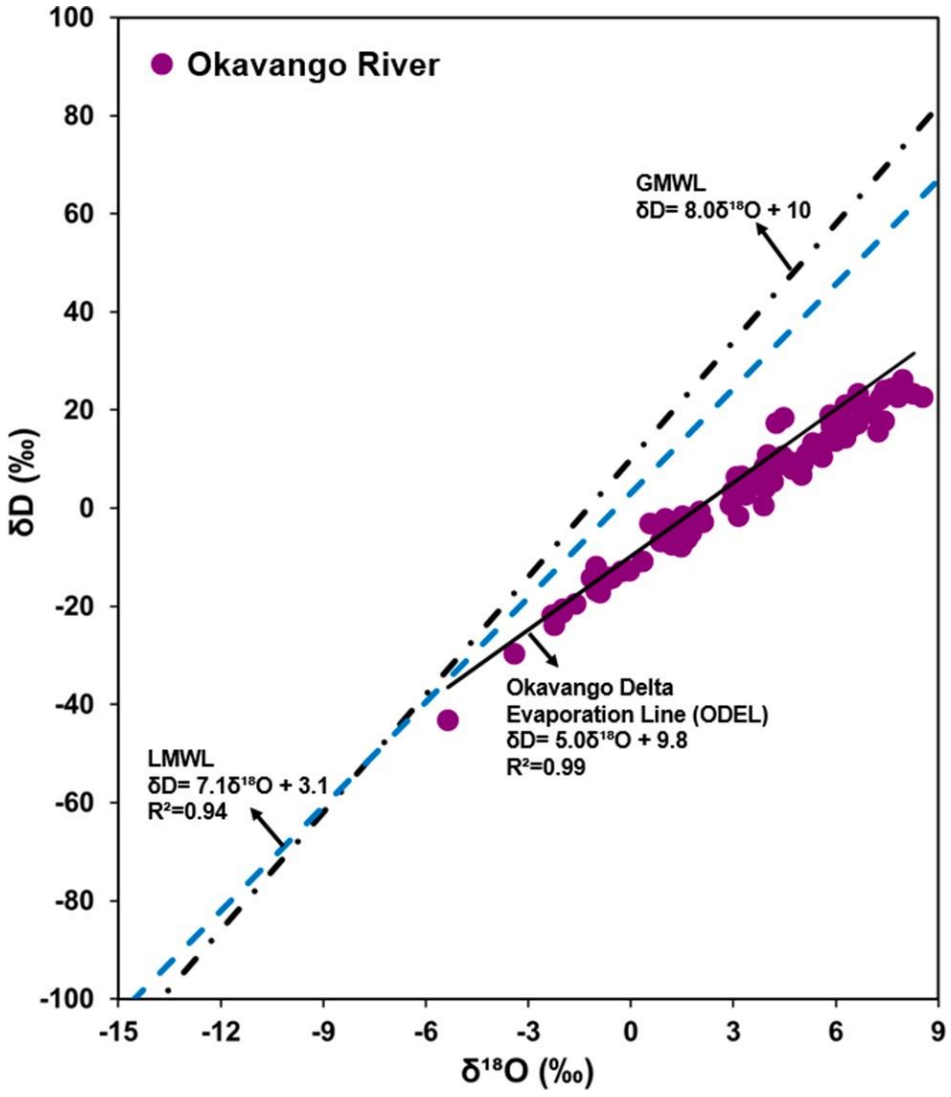

Figure 3: Plot of the stable oxygen isotopic composition ($\delta^{18}O$) vs. the stable hydrogen isotope (δD) for the Okavango River samples measured at the Delta outlet in Maun. The global meteoric water line (GMWL; Craig, 1961), local meteoric water line from Maun rain (LMWL) from Akondi et al. (2019) and the Okavango Delta evaporation line (ODEL) of Atekwana et al. (2016) are included.

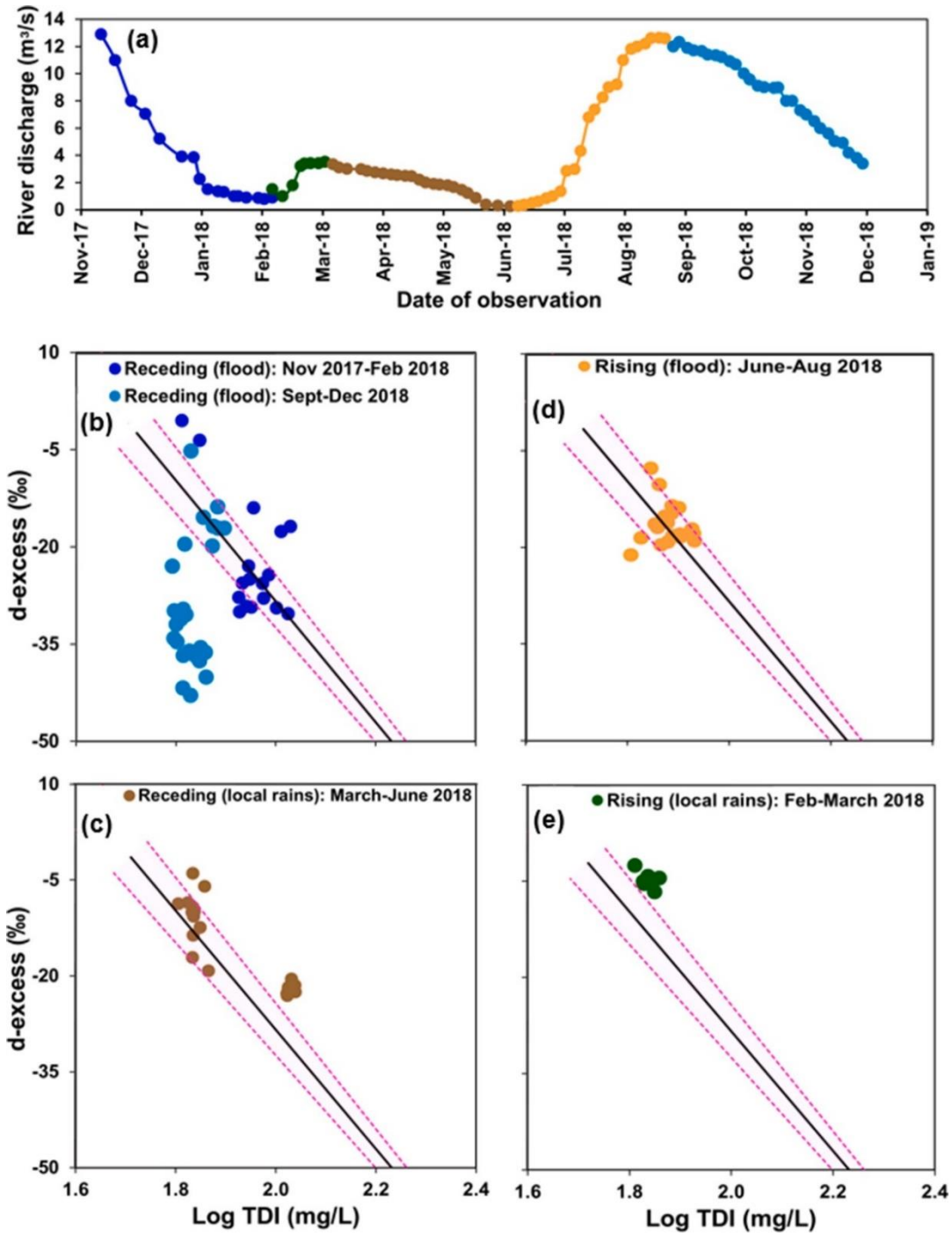

Figure 4: Temporal plot of (a) river discharge and cross plots of deuterium excess (d-excess) vs. log total dissolved ions (TDI) in the Okavango River during (b) flood recession (November 2017 to February 2018 and September to December 2018), (c) receding limb of the rain hydrograph between March and June 2018, (d) flood expansion between June and August 2018 and (e) rising

limb of the rain hydrograph between February and March 2018. The regression line in plots b-e depicted by the solid (black) line is for evaporated river water collected in Maun in 2010 adapted from Atekwana et al. (2016). The dashed lines show the upper and lower bounds of the 95% confidence interval for the regression.

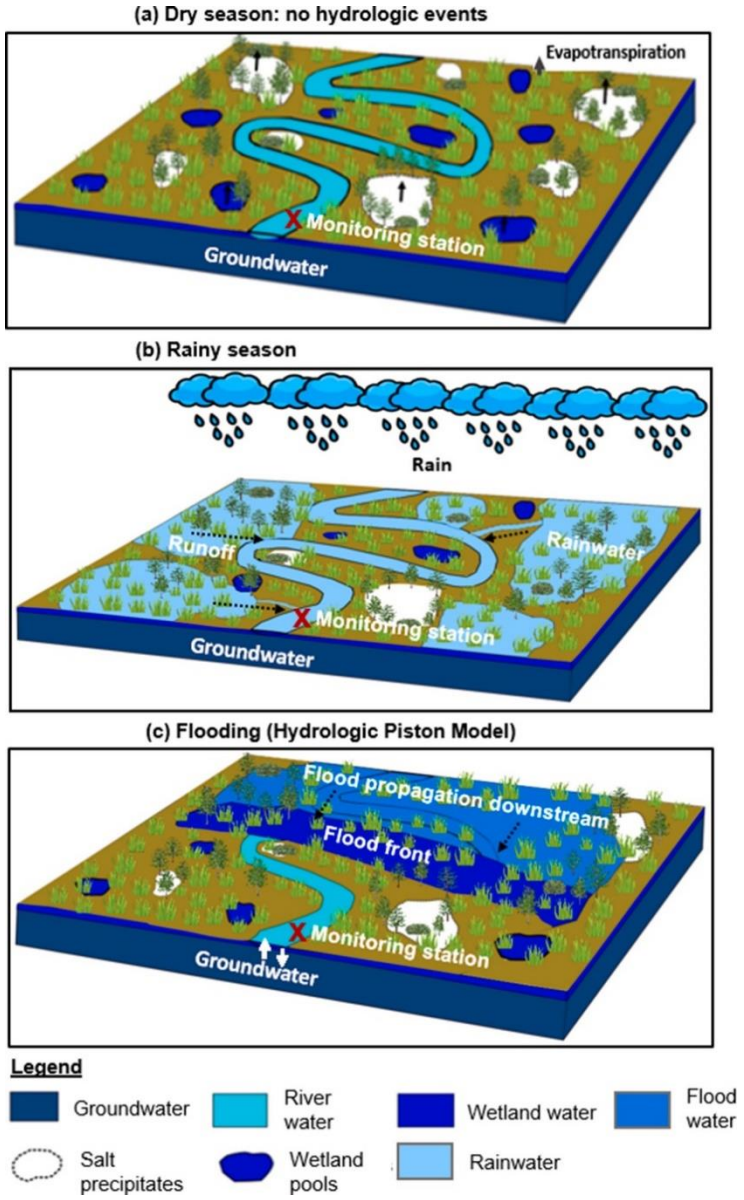

Figure 5: Conceptual model showing (a) the accumulation of solutes in solute stores on the river floodplains, islands and wetlands induced by evapotranspiration, (b) dissolution of salt precipitates on the surfaces of floodplains and islands and their transfer to the river by rains and (c) dissolution

of salt precipitates on the floodplains, and islands and their transfer to the river along with evaporated wetland water pushed by the flood pulse front.

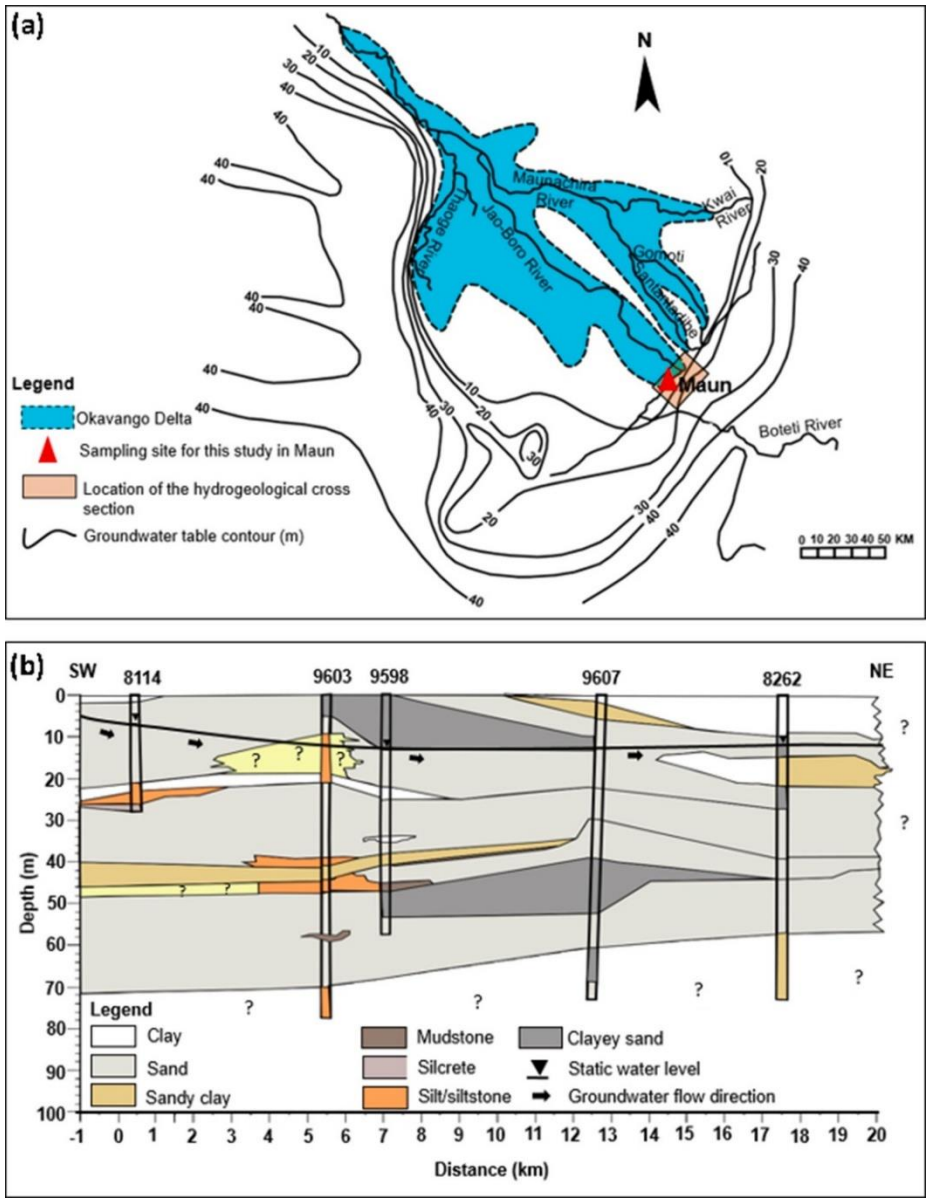

Figure 6: (a) Map of the Okavango Delta showing depth to the groundwater table adapted from McCarthy et al. (1997) and (b) hydrogeological cross section con- structed from 5 wells in the Maun area adapted from Mangisi (2004). The location of the hydrogeologic section is shown in (a).

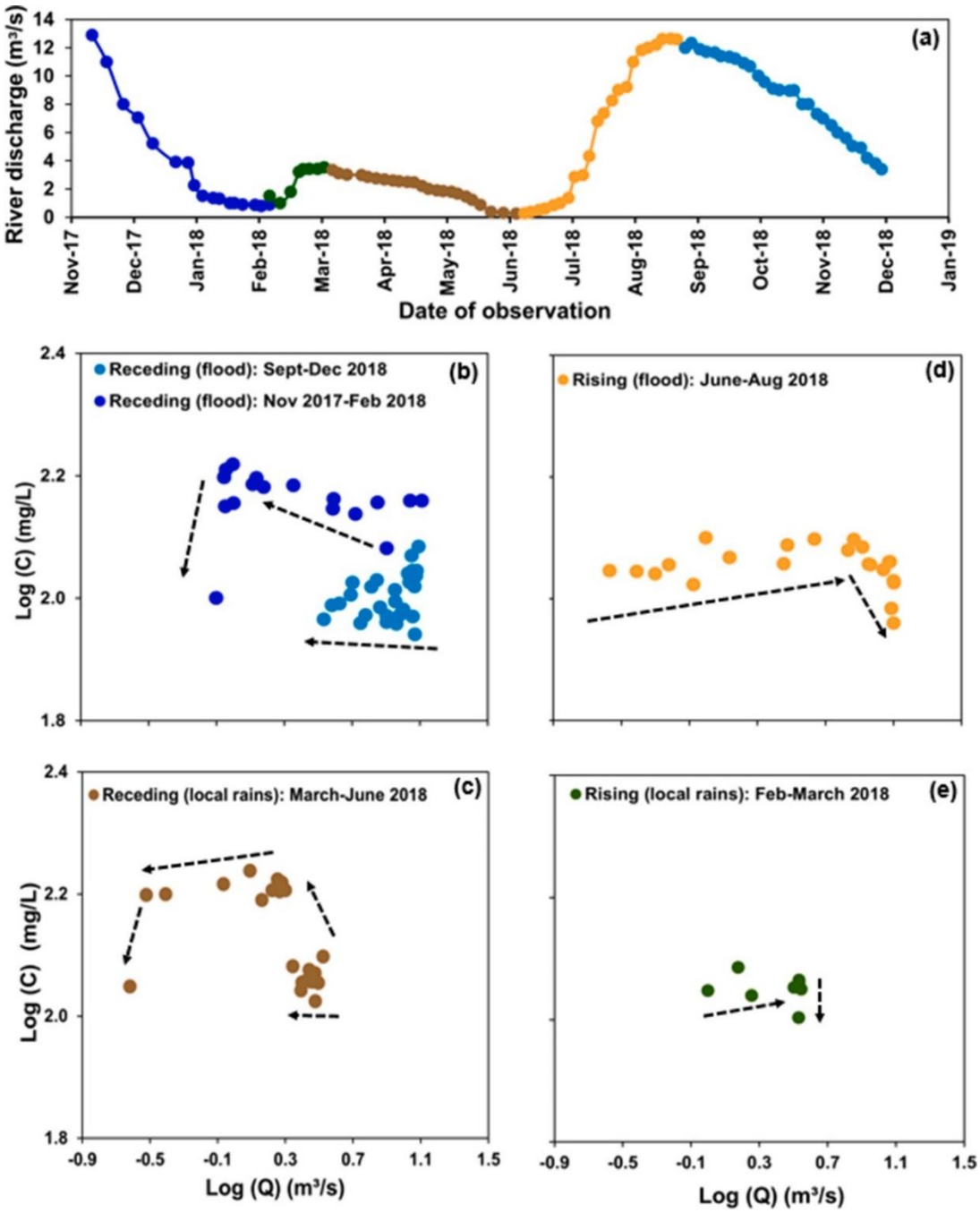

Figure 7: Temporal plot of (a) river discharge and cross plots of Log concentration (C) vs. Log discharge (Q) in the Okavango River during (b) flood recession (November 2017 to February 2018 and September to December 2018), (c) receding limb of the rain hydrograph between March and June 2018, (d) flood expansion between June and Aug 2018, and (e) rising limb of the rain

hydrograph between February and March 2018. The arrows show the direction of change in concentrations relative to discharge.

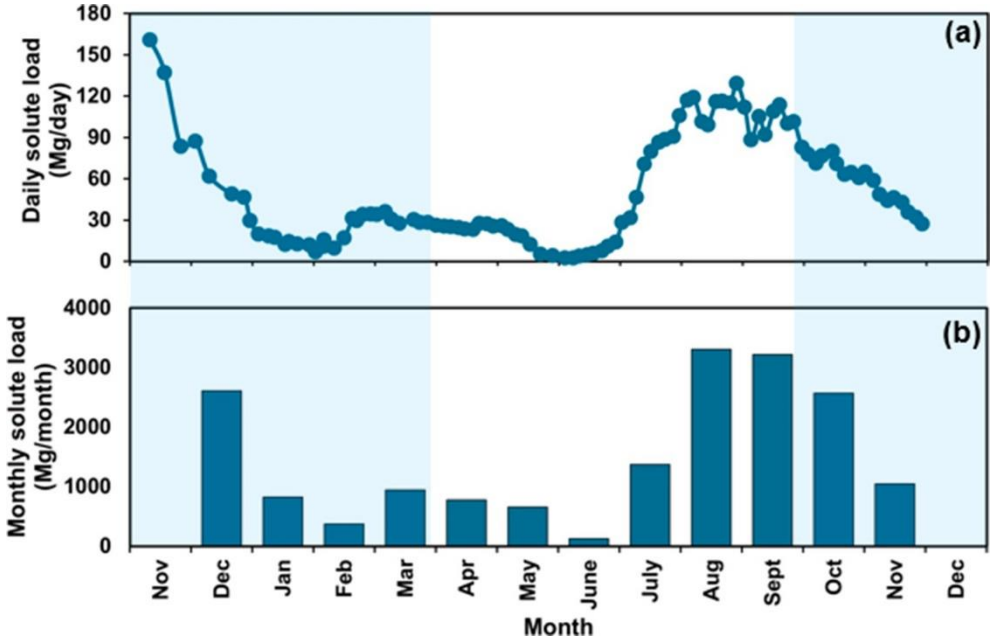

Figure 8: Temporal variations of (a) the daily solute load and (b) the monthly solute load measured in the Okavango River at the distal portion of the Okavango Delta in Maun. The blue shade represents the rainy season, and the unshaded portion is the dry season.

8. Tables

Table 1: Descriptive statistics for measured parameters. Min=minimum; Max=maximum; SD=Standard deviation; TDI=total dissolved ions; TDS=total dissolved solids

Parameter	Mean	Min.	Max.	SD	No. of samples (n)
TDI (mg/L)	78.1	62.1	109.6	14.0	98
Silica (mg/L)	42.3	24.8	63.4	10.1	98
TDS (TDI + Silica) (mg/L)	120.3	87.3	173.0	22.5	98
Na^+ (mg/L)	13.6	9.6	21.1	2.9	98
K^+ (mg/L)	8.1	3.7	13.6	2.8	98
Mg^{2+} (mg/L)	3.1	1.5	4.3	0.6	98
Ca^{2+} (mg/L)	1.6	0.5	2.8	0.5	98
Mean monthly air temperature (°C)	26.4	18	34	4.9	14 months
River discharge (m^3/s)	5.2	0.2	12.9	4.1	98
δD of river water (‰)	0.3	-43	26	14	98
$\delta^{18}O$ of river water (‰)	2.5	-5.3	8.3	3.0	98
Rainfall (mm)	5.6	0.1	48	9.4	14 months
δD of rain (‰)	-24	-94	37	32	51
$\delta^{18}O$ of rain (‰)	-3.5	-13.6	5.9	4.5	51
Daily solute load (Mg/d)	50.7	2.3	160.8	38.6	98
Monthly solute load (Mg/mo)	1528.7	128.7	3304.6	1117.1	12 months
					Total: 17,838 Mg/y

Table 2: Temporal δD and $\delta^{18}O$ composition of river water, total dissolved ions (TDI), silica, Na^+, K^+, Mg^{2+}, Ca^{2+} and daily solute load measured in the Okavango River in Maun, Botswana.

Date of observation	δD (‰)	$\delta^{18}O$ (‰)	TDI (mg/L)	Silica (mg/L)	Na^+ (mg/L)	K^+ (mg/L)	Mg^{2+} (mg/L)	Ca^{2+} (mg/L)	Daily solute load (Mg/d)
11/21/2017	18.9	5.84	84.40	59.91	15.61	5.03	3.02	1.60	160.84
11/28/2017	17.6	5.86	87.60	56.79	17.19	6.15	3.38	1.73	137.23
12/6/2017	-21.9	-2.29	70.45	50.28	12.41	8.00	2.29	1.39	83.45
12/13/2017	20.9	6.28	89.50	53.93	18.15	8.13	3.58	1.84	87.36
12/20/2017	23.2	6.65	84.80	52.52	16.29	8.03	3.21	1.50	61.93
12/31/2017	10.5	4.44	88.85	56.47	16.36	8.03	3.15	1.76	48.97
1/6/2018	8.3	3.91	88.39	51.71	15.58	8.75	3.37	1.70	46.60
1/9/2018	8.6	4.28	94.15	58.78	18.00	9.35	3.28	1.79	29.73
1/13/2018	2.7	3.38	97.00	54.91	17.46	10.47	3.20	1.76	19.69
1/18/2018	13.2	5.33	100.40	56.80	18.12	10.56	3.45	1.86	18.47
1/21/2018	5.4	4.17	94.75	58.78	18.50	10.50	3.44	1.95	17.24
1/26/2018	-6.2	0.98	90.40	52.57	15.63	9.23	2.68	1.49	12.35
1/28/2018	13.0	5.41	106.05	59.48	18.19	10.90	3.68	2.09	14.16
2/1/2018	17.3	4.27	107.20	55.07	21.09	13.43	3.05	1.67	12.62
2/7/2018	18.3	4.49	102.60	55.00	18.58	12.59	2.96	1.61	11.98
2/10/2018	-43.3	-5.35	64.90	35.23	11.65	9.43	1.89	1.09	6.83
2/14/2018	5.6	3.91	93.55	55.49	12.04	7.90	2.25	1.41	10.87
2/14/2018	-20.6	-1.97	70.10	51.71	17.05	10.00	3.04	1.80	15.79
2/19/2018	-21.4	-2.05	67.25	44.33	10.93	8.11	2.33	1.45	9.64
2/24/2018	-19.6	-1.62	70.70	38.84	11.13	8.74	2.12	1.44	17.04
2/28/2018	-22.1	-2.23	68.60	44.34	11.74	8.36	2.37	1.48	31.23
3/2/2018	-29.7	-3.40	64.70	36.11	10.48	8.52	2.10	1.14	29.61
3/5/2018	-21.8	-2.11	68.65	46.59	11.67	9.19	2.62	0.99	33.95
3/9/2018	-21.6	-2.14	72.25	43.77	13.59	9.65	2.71	1.02	34.29
3/12/2018	-21.3	-1.99	67.45	44.72	11.39	8.37	2.56	0.96	34.12
3/16/2018	-23.9	-2.24	72.15	53.11	14.02	8.66	2.50	0.94	36.04
3/19/2018	-22.0	-2.26	68.35	45.09	11.67	7.47	2.46	0.91	30.58

3/23/2018	-16.9	-1.01	64.00	41.79	10.45	10.10	2.51	0.87	27.42
3/30/2018	-14.6	-0.66	68.40	49.24	13.34	8.26	2.62	0.93	30.29
4/2/2018	-14.7	-0.76	66.85	47.04	14.92	7.58	2.53	0.90	28.14
4/6/2018	-12.8	-0.04	70.70	48.41	14.25	8.51	2.70	0.93	28.30
4/10/2018	-12.9	-0.27	68.65	45.73	11.67	8.32	1.45	0.53	26.29
4/14/2018	-14.3	-0.54	68.90	44.91	12.26	7.34	1.92	0.92	25.47
4/17/2018	-17.3	-0.90	68.15	45.50	12.68	7.59	1.99	1.12	25.04
4/21/2018	-7.5	1.21	68.25	45.32	13.07	6.16	2.40	1.40	24.53
4/24/2018	-14.1	-0.60	68.35	41.91	13.40	8.19	2.67	1.55	23.43
4/28/2018	-10.9	0.35	68.45	52.31	15.30	12.17	2.54	1.45	23.06
5/1/2018	2.6	3.04	106.10	54.83	18.32	13.08	4.11	2.66	27.67
5/5/2018	2.8	3.04	108.30	57.23	19.88	13.62	4.26	2.75	27.17
5/8/2018	3.3	2.98	107.70	52.57	18.56	13.45	4.22	2.70	25.48
5/12/2018	3.7	3.16	108.95	58.48	19.75	13.38	4.12	2.67	25.89
5/15/2018	3.6	3.14	109.30	51.59	19.30	13.09	4.05	2.66	23.08
5/19/2018	0.6	2.93	105.50	49.43	16.91	13.05	4.09	2.62	19.41
5/22/2018	3.7	3.28	109.60	63.39	20.62	13.47	4.18	2.75	18.38
5/26/2018	4.0	3.22	108.00	56.65	18.36	12.83	3.98	2.57	12.23
5/31/2018	2.6	3.10	106.00	52.38	17.76	13.26	4.17	2.67	5.34
6/6/2018	4.1	3.41	105.55	52.41	18.05	13.54	4.19	2.72	4.09
6/12/2018	-5.0	1.80	73.45	38.49	11.04	8.32	3.07	1.68	2.32
6/16/2018	-5.5	1.20	74.70	36.46	11.33	8.39	3.10	1.73	2.59
6/19/2018	-6.3	1.30	71.55	39.32	11.35	8.02	3.04	1.67	3.74
6/23/2018	-6.5	1.10	74.10	35.69	11.48	8.15	3.14	1.63	4.74
6/26/2018	-6.3	1.70	73.40	40.27	12.09	8.24	3.19	1.63	5.89
6/30/2018	-7.0	1.20	72.35	33.17	11.62	8.51	3.17	1.62	7.66
7/3/2018	-5.9	1.50	80.05	45.87	13.21	8.70	3.24	1.66	10.77
7/7/2018	-6.9	0.90	79.60	37.21	12.15	8.19	3.13	1.61	13.83
7/10/2018	-3.1	2.00	75.70	38.42	12.37	8.19	3.16	1.65	28.10
7/14/2018	-2.5	2.00	80.15	42.39	11.55	7.61	2.98	1.50	31.66
7/17/2018	-2.7	2.00	85.40	39.88	11.99	8.31	3.14	1.61	46.65
7/21/2018	-4.1	1.70	85.10	35.05	10.74	8.23	3.14	1.63	70.48
7/24/2018	-3.9	1.70	84.55	40.54	11.63	8.31	3.15	1.62	79.66

7/28/2018	-3.4	1.90	77.45	44.04	12.74	8.22	3.11	1.58	86.60
7/31/2018	-3.5	1.40	77.05	36.87	12.89	8.80	3.20	1.64	88.58
8/4/2018	-2.4	1.70	75.40	38.34	13.70	8.23	3.11	1.60	90.60
8/7/2018	-2.7	1.70	75.60	35.93	14.05	8.19	3.18	1.59	106.00
8/11/2018	-2.0	1.60	75.00	39.86	12.82	7.88	3.09	1.53	117.11
8/14/2018	-3.2	1.30	77.25	37.72	13.84	8.68	3.27	1.63	119.20
8/18/2018	6.3	3.10	67.05	29.30	12.65	5.52	3.08	1.51	101.56
8/21/2018	10.8	4.00	64.05	27.12	12.88	3.99	2.96	1.43	99.26
8/25/2018	-2.2	1.00	72.85	33.36	12.51	8.30	3.20	1.61	115.90
8/28/2018	-3.2	0.60	70.15	36.83	13.14	8.42	3.19	1.61	116.37
9/1/2018	-14.2	-1.10	67.60	43.44	12.86	7.07	2.32	1.27	115.13
9/4/2018	-0.8	2.00	78.90	42.54	14.26	9.16	3.42	1.70	129.27
9/8/2018	-1.7	1.50	76.55	32.31	13.01	8.75	3.20	1.65	111.93
9/11/2018	6.3	3.70	62.05	25.28	12.23	3.90	2.86	1.40	88.28
9/15/2018	-5.1	1.30	71.65	33.01	11.84	8.10	3.11	1.60	105.35
9/18/2018	9.1	4.80	65.25	28.22	13.50	4.03	2.93	1.43	92.06
9/22/2018	-2.9	2.10	74.55	36.44	13.55	8.12	3.12	1.58	108.86
9/25/2018	-2.0	1.90	76.65	40.80	14.15	8.76	3.22	1.66	113.86
9/29/2018	-3.1	1.30	76.45	29.75	12.17	8.88	3.29	1.72	100.01
10/2/2018	-3.1	1.70	74.95	34.87	12.50	8.77	3.29	1.63	101.34
10/6/2018	6.4	3.20	65.75	30.12	12.04	5.38	3.04	1.48	82.83
10/9/2018	8.6	4.90	63.70	30.29	12.99	3.91	2.89	1.43	77.79
10/13/2018	8.6	4.80	62.65	28.19	12.66	4.14	3.04	1.50	71.43
10/16/2018	17.7	7.43	65.16	33.68	9.90	3.83	3.11	1.57	76.86
10/21/2018	22.6	7.83	72.46	30.73	11.49	4.59	3.77	1.84	79.80
10/23/2018	17.4	6.17	63.16	28.29	9.58	3.87	3.23	1.63	70.87
10/27/2018	16.6	5.88	66.08	25.41	10.96	3.93	3.36	1.74	63.24
10/30/2018	16.5	5.94	64.55	29.15	10.89	4.05	3.38	1.73	64.68
11/3/2018	19.3	7.00	65.26	31.36	10.16	4.02	3.29	1.71	60.94
11/6/2018	22.2	7.31	72.28	34.80	12.13	4.51	3.49	1.85	64.76
11/10/2018	24.4	7.65	69.09	35.39	11.42	4.53	3.45	1.81	58.68
11/13/2018	20.1	6.78	62.50	31.39	9.56	3.85	3.06	1.60	48.68
11/17/2018	16.6	6.41	63.41	27.70	10.26	3.73	3.06	1.59	44.08

11/20/2018	26.2	7.97	70.35	35.81	11.41	4.62	3.49	1.86	46.14
11/24/2018	23.2	8.27	67.53	33.79	10.12	4.09	3.21	1.71	42.89
11/27/2018	20.4	7.05	67.09	30.94	10.25	4.07	3.23	1.71	35.57
12/1/2018	23.9	7.43	70.76	26.68	10.29	4.18	3.22	1.72	31.99
12/4/2018	22.6	7.34	67.54	24.84	9.87	4.25	3.30	1.77	27.14

Table 3: Temporal δD and $\delta^{18}O$ composition of rain collected in Maun, Botswana

Date	δD (‰)	$\delta^{18}O$ (‰)	Date	δD (‰)	$\delta^{18}O$ (‰)
11/24/17	16.5	2.14	3/5/18	-34.7	-5.33
11/26/17	20.8	3.29	3/6/18	-43.7	-6.85
12/3/17	6.2	0.99	3/8/18	-7.5	-2.23
12/5/17	36.7	5.71	3/22/18	-23.5	-4.52
12/8/17	12.5	2.36	3/22/18	-8.7	-2.31
12/11/17	35.1	5.89	3/25/18	-23.6	-3.68
12/19/17	9.6	1.21	3/30/18	-18.8	-3.32
12/23/17	-89.7	-12.14	4/5/18	18.1	0.80
1/28/18	14.8	1.88	1/29/18	-25.2	-4.03
1/31/18	12.5	0.73	10/21/18	-21.5	-2.99
2/1/18	-31.2	-5.23	12/3/18	0.7	0.86
2/2/18	-8.4	-1.70	12/30/18	-42.7	-4.07
2/3/18	-70.7	-10.21	12/31/18	-36.8	-2.12
2/4/18	-64.8	-9.59	1/2/19	-16.8	-1.33
2/7/18	-76.1	-10.30	1/5/19	31.2	3.70
2/14/18	-47.2	-6.17	1/7/19	-17.3	-1.29
2/15/18	-46.5	-7.34	1/12/19	-19.3	-1.93
2/17/18	-28.7	-3.74	1/13/19	-22.1	-3.26
2/19/18	-30.7	-5.29	1/14/19	-21.6	-3.24
2/20/18	-28.4	-5.27	1/15/19	-22.4	-0.72
2/21/18	-52.8	-8.84	1/16/19	-26.8	-3.61
2/23/18	-52.6	-8.20	1/17/19	-23.8	-4.55
2/24/18	-94.5	-13.63	1/18/19	-11.6	-2.04
2/26/18	-36.8	-6.14	2/11/19	-82.5	-10.01
3/3/18	-27.9	-3.23	2/12/19	-83.6	-10.32
3/4/18	-41.0	-6.76			

Table 4: Temporal river discharge and water level measured in the Okavango River in Maun.

Date	River discharge (m^3/s)	Water level (m)
6/16/2016	0.83	0.88
6/23/2016	1.57	1.02
6/27/2016	3.62	1.23
6/30/2016	4.22	1.32
7/4/2016	5.66	1.41
7/5/2016	5.66	1.41
8/8/2016	7.31	1.78
8/9/2016	9.79	1.92
8/18/2016	9.84	1.95
8/29/2016	7.40	1.74
9/15/2016	5.92	1.72
9/26/2016	4.44	1.69
9/27/2016	4.44	1.69
10/29/2016	1.73	1.44
11/24/2016	0.84	1.20
12/9/2016	0.34	1.02
12/29/2016	0.27	0.98

9. Citations:

Akoko, E., Atekwana, E.A., Cruse, A.M., Molwalefhe, L., Masamba, W.R., 2013. River- wetland interaction and carbon cycling in a semi-arid riverine system: the Okavango Delta, Botswana. Biogeochemistry 114 (1–3), 359–380.

Akondi, R.N., Atekwana, E.A., Molwalefhe, L., 2019. Origin and chemical and isotopic evolution of dissolved inorganic carbon (DIC) in groundwater of the Okavango Delta, Botswana. Hydrol. Sci. J. 64 (1), 105–120.

Ala-Aho, P., Soulsby, C., Pokrovsky, O.S., Kirpotin, S.N., Karlsson, J., Serikova, S., Vorobyev, S.N., Manasypov, R.M., Loiko, S., Tetzlaff, D., 2018. Using stable isotopes to assess surface water source dynamics and hydrological connectivity in a high- latitude wetland and permafrost influenced landscape. J. Hydrol. 556, 279–293.

Atekwana, E.A., Molwalefhe, L., Kgaodi, O., Cruse, A.M., 2016. Effect of evapotranspiration on dissolved inorganic carbon and stable carbon isotopic evolution in rivers in semi-arid climates: the Okavango Delta in North West Botswana. J. Hydrol. Reg. Stud. 7, 1–13.

Aulenbach, B.T., Burns, D.A., Shanley, J.B., Yanai, R.D., Bae, K., Wild, A.D., Yang, Y., Yi, D., 2016. Approaches to stream solute load estimation for solutes with varying dynamics from five diverse small watersheds. Ecosphere 7 (6), e01298.

Baskaran, S., Ransley, T., Brodie, R.S., Baker, P., 2009. Investigating groundwater–river interactions using environmental tracers. Aust. J. Earth Sci. 56 (1), 13–19.

Batlle-Aguilar, J., Harrington, G.A., Leblanc, M., Welch, C., Cook, P.G., 2014. Chemistry of groundwater discharge inferred from longitudinal river sampling. Water Resour. Res. 50 (2), 1550–1568.

Bauer, P., Supper, R., Zimmermann, S., Kinzelbach, W., 2006. Geoelectrical imaging of groundwater salinization in the Okavango Delta, Botswana. J. Appl. Geophys. 60 (2), 126–141.

Bauer, P., 2004. Flooding and salt transport in the Okavango Delta, Botswana: key issues for sustainable wetland management (Doctoral dissertation, ETH Zurich).

Bauer-Gottwein, P., Langer, T., Prommer, H., Wolski, P., Kinzelbach, W., 2007. Okavango Delta Islands: interaction between density-driven flow and geochemical reactions under evapo-concentration. J. Hydrol. 335 (3–4), 389–405.

Bereslawski, E., 1997. Geohydrology, Geology, and Soils of the Cubango River Basin (Angolan Sector). OKACOM Okavango River Basin Preparatory Assessment Study, Specialist's Report.

Boyer, E.W., Hornberger, G.M., Bencala, K.E., McKnight, D.M., 1997. Response characteristics of DOC flushing in an alpine catchment. Hydrol. Process. 11 (12), 1635–1647.

Bufford, K.M., Atekwana, E.A., Abdelsalam, M.G., Shemang, E., Atekwana, E.A., Mickus, K., Moidaki, M., Modisi, M.P., Molwalefhe, L., 2012. Geometry and faults tectonic activity of the Okavango Rift Zone, Botswana: Evidence from magnetotelluric and electrical resistivity tomography imaging. J. Afr. Earth Sc. 65, 61–71.

Catuneanu, O., Wopfner, H., Eriksson, P.G., Cairncross, B., Rubidge, B.S., Smith, R.M.H., HancoX, P.J., 2005. The Karoo basins of south-central Africa. J. Afr. Earth Sci. 43 (1–3), 211–253.

Chorover, J., Derry, L.A., McDowell, W.H., 2017. Concentration-discharge relations in the critical zone: implications for resolving critical zone structure, function, and evolution. Water Resour. Res. 53 (11), 8654–8659.

Clark, I.D., Fritz, P., 1997. Environmental isotopes in hydrogeology. CRC Press.

Covino, T., 2017. Hydrologic connectivity as a framework for understanding biogeochemical fluX through watersheds and along fluvial networks. Geomorphology 277, 133–144.

Craig, H., 1961. Isotopic variations in meteoric waters. Science 133 (3465), 1702–1703.

Cronberg, G., Gieske, A., Martins, E., Nengu, J.P. and Stenstro¨m, I.M., 1996. Major ion chemistry, plankton, and bacterial assemblages of the Jao/Boro River, Okavango Delta, Botswana: the swamps and floodplains. Archiv für Hydrobiologie. Supplement band. Monographische Beitra¨ge, 107(3), pp.335-407.

Dalzell, B.J., Filley, T.R., Harbor, J.M., 2007. The role of hydrology in annual organic carbon loads and terrestrial organic matter export from a midwestern agricultural watershed. Geochim. Cosmochim. Acta 71 (6), 1448–1462.

Dansgaard, W., 1964. Stable isotopes in precipitation. Tellus 16 (4), 436–468.

Darracq, A., Destouni, G., Persson, K., Prieto, C., Jarsjo¨, J., 2010. Quantification of advective solute travel times and mass transport through hydrological catchments. Environ. Fluid Mech. 10 (1–2), 103–120.

Diamond, J.S., Cohen, M.J., 2018. Complex patterns of catchment solute–discharge relationships for coastal plain rivers. Hydrol. Process. 32 (3), 388–401.

Dincer, T., Hutton, L.G. and Kupee, B.B.J., 1979. Study, using stable isotopes, of flow distribution, surface-groundwater relations and evapotranspiration in the Okavango Swamp, Botswana. In Isotope hydrology 1978.

Drever, J.I., 1971. Chemical weathering in a subtropical igneous terrain, Rio Ameca, Mexico. J. Sedimen. Res. 41 (4), 951–961.

Duvert, C., Hutley, L.B., Birkel, C., Rudge, M., Munksgaard, N.C., Wynn, J.G., Setterfield, S.A., Cendo´n, D.I., Bird, M.I., 2020. Seasonal shift from biogenic to geogenic fluvial carbon caused by changing water sources in the wet-dry tropics. J. Geophys. Res. Biogeosci. 125 (2).

Ehhalt, D., Knott, K., Nagel, J.F., Vogel, J.C., 1963. Deuterium and oXygen 18 in rain water. J. Geophys. Res. 68 (13), 3775–3780.

Ellery, W.N., McCarthy, T.S., Smith, N.D., 2003. Vegetation, hydrology, and sedimentation patterns on the major distributary system of the Okavango Fan, Botswana. Wetlands 23 (2), 357.

Foster, S.S.D., Bath, A.H., Farr, J.L., Lewis, W.J., 1982. The likelihood of active groundwater recharge in the Botswana Kalahari. J. Hydrol. 55 (1–4), 113–136.

Fovet, O., Humbert, G., Dupas, R., Gascuel-OdouX, C., Gruau, G., Jaffr´ezic, A., Thelusma, G., FaucheuX, M., Gilliet, N., Hamon, Y., Grimaldi, C., 2018. Seasonal variability of stream water quality response to storm events captured using high- frequency and multi-parameter data. J. Hydrol. 559, 282–293.

Frings, P.J., De La Rocha, C., Struyf, E., Van Pelt, D., Schoelynck, J., Hudson, M.M., Gondwe, M.J., Wolski, P., Mosimane, K., Gray, W., Schaller, J., 2014. Tracing silicon cycling in the

Okavango Delta, a sub-tropical flood-pulse wetland using silicon isotopes. Geochim. Cosmochim. Acta 142, 132–148.

Fro¨hlich, K., Gibson, J.J. and Aggarwal, P.K., 2002. Deuterium excess in precipitation and its climatological significance (No. IAEA-CSP–13/P).

Geeraert, N., Omengo, F.O., Borges, A.V., Govers, G., Bouillon, S., 2017. Shifts in the carbon dynamics in a tropical lowland river system (Tana River, Kenya) during flooded and non-flooded conditions. Biogeochemistry 132 (1–2), 141–163.

Gieske, A., 1996. Modelling of surface outflow from the Okavango Delta. Botswana Notes Rec. 28 (1), 165–192.

Glover, B.J., Johnson, P., 1974. Variations in the natural chemical concentration of river water during flood flows, and the lag effect. J. Hydrol. 22 (3–4), 303–316.

Godsey, S.E., Kirchner, J.W., Clow, D.W., 2009. Concentration–discharge relationships reflect chemostatic characteristics of US catchments. Hydrol. Process. Int. J. 23 (13), 1844–1864.

Gondwe, M.J., Masamba, W.R.L., 2016. Variation of physico-chemical parameters along a river transect through the Okavango Delta, Botswana. Afr. J. Aquat. Sci. 41 (2), 205–215.

Gondwe, M.J., Masamba, W.R.L., Gondwe, M.J., Murray-Hudson, M., 2017. Water balance and variations of nutrients and major solutes along a river transect through the Okavango Delta, Botswana. Botswana Notes Rec. 49, 26–43.

Good, S.P., Mallia, D.V., Lin, J.C., Bowen, G.J., 2014. Stable isotope analysis of precipitation samples obtained via crowdsourcing reveals the spatiotemporal evolution of Superstorm Sandy. PLoS ONE 9 (3).

Gooseff, M.N., Bencala, K.E. and Wondzell, S.M., 2008. Solute transport along stream and river networks. River confluences, tributaries and the fluvial network, pp.395–417.

Govender, Y., Cuevas, E., Sternberg, L.D.S., Jury, M.R., 2013. Temporal variation in stable isotopic composition of rainfall and groundwater in a tropical dry forest in the northeastern Caribbean. Earth Interact 17 (27), 1–20.

Gumbricht, T., McCarthy, T.S., Merry, C.L., 2001. The topography of the Okavango Delta, Botswana, and its tectonic and sedimentological implications. S. Afr. J. Geol. 104 (3), 243–264.

Gumbricht, T., McCarthy, T.S., 2003. Spatial patterns of islands and salt crusts in the Okavango Delta, Botswana. S. Afr. Geograph. J. 85 (2), 164–169.

Gumbricht, T., McCarthy, J., McCarthy, T.S., 2004. Channels, wetlands and islands in the Okavango Delta, Botswana, and their relation to hydrological and sedimentological processes. Earth Surf. Process. Landforms J. Br. Geomorphol. Res. Group 29 (1), 15–29.

Hem, J.D., 1985. Study and interpretation of the chemical characteristics of natural water (Vol. 2254). Department of the Interior, US Geological Survey.

Herndon, E.M., Steinhoefel, G., Dere, A.L., Sullivan, P.L., 2018. Perennial flow through convergent hillslopes explains chemodynamic solute behavior in a shale headwater catchment. Chem. Geol. 493, 413–425.

Hodson, A., Heaton, T., Langford, H., Newsham, K., 2010. Chemical weathering and solute export by meltwater in a maritime Antarctic glacier basin. Biogeochemistry 98 (1–3), 9–27.

Hope, D., Billett, M.F., Cresser, M.S., 1994. A review of the export of carbon in river water: fluXes and processes. Environ. Pollut. 84 (3), 301–324.

Horgby, Å., BoiX Canadell, M., Ulseth, A.J., Vennemann, T.W., Battin, T.J., 2019. High-Resolution Spatial Sampling Identifies Groundwater as Driver of CO2 Dynamics in an Alpine Stream Network. J. Geophys. Res. Biogeosci. 124 (7), 1961–1976.

Huang, T., Pang, Z., 2012. The role of deuterium excess in determining the water salinisation mechanism: A case study of the arid Tarim River Basin, NW China. Appl. Geochem. 27 (12), 2382–2388.

Humphries, M.S., McCarthy, T.S., Cooper, G.R.J., Stewart, R.A., Stewart, R.D., 2014. The role of airborne dust in the growth of tree islands in the Okavango Delta, Botswana. Geomorphology 206, 307–317.

Huntsman-Mapila, P., Kampunzu, A.B., Vink, B., Ringrose, S., 2005. Cryptic indicators of provenance from the geochemistry of the Okavango Delta sediments, Botswana. Sedim. Geol. 174 (1–2), 123–148.

Imes, J.L., Wood, W.W., 2007. Solute and isotope constraint of groundwater recharge simulation in an arid environment, Abu Dhabi Emirate, United Arab Emirates. Hydrogeol. J. 15 (7), 1307–1315.

Jones, M.J., 2010. The groundwater hydrology of the Okavango basin. OKACOM Okavango River Basin Transboundary Diagnostical Analysis Technical Report.

Kalscheuer, T., Blake, S., Podgorski, J.E., Wagner, F., Green, A.G., Maurer, H., Jones, A. G., Muller, M., Ntibinyane, O., Tshoso, G., 2015. Joint inversions of three types of electromagnetic data explicitly constrained by seismic observations: results from the central Okavango Delta, Botswana. Geophys. J. Int. 202 (3), 1429–1452.

Kanduˇc, T., Szramek, K., Ogrinc, N., Walter, L.M., 2007. Origin and cycling of riverine inorganic carbon in the Sava River watershed (Slovenia) inferred from major solutes and stable carbon isotopes. Biogeochemistry 86 (2), 137–154.

Kgathi, D.L., Kniveton, D., Ringrose, S., Turton, A.R., Vanderpost, C.H.M., Lundqvist, J., Seely, M., 2006. The Okavango; a river supporting its people, environment and economic development. J. Hydrol. 331 (1–2), 3–17.

Kinabo, B.D., Atekwana, E.A., Hogan, J.P., Modisi, M.P., Wheaton, D.D., Kampunzu, A. B., 2007. Early structural development of the Okavango rift zone, NW Botswana. J. Afr. Earth Sc. 48 (2–3), 125–136.

Kinabo, B.D., Hogan, J.P., Atekwana, E.A., Abdelsalam, M.G., Modisi, M.P., 2008. Fault growth and propagation during incipient continental rifting: Insights from a combined aeromagnetic and Shuttle Radar Topography Mission digital elevation model investigation of the Okavango Rift Zone, northwest Botswana. Tectonics 27 (3).

Koeniger, P., Leibundgut, C., Stichler, W., 2009. Spatial and temporal characterisation of stable isotopes in river water as indicators of groundwater contribution and confirmation of modelling results; a study of the Weser River, Germany. Isot. Environ. Health Stud. 45 (4), 289–302.

Krishan, G., Prasad, G., Kumar, C.P., Patidar, N., Yadav, B.K., Kansal, M.L., Singh, S., Sharma, L.M., Bradley, A., Verma, S.K., 2020. Identifying the seasonal variability in source of groundwater salinization using deuterium excess-a case study from Mewat, Haryana, India. J. Hydrol. Reg. Stud. 31, 100724.

Leseane, K., Atekwana, E.A., Mickus, K.L., Abdelsalam, M.G., Shemang, E.M., Atekwana, E.A., 2015. Thermal perturbations beneath the incipient Okavango Rift Zone, northwest Botswana. J. Geophys. Res. Solid Earth 120 (2), 1210–1228.

Li, J., 2014. Terminal fluvial systems in a semi-arid endorheic basin. Salar de Uyuni (Bolivia).

Liu, J., Chen, B., Xu, Z.Y., Wei, Y., Su, Z.H., Yang, R., Ji, Y.X., Wang, X.D., Zhang, L.L., An, N., Yang, F., 2020. Tracing solute sources and carbon dynamics under various hydrological conditions in a karst river in southwestern China. Environ. Sci. Pollut. Res. 1–12.

Liu, F., Parmenter, R., Brooks, P.D., Conklin, M.H. and Bales, R.C., 2008. Seasonal and interannual variation of streamflow pathways and biogeochemical implications in semi-arid, forested catchments in Valles Caldera, New Mexico. Ecohydrology: Ecosystems, Land and Water Process Interactions, Ecohydrogeomorphology, 1(3), pp.239–252.

Mackay, A.W., Davidson, T., Wolski, P., Mazebedi, R., Masamba, W.R., Huntsman- Mapila, P., Todd, M., 2011. Spatial and seasonal variability in surface water chemistry in the Okavango Delta, Botswana: a multivariate approach. Wetlands 31 (5), 815.

Mangisi, N., 2004. Hydrogeological verification of magnetic resonance sounding Maun area, Botswana. Unpublished MS Thesis. International Institute for GeoInformation Science and Earth Observation Enschede, The Netherlands, 118.

Masamba, W.R., Muzila, A., 2005. Spatial and seasonal variation of major cation and selected trace metal ion concentrations in the Okavango-Maunachira-Khwai channels of the Okavango Delta. Botswana Notes Rec. 37 (1), 218–226.

Mazor, E., Verhagen, B.T., Sellschop, J.P.F., Jones, M.T., Robins, N.E., Hutton, L., Jennings, C.M.H., 1977. Northern Kalahari groundwaters: Hydrologic, isotopic and chemical studies at Orapa, Botswana. J. Hydrol. 34 (3–4), 203–234.

McCarthy, T.S., 2006. Groundwater in the wetlands of the Okavango Delta, Botswana, and its contribution to the structure and function of the ecosystem. J. Hydrol. 320 (3–4), 264–282.

McCarthy, T.S., McIver, J.R., Verhagen, B.T., 1991. Groundwater evolution, chemical sedimentation and carbonate brine formation on an island in the Okavango Delta swamp, Botswana. Appl. Geochem. 6 (6), 577–595.

McCarthy, T.S., Ellery, W.N., Stanistreet, I.G., 1992. Avulsion mechanisms on the Okavango fan, Botswana: the control of a fluvial system by vegetation. Sedimentology 39 (5), 779–795.

McCarthy, T.S., Ellery, W.N., Ellery, K., 1993. Vegetation-induced, subsurface precipitation of carbonate as an aggradational process in the permanent swamps of the Okavango (delta) fan, Botswana. Chem. Geol. 107 (1–2), 111–131.

McCarthy, T.S., Barry, M., Bloem, A., Ellery, W.N., Heister, H., Merry, C.C., Ruther, H., Stromberg, H., 1997. The gradient on the Okavango fan, Botswana. and its sedimentological and tectonic implications. J. Afr. Earth Sci. 24, 65–78.

McCarthy, T.S., Ellery, W.N., 1994. The effect of vegetation on soil and ground water chemistry and hydrology of islands in the seasonal swamps of the Okavango Fan, Botswana. J. Hydrol. 154 (1–4), 169–193.

McCarthy, T.S., Ellery, W.N., 1998. The Okavango delta. Trans. R. Soc. S. Afr. 53 (2), 157–182.

McCarthy, J.M., Gumbricht, T., McCarthy, T., Frost, P., Wessels, K., Seidel, F., 2003.

Flooding patterns of the Okavango wetland in Botswana. Ambio: A J. Hum. Environ. 32 (7), 453–457 between 1972 and 2000.

McCarthy, T.S., Humphries, M.S., Mahomed, I., Le RouX, P., Verhagen, B.T., 2012. Island forming processes in the Okavango Delta, Botswana. Geomorphology 179, 249–257.

McCarthy, T.S., Metcalfe, J., 1990. Chemical sedimentation in the semi-arid environment of the Okavango Delta, Botswana. Chem. Geol. 89 (1–2), 157–178.

McCarthy, T.S., Bloem, A., Larkin, P.A., 1998. Observations on the hydrology and geohydrology of the Okavango Delta. S. Afr. J. Geol. 101 (2), 101–117.

McClain, M.E., Boyer, E.W., Dent, C.L., Gergel, S.E., Grimm, N.B., Groffman, P.M.,

Hart, S.C., Harvey, J.W., Johnston, C.A., Mayorga, E., McDowell, W.H., 2003. Biogeochemical hot spots and hot moments at the interface of terrestrial and aquatic ecosystems. Ecosystems 301–312.

Miller, W.R., Drever, J.I., 1977. Chemical weathering and related controls on surface water chemistry in the Absaroka Mountains, Wyoming. Geochim. Cosmochim. Acta 41 (12), 1693–1702.

Milzow, C., Kgotlhang, L., Bauer-Gottwein, P., Meier, P., Kinzelbach, W., 2009. Regional review: the hydrology of the Okavango Delta, Botswana—processes, data and modelling. Hydrogeol. J. 17 (6), 1297–1328.

Mladenov, N., McKnight, D.M., Wolski, P., Ramberg, L., 2005. Effects of annual flooding on dissolved organic carbon dynamics within a pristine wetland, the Okavango Delta, Botswana. Wetlands 25 (3), 622–638.

Modie, B.N., 2000. Geology and mineralisation in the Meso-to Neoproterozoic Ghanzi- Chobe Belt of northwest Botswana. J. Afr. Earth Sci. 30 (3), 467–474.

Modisi, M.P., Atekwana, E.A., Kampunzu, A.B., Ngwisanyi, T.H., 2000. Rift kinematics during the incipient stages of continental extension: Evidence from the nascent Okavango rift basin, northwest Botswana. Geology 28 (10), 939–942.

Mogobe, O., Mosimanyana, E., Masamba, W.R.L., Mosepele, K., 2018. Monitoring water quality of the Upper Okavango Delta. Climate Change and Adaptive Land Management in Southern Africa—Assessments, Changes, Challenges, and Solutions. Biodivers. Ecol. 6, 106–111.

Molwalefhe, L.N., 2003. Geochemical and Isotopic Characterization of Shallow Basinal Brines from the Makgadikgadi Pans Complex, Northeastern Botswana: Determination of the Sources of Salinity. Doctor of Philosophy thesis. Western Michigan University, USA.

Mosepele, K., Ngwenya, B.N. and Bernard, T., 2006. Artisanal fishing and food security in the Okavango Delta, Botswana. World Sustainable Development Outlook: Global and Local Resources in Achieving Sustainable Development, Inderscience, Geneva, pp.159–168.

Mosepele, K., Moyle, P.B., Merron, G.S., Purkey, D.R., Mosepele, B., 2009. Fish, floods, and ecosystem engineers: aquatic conservation in the Okavango Delta, Botswana. Bioscience 59 (1), 53–64.

Moses, O., Gondwe, M., 2019. Simulation of changes in the twenty-first century maximum temperatures using the statistical downscaling model at some stations in Botswana. Model. Earth Syst. Environ. 5 (3), 843–855.

Mosimane, K., Struyf, E., Gondwe, M.J., Frings, P., van Pelt, D., Wolski, P., Schoelynck, J., Schaller, J., Conley, D.J., Murray-Hudson, M., 2017. Variability in chemistry of surface and soil waters of an evapotranspiration-dominated flood- pulsed wetland: solute processing in the Okavango Delta, Botswana. Water SA 43 (1), 104–115.

Murray-Hudson, M., Wolski, P., Murray-Hudson, F., Brown, M.T., Kashe, K., 2014. Disaggregating hydroperiod: components of the seasonal flood pulse as drivers of plant species distribution in floodplains of a tropical wetland. Wetlands 34 (5), 927–942.

Nyberg, B., Gawthorpe, R.L., Helland-Hansen, W., 2018. The distribution of rivers to terrestrial sinks: implications for sediment routing systems. Geomorphology 316, 1–23.

Obakeng, O.T. and Gieske, A.S.M., 1997. Hydraulic conductivity and transmissivity of a water-table aquifer in the Boro River system, Okavango Delta. Botswana Geological Survey Department bulletin series, 46.

Oromeng, K.V., Atekwana, E.A., Molwalefhe, L., Ramatlapeng, G.J., 2020. Time-series Variability of Solute Transport and Processes in Rivers in Semi-arid Endorheic Basins: The Okavango Delta. Science of The Total Environment, Botswana, p. 143574.

Peel, M.C., Finlayson, B.L. and McMahon, T.A., 2007. Updated world map of the Ko¨ppen-Geiger climate classification.

Podgorski, J.E., Green, A.G., Kgotlhang, L., Kinzelbach, W.K., Kalscheuer, T., Auken, E., Ngwisanyi, T., 2013. Paleo-megalake and paleo-megafan in southern Africa. Geology 41 (11), 1155–1158.

Podgorski, J.E., Green, A.G., Kalscheuer, T., Kinzelbach, W.K., Horstmeyer, H., Maurer, H., Rabenstein, L., Doetsch, J., Auken, E., Ngwisanyi, T., Tshoso, G., 2015. Integrated interpretation of helicopter and ground-based geophysical data recorded within the Okavango Delta, Botswana. J. Appl. Geophys. 114, 52–67.

Pombo, S., de Oliveira, R.P., Mendes, A., 2015. Validation of remote-sensing precipitation products for Angola. Meteorol. Appl. 22 (3), 395–409.

Ramberg, L., Wolski, P., 2008. Growing islands and sinking solutes: processes maintaining the endorheic Okavango Delta as a freshwater system. Plant Ecol. 196 (2), 215–231.

Ringrose, S., Harris, C., Huntsman-Mapila, P., Vink, B.W., Diskins, S., Vanderpost, C., Matheson, W., 2009. Origins of strandline duricrusts around the Makgadikgadi Pans (Botswana Kalahari) as deduced from their chemical and isotope composition. Sed. Geol. 219 (1–4), 262–279.

Rose, L.A., Karwan, D.L., Godsey, S.E., 2018. Concentration–discharge relationships describe solute and sediment mobilization, reaction, and transport at event and longer timescales. Hydrol. Process. 32 (18), 2829–2844.

Runkel, R.L., Bencala, K.E., 1995. Transport of reacting solutes in rivers and streams. In: Environmental Hydrology. Springer, Dordrecht, pp. 137–164.

Sawula, G., Martins, E., 1991. Major ion chemistry of the lower Boro River, Okavango Delta. Botswana. Freshwater Biology 26 (3), 481–493.

Seely, M., Henderson, J., Heyns, P., Jacobson, P., Nakale, T., Nantanga, K. and Schachtschneider, K., 2003. Ephemeral and endoreic river systems: Relevance and management challenges.

Transboundary Rivers, Sovereignty and Development: Hydropolitical Drivers in the Okavango River Basin, pp.187-212.

Sheng, Y., 2014. Endorheic lake dynamics: Remote sensing. Taylor & Francis, pp. 687–695.

Steudel, T., Go¨hmann, H., Flügel, W.A., Helmschrot, J., 2013. Assessment of hydrological dynamics in the upper Okavango River Basins. Biodivers. Ecol. 5, 247–262.

Thangarajan, M., Linn, F., Uhl, V., Bakaya, T.B., Gabaake, G.G., 1999. Modelling an inland Delta aquifer system to evolve pre-development management schemes: a case study in Upper Thamalakane River valley, Botswana, southern Africa. Environ. Geol. 38 (4), 285–295.

Verhagen, B.T., 1992. Detailed geohydrology with environmental isotopes: A case study at Serowe, Botswana. In Isotope techniques in water resources development 1991.

Walker, C.D., Richardson, S.B., 1991. The use of stable isotopes of water in characterising the source of water in vegetation. Chem. Geol. Isotope Geosci. Sect. 94 (2), 145–158.

Wilson, B.H. and Dincer, T., 1976, August. An introduction to the hydrology and hydrography of the Okavango Delta. In Symposium on the Okavango Delta (pp. 33–48). Botswana Soc. Gaborone Botswana.

Wolski, P. and Murray-Hudson, M., 2008. Alternative futures' of the Okavango Delta simulated by a suite of global climate and hydro-ecological models. Water SA, 34(5), pp.605–610.

Wolski, P., Murray-Hudson, M., Savenije, H. and Gumbricht, T., 2005. Modeling of the hydrology of the Okavango Delta. Publication of the Water and Ecosystem Resources for Regional Development (WERRD) project, HOORC, Maun, Botswana.

Wolski P., Murray-Hudson M., Mazvimavi D., Ringrose S., 2008. Change and variability of flooding in the Okavango Delta, Botswana, and their consequences for water resources management. Harry Oppenheimer Okavango Research Centre, University of Botswana. In Proceedings of the Second IASTED Africa Conference (Vol. 604, p. 055).

Wymore, A.S., Leon, M.C., Shanley, J.B. and McDowell, W.H., 2020. Hysteretic response of solutes and turbidity at the event scale across forested tropical montane watersheds. Critical Zone (CZ) EXport to Streams as Indicator for CZ Structure and Function.

Yapiyev, V., Sagintayev, Z., Inglezakis, V.J., Samarkhanov, K., Verhoef, A., 2017. Essentials of endorheic basins and lakes: a review in the context of current and future water resource management and mitigation activities in Central Asia. Water 9 (10), 798.

Zimmermann, S., Bauer, P., Held, R., Kinzelbach, W., Walther, J.H., 2006. Salt transport on islands in the Okavango Delta: numerical investigations. Adv. Water Resour. 29 (1), 11–29.

Chapter 2: Spatial and temporal controls on the solute behavior of rivers in arid watersheds: The Okavango River, NW Botswana

This chapter is reproduced from the original publication: Ramatlapeng, G.J., Atekwana, E.A. and Molwalefhe, L., 2023. Spatial and temporal controls on the solute behavior of rivers in arid watersheds: The Okavango River, NW Botswana. Journal of Hydrology, 618, p.129141.

Abstract

Solute cycling models for rivers in arid watersheds must identify solute sources and their spatial and temporal connectivity to rivers to assess the processes that control the solute behavior in these rivers. In this study, we collected hourly time series of total dissolved ions (TDI) concentrations, water levels, water temperatures and air temperatures at select stations distributed longitudinally in a river in an arid watershed. Our objectives were to: (1) document the spatial and temporal variations in solute concentrations and (2) determine the processes controlling the spatial and temporal variations in solute concentrations. We conducted this investigation over a two-year period at four stations along the Okavango River flowing through the Okavango Delta (Delta) in the middle Kalahari Desert, Botswana. At the spatial scale, we observed progressive downriver enrichment in TDI concentrations associated with evapotranspiration of river water because of the 5 months river transit across the hot Delta. At a temporal scale, the TDI concentrations increased seasonally from evapoconcentration and sub- seasonally from solute transfer from the watershed to the river. We analyzed sub-seasonal TDI concentration perturbations using the slope (β) of the relationship between TDI concentrations and normalized water level (C- NWL) relationships. We find that at low discharge during flow recession and at the beginning of rising discharge from flooding, the solute enrichment anomalies with $\beta > 0$ are related to hydrologic connectivity between the river and solute stores in the river floodplains, hundreds of thousands of salt islands

and isolated evapoconcentrated wetland pools. Our findings indicate that hydrologically driven river connectivity to solute stores in the local watershed and evapotranspiration jointly control the solute behavior at variable spatial and temporal scales in rivers in arid watersheds. We anticipate that our findings will inform solute transport and solute cycling models for rivers in arid watersheds.

1. Introduction

Rivers act as conduits of water and solutes (dissolved ions in water) out of the river basin in exorheic basins and to the terminus of endorheic basins. Solute transformation across river basins and the role of rivers in solute transport make rivers an important component of the global so- lute cycle. Studies in exorheic basins typically found in humid environments have advanced our knowledge and understanding of source(s) of solutes, solute transport, in-stream processes, and catchment specific characteristics that control the spatial and temporal variability in solute behavior (Fovet et al., 2018; Herndon et al., 2018; Rose et al., 2018; Wymore et al., 2020; Liu et al., 2020). Knowledge on solute cycling in exorheic basins is critical for quantifying weathering fluxes, solute load, and solute export out of basins to oceans, which has implications for the global oceanic solute cycle. Comparatively, limited studies (e.g., Oromeng et al., 2021; Letshele et al., 2023) have been conducted in rivers draining endorheic basins in arid environments to understand the processes controlling the spatial and temporal variability of solutes and solute cycling, perhaps because endorheic basins are disconnected from the ocean, and thus are regarded as unimportant in the global cycling of solutes. Nevertheless, endorheic basins occupy 20-23 % of the Earth's surface (Nichols, 2007; Nyberg et al., 2018), which we use to suggest that substantial amounts of solutes transferred from the upper portions of watersheds are transformed in the rivers and stored at the terminus of endorheic basins. In spite of the potential importance of terrestrial solute cycling

at the local and regional levels in endorheic basins, the processes that control the cycling of solutes are not well understood because of limited investigations. A study by Oromeng et al. (2021) conducted in the endorheic Okavango River basin provided much needed insights on the hydrologic and biogeochemical controls on the river solute behavior. A study of the Okavango River by Letshele et al. (2023) showed that downriver solute enrichment was related to the d-excess parameter derived from the stable hydrogen and oxygen isotopic composition of river water. Additionally, the Letshele et al. (2023) study also found marked disagreement between the mean TDI-mean d-excess model and TDI-d-excess data from previous studies, which was used to invoke non- evaporative solute enrichment in the Okavango Delta. The Oromeng et al. (2021) and the Letshele et al. (2023) studies can be used to suggest that more work still needs to be done to constrain the spatio-temporal controls of solute cycling across large spatial scales and over short to long-term timescales in endorheic basins. Understanding solute cycling in endorheic basins has implications for knowing the river salinity status which impacts water quality and river ecology.

Unlike exorheic basins in humid environments, the hydrology of rivers in endorheic basins in arid environments is characterized by highly variable river flow and downriver water transmission losses to groundwater and evapotranspiration. Yet, little is known on how the downriver modifications of water and solutes modulates solute behavior at various temporal scales. Understanding the spatial and temporal river solute dynamics across river basins requires assessments of river discharge and solute concentrations with a temporal resolution adequate to capture processes occurring at multiple locations across the basin. Hydrochemical investigations utilize river discharge to constrain hydrologic controls on solute behavior in rivers (e.g., Evans and Davies, 1998; Godsey et al., 2009; Moatar et al., 2017; Zhi et al., 2018; Oromeng et al., 2021). However, there are many rivers that are ungauged, and those that are gauged may not be gauged

at locations useful for experiments that investigate the spatial evolution of the hydrochemistry of rivers. The lack of discharge measurements for many ungauged rivers and at select river segments may be due to difficulties in defining river channel cross-sectional area and measuring flow velocity. For example, measuring discharge in braided stream reaches and reaches with extensive wetlands can be challenging, and thus will impact our ability to assess discharge related solute behavior. A way to meet this challenge in studying discharged-based solute behavior is a qualitative comparison, where relative water level changes at multiple river reaches can be considered a proxy for discharge (supplementary Fig. 1). The water levels for each measured reach are normalized and used as a relative indicator of discharge. The normalization can be tested by comparing the solute behavior using normalized water levels with the solute behavior where river discharge is measured along the river (supplementary Fig. 1). If the solute-discharge and solute-normalized water levels relationships show similar temporal behavior, then the normalized water levels can be used as a proxy for discharge in ungauged river segments.

Hydrochemical studies of solute behavior in rivers take into consideration both river discharge and solute concentrations. The solute dynamics can be characterized using the total dissolved ions (TDI) which are reflective of the gross river solute composition (e.g., Oromeng et al., 2021). TDI concentrations can be measured by electronic meters and recorded and stored in data loggers at a much higher frequency than can be measured manually. Thus, assessing the relationship between solute concentrations as TDI and normalized water levels (C-NWL relationship) at high frequency during different flow regimes across a river basin will allow us to tease out salient solute behavior patterns driven by variable processes.

We investigated the processes controlling the spatial and temporal solute behavior in the Okavango River in northwestern Botswana. The Okavango River flows in an endorheic basin (the

Okavango River Basin; hereafter referred to as the ORB). The ORB covers two climatic regimes from a higher rainfall temperate region in Angola to the steppe middle Kalahari Desert in Botswana (Ellery et al., 2003; Peel et al., 2007). Near the terminus of the ORB lies the Okavango Delta (Delta). The Okavango River meanders extensively through a narrow valley of the Panhandle region of the Delta before it disperses into a series of distributary channels on a large alluvial fan forming the lower delta region. In the lower delta region, the river is mostly characterized by braided flow through the Okavango Delta wetlands. The hydrology of the Delta is highly variable and controlled by an annual flood pulse initiated by rains from the upper watershed in Angola and by local rains (e.g., Wolski et al., 2005). The Delta and its wetlands are subjected to high evapotranspiration (ET) rates which cause salt precipitation on floodplains and on the numerous tree islands in the Delta wetlands (e.g., McCarthy et al., 1991, 1998; Gumbricht and McCarthy, 2003; Gumbricht et al., 2004, Akondi et al., 2019). Evapotranspiration also causes enrichment of solutes in isolated wetland pools scattered across the Delta (e.g., Dincer et al., 1979). The role that these solute stores (ie., floodplains, salt islands and isolated wetland pools) which are distributed differentially across the Delta have on the Okavango River solute cycling is yet to be investigated.

Investigations of the solute behavior in the Okavango River in the Delta conducted at the proximal portion of the Delta in Mohembo (Oromeng et al., 2021) and distal portion of the Delta in Maun (Oromeng et al., 2021; Ramatlapeng et al., 2021) have suggested that hydrologic connectivity between the Okavango River and solute stores in the local watershed and evapotranspiration control the spatial and temporal river solute behavior. Although the Oromeng et al. (2021) and Ramatlapeng et al. (2021) studies have provided insights on the role of hydrology and evapotranspiration in controlling solute behavior at the inlet and outlet of the Delta, there is still a lack of understanding of the processes driving the variations in river solute concentrations

both in space and time for the nearly 450 km river distance between the Delta inlet and outlet (e.g., Letshele et al, 2023). The Delta serves as an important source of potable water and food (fish, water lily) to the riparian communities (Mosepele et al., 2006, 2009; Kgathi et al., 2006) and therefore, studying the processes that may affect the solute behavior in the Delta is crucial for water quality monitoring and ecological sustainability.

In this study, we made hourly measurements of TDI concentrations, water level, air temperature and water temperature at 4 stations located spatially across the Delta. Our objectives were to (1) document the spatial and temporal variations of solutes and (2) determine the processes controlling variations in solute concentrations in the Okavango River. We used TDI concentrations to characterize solute behavior and air temperature and water temperature to assess seasonality and climatic controls on solute behavior in the river. We utilized normalized water levels to elucidate the influence of hydrological changes on solute behavior. Monitoring hydrologic (water level), hydrochemical (TDI concentrations) and climatic (water and air temperature) controls at a high frequency allowed us to assess solute behavior dynamics occurring at seasonal and sub-seasonal timescales across the Delta. The placement of one of our stations at the inlet of the Delta captured solute transport and processes influenced by the upper headwater catchments. Localized chemical transformation in the Delta which controls the solute dynamics that affect the Delta and its wetlands was assessed for two stations within the Delta and a station at the river exit from the Delta. The findings from our study provide insights on the hydrologic, climatic, and geomorphological processes controlling the spatio-temporal solute behavior in Okavango Delta and is applicable to other rivers in endorheic basins.

2. The Okavango Delta

2.1. Location

The Delta lies near the terminus of the endorheic ORB. This study was conducted along the Okavango River located between latitudes 18º and 21ºS and longitudes 22º and 24ºE in the Okavango Delta in northwest Botswana (Fig. 1). The upper watershed of the ORB comprises the Cubango and Cuito basins which are drained by the Cubango River and Cuito River, respectively, and merge in Angola to form the Okavango River. The Okavango River enters the Delta in Botswana at Mohembo and flows for ~450 km from the inlet to the outlet of the Delta in Maun. The Delta consists of a Panhandle region and a lower delta region. The Panhandle of the Delta is a ~6,000 km^2 valley through which the Okavango River meanders before branching out into distributary channels forming the lower delta. The lower delta is an alluvial fan with a surface area of ~22,000 km^2 (McCarthy et al., 1992) and lies in the Quaternary half-graben of the Okavango Rift Zone (McCarthy et al., 1993; Modisi et al., 2000; Kinabo et al., 2007, 2008; Bufford et al., 2012). The landscape of the Delta has been shaped by neotectonics, river sedimentation, formation of channels, channel avulsion and wetland development (McCarthy and Ellery, 1994; McCarthy et al., 1998). The topographical elevations vary from 1025 m where the Okavango River flows into the Delta at Mohembo to 920 m in the Mababe Depression (Gumbricht et al., 2001). The topography of the Delta is relatively flat (McCarthy et al., 1998; McCarthy, 2006) with gentle undulations where the local relief rarely exceeds 2 m, except for areas with termite mounds and islands (McCarthy et al., 1998; Gumbricht et al., 2001; McCarthy, 2006).

2.2. Geology

The Cubango and Cuito sub-basins in the upper ORB in Angola lie on the Precambrian Congo Craton. The Cuito basin and southern part of the Cubango sub-basins are covered by the Karoo

Supergroup sedimentary rocks, overlain by thick unconsolidated Kalahari sands, clays, lime rock and lateritic layers of the Kalahari Superior Formation (Bereslawski, 1997; Catuneanu et al., 2005; Jones, 2010). The headwater portion of the Cubango sub-basin is underlain by a crystalline Precambrian bedrock comprising granite and dolerite (Bereslawski, 1997; Jones, 2010).

In the Okavango Delta, the bedrock geology is comprised of Precambrian crystalline rocks of the Damara and Ghanzi-Chobe orogenic belt (Modie, 2000; Milzow et al., 2009). The surficial geology consists of the Quaternary Kalahari alluvium and recent swamp sediments over- lying 105–175 m of lacustrine and fluvio-deltaic sediments (Ringrose et al., 2009). At the surface, the sediments in the Okavango Delta are mostly sands with varying proportions of silt, clays, and carbonates (Huntsman-Mapila et al., 2005). The surficial sediments originate from a mixture of aeolian quartz, diagenetic carbonates and components of weathered Proterozoic granitoids and mafic–ultramafic rocks exposed in the northwestern part of Botswana (Huntsman-Mapila et al., 2005).

2.3. Climate

The climate of the ORB ranges from a temperate climate in the Angolan highlands to a steppe arid Kalahari Desert in northwestern Botswana (Peel et al., 2007). The climate is characterized by a wet season which spans from November to March and a dry season which spans from April to October (McCarthy and Ellery, 1994; Milzow et al., 2009; Steudel et al., 2013). The mean annual rainfall in the upper watershed is 1100 mm (Pombo et al., 2015). In the Delta, the mean annual rainfall ranges between 455 and 490 mm (McCarthy et al., 2000). Temperatures in the upper ORB range between 13 and 17 ℃ during the dry season and from 20 to 25 ℃ during the wet season (Baumberg et al., 2014). The highest mean monthly maximum temperatures over the Delta ranges between 32 and 35 ℃ during the wet season and the lowest mean monthly minimum temperatures

range from 2 to 7 ℃ during the dry season (Moses and Gondwe, 2019). The Delta is subjected to high temperatures with an estimated potential evapotranspiration of ~2172 mm/y which is 4 times greater than the rainfall received in the Delta (Wilson and Dincer, 1976). Thus, evapotranspiration has a profound effect on the water balance in the Delta and contributes to the development and growth of the ~150,000 tree island complexes scattered across the Delta (Gumbricht and McCarthy, 2003). The tree islands cover 5 % of the permanently flooded ecotone, 25 % of the seasonal ecotone and 50 % of the occasionally flooded ecotone (Gumbricht et al., 2004; Humphries et al., 2014). Evapoconcentration also causes enrichment of solutes in the numerous isolated surface water pools scattered in the Delta's seasonally and occasionally flooded eco- tones (McCarthy et al., 1998).

2.4. Hydrology

The Cuito and Cubango Rivers in the upper watershed in Angola contribute about 45 % and 55 % of the discharge, respectively, to the Okavango River flowing through the Delta (Mendelsohn and el Obeid, 2004). The hydrology of the Okavango River and Delta is primarily driven by an annual flood derived from the highlands of Angola and by local rains. The mean annual inflow of water from the upper watershed to the Delta is 9.2×10^9 m^3/y and the seasonal rains contribute an additional 6×10^9 m^3/y (McCarthy and Ellery, 1998; Merron, 1991). The annual flood pulse reaches the inlet to the Delta in Mohembo be- tween February and May and gradually flows across the Delta as a progressive wave to the outlet of the Delta in Maun for 4–6 months (McCarthy and Metcalfe, 1990; McCarthy and Ellery, 1998). As the flood advances across the Delta, the area inundated varies from an annual low of 4500–6000 km2 to an annual high of 9000–12,000 km2 (Ramberg and Wolski, 2008). Because the Kalahari sands in the Delta have relatively high hydraulic conductivity (10–30 m/day) and porosity (30 %) (Obakeng and Gieske, 1997), the slow

propagation of the flood wave is accompanied by groundwater recharge in the shallow unconfined aquifer (McCarthy, 2006), making the Okavango River influent. The deepening of the groundwater table away from the Okavango River and Delta wetlands is evidence for groundwater recharge by the Okavango River (McCarthy et al., 1997; Ellery et al., 2003; McCarthy, 2006; Milzow et al., 2009; Akondi et al., 2019).

The variable flooding in the Delta creates vegetation zonations (Mladenov et al., 2005; Wolski et al., 2006). The Panhandle region is in the permanently flooded ecotone dominated by grass (*Miscanthus junceus*), reeds (*Phragmites australis*) and giant sedges (*Cyperus papyrus*) (Ellery et al., 2003) on the channel margins. Water depths average 1.5 m (Wilson and Dincer, 1976), average river gradient is 1:5500 (Gumbricht et al., 2004), and the river flows at a velocity of 0.4–0.8 m/s within the channel (Wolski et al., 2006). The lower delta has seasonally flooded and occasionally flooded ecotones. The seasonally flooded ecotone is dominated by *Cyperus papyrus* and *Phragmites mauritianus* and the occasionally flooded ecotone is dominated by *Miscanthus junceus* (Ellery et al., 2003). In the lower delta, water depths generally decrease downriver and average 1 m (Wilson and Dincer, 1976). The Okavango River's gradient in the lower delta averages 1:3,300 (Gumbricht et al., 2004) and the average river velocity is 0.01 m/s (Wolski et al., 2006).

3. Methods

3.1. Data collection

3.1.1. Water level, water temperature, river specific conductance, air temperature and barometric pressure

We deployed Solinst™ LTC (level, temperature, conductivity) leveloggers at the inlet to the Delta in Mohembo (18º16′ 38.82″ S, 21º47′ 12.66″ E), near the end of the Panhandle of the Delta at Seronga (18º49′ 19.38″ S, 22º24′ 52.62″ E), in the lower delta at the Okavango Research Institute (ORI) Island (19º32′ 53.40″ S, 23º10′ 40.68″ E) and at the outlet of the Delta in Maun (20º0′ 18.14″ S, 23º25′ 34.40″ E) (Fig. 1). Prior to deploying the Solinst™ LTC leveloggers in the river, we gently cleaned the conductivity cell and sensor pins using soft Q-tips and per- formed conductivity calibration on the leveloggers according to Solinst™'s instructions to ensure accurate readings. The Solinst™ LTC leveloggers are equipped with sensors which record river water level (m), water temperature (℃) and specific conductance (SC; µS/cm). The water level sensor of the Solinst™ LTC has an automatic temperature compensation for normalization. The sensor records water level with an accuracy of 0.1 % percentage of full scale and a temperature compensation range from 10 ◦C to 40 ℃. The 4-electrode conductivity sensor of the Solinst™ LTC has a resolution of 1 µS/cm with the ability to measure on a full range of 0 to 80,000 µS/cm. The conductivity sensor can operate in water temperatures ranging from -20 ℃ to 80 ℃.

We also deployed Solinst™ barologgers at the Mohembo, Seronga, ORI Island and Maun stations. The Solinst™ barologgers record air temperature (℃) and were programmed to record and convert barometric pressure to equivalent water level (m) using a conversion factor of 0.101972 m/kPa. The accuracy of the air temperature sensor is ±0.05 ℃ with a resolution of 0.003 ℃, whilst the accuracy of the barologger pressure sensor is 0.05 kPa. The Solinst™ LTC barologgers were set to an altitude of 1006 m above sea level (a.s.l) for the Mohembo and Seronga stations, 0 m a.s.l for the ORI Island station and 929 m a.s.l for the Maun station.

At each of the 4 stations, the levelogger was deployed in the water column in a perforated PVC tube and the barologger was deployed in the same PVC tube above the surface of the water. The

perforated tubes allowed for free flow of water to the leveloggers and air to the barologgers, while also providing protection to the dataloggers from external interferences like curious wildlife and people. The perforated tubes were strategically placed in locations along the river where there would be little to no external interferences. The leveloggers and barologgers were set to collect data in a linear sampling mode at hourly intervals and data was collected from July 2010 to July 2012.

Upon completion of the monitoring, the leveloggers were examined for presence of biofilm on the sensor surfaces to ensure that the recorded readings were accurate. We found that there was no biofilm and coatings on the sensors. As part of our data quality control for missing data in our long-term monitoring, data correction was performed using the regression imputation method where the regression equation of the variables of interest is employed instead of data removal or data smoothing. For instance, attempts to remove the barologger from the PVC casing by unknown individual(s) failed. However, the cord holding the barologger was cut in that attempt and the barologger fell to the bottom of the tube and was immersed in river, thus it did not record the air temperature. Missing air temperature values (n=11,291) from Seronga were corrected using a regression equation of the relationship between the air temperature at the Seronga station and that of Mohembo station (Seronga air temperature = (0.57*Mohembo air temperature) + 9.97, R^2 = 0.45, n = 15,080)

3.1.2 Monthly rainfall

In the upper Delta, we selected the Shakawe weather station to represent rainfall in the Panhandle of the Delta covering the Mohembo and Seronga stations. We selected the Okavango Research Institute (ORI) weather station to represent rainfall for the lower delta covering ORI

Island and Maun. Monthly rainfall data for the Shakawe and ORI weather stations were obtained from the archives of ORI (https://o kavangodata.ub.bw/ori/monitoring/water/).

3.2. Data analyses

3.2.1. Total dissolved ions (TDI) estimates

The total dissolved ions (mg/L) were estimated from the specific conductance (µS/cm) measurements recorded by leveloggers at the 4 stations (e.g., Oromeng et al., 2021). The relationship between TDI and SC was established based on the assumption that TDI represents all the electrically conductive ionic species in river water (Lloyd and Heath- cote, 1985). The TDI was estimated using a linear regression equation developed from the relationship between SC and TDI for 57 measurements across the Delta (Oromeng et al., 2021; Atekwana, unpublished):

$$TDI = (0.65*SC) + 0.38 \quad (1)$$

where TDI is the total dissolved ions, 0.65 is the slope of the linear regression, 0.38 is the y-intercept and SC is the specific conductance.

3.2.2. Normalization of river levels

River water levels from the leveloggers were corrected for barometric pressure changes by subtracting the time equivalent barometric pressure values recorded by the barologger. After compensating for barometric pressure changes, we normalized water levels using the Min-Max normalization method (Dawam and Ku-Mahamud, 2019) given by:

$$NWL = (WL_i — WL_{min})/WL_{max} — WL_{min}) \quad (2)$$

where NWL is the normalized water level, WL_i is the instantaneous water level at any time of interest, WL_{min} is the minimum water level and WL_{max} is the highest water level measured for

either the rising or receding limbs of an annual discharge hydrograph. For the data with incomplete water level measurements (i.e., unknown highest water level value) for periods where discharge was measured, we used the highest river discharge from data from the archives of ORI discharge database during that time frame to determine the corresponding water level value using the following equations developed for the Mohembo (Eqn. (3)) and the Maun (Eqn. (4)) discharge measuring stations:

$$\text{Log discharge} = 1.5574(\log \text{water level}) + 1.9071 \quad (3)$$

$$\text{Log discharge} = 2.7623(\log \text{water level}) + 0.4572 \quad (4)$$

3.2.3. Concentration-normalized water level analysis

Concentration (TDI concentrations) data were log-transformed before developing the concentration-normalized water level (C-NWL) relationships. C-NWL matrix of linear slope (β) of the log C-normalized water level regression was derived from log-transformed TDI concentrations and normalized water level following methods from previous studies (Godsey et al., 2009; Musolff et al., 2015; Thompson et al., 2011) which utilized log discharge instead of normalized water level. The β was derived from the best-fit equation of the linear regression of Log C vs normalized water level. In this case, the C-NWL relationships are defined by a power law function:

$$C = \alpha NWL\beta \quad (5)$$

where C is the instantaneous TDI concentration and NWL is the corresponding normalized water level. The intercept (α) and the slope (β) of the power law are derived from the linear regressions of log C vs normalized water level. A slope (β) near zero indicate little to no changes in concentration despite high variability in water levels (Chemostatic behavior), a slope < 0 depicts

solute dilution and slope > 0 depicts solute enrichment (Basu et al., 2011; Clow and Mast, 2010; Godsey et al., 2009). The slope (β) values were estimated on a daily timescale using the hourly measurements for every 24 h, under the assumption that this is an adequate frequency to capture the temporal changes in solute concentrations and solute transport regimes (Oromeng et al., 2021).

The statistical analysis of the C-NWL data was performed in Micro soft Excel™ and R studio.

4. Results

4.1. Summary statistics

The temporal measurements of TDI concentrations, air temperature, water temperature, monthly rainfall amount and water levels from the Mohembo, Seronga, ORI Island and Maun stations are presented in Supplementary Table 1. The summary statistics of the TDI concentrations, air temperature, water temperature, monthly rainfall amount and normalized water levels are presented in Table 1.

4.2. Spatial and temporal variations in TDI concentrations

The TDI concentrations increase across the 4 stations (Mohembo, Seronga, ORI Island and Maun) in the downriver direction (Fig. 2a, b, c and d; Fig. 3a). The TDI concentrations in the Panhandle of the Delta at Mohembo station ranged between 6 and 84 mg/L with a mean of 17 ± 11 mg/L (Table 1), while at the Seronga station, the TDI concentrations ranged from 11 to 71 mg/L with a mean of 27 ± 13 mg/L (Table 1). In the lower delta at ORI Island, the TDI concentrations ranged between 28 and 61 mg/L, with a mean of 47 ± 8 mg/L and between 40 and 97 mg/L with a mean of 71 ± 9 mg/L at the Maun station (Table 1).

At a temporal scale, the TDI concentrations from the 4 stations showed distinct interannual, seasonal and sub-seasonal (monthly, weekly, and daily) variations (Fig. 2a, b, c and d). At an interannual scale, the TDI concentrations were generally lower in 2011 compared to 2010 and 2012. At the seasonal scale, the TDI concentrations in Mohembo increased continuously from July to January, which was followed by a sudden decrease to low TDI concentrations from February to July (Fig. 2a). The six-month long period of low TDI concentrations was characterized by two prominent TDI concentration peaks in September and January, followed by a general decrease in TDI concentrations to the next seasonal cycle. In Seronga, we observed a continuous increase in TDI concentrations from August to December followed by a continuous decrease to lower concentration spanning January to August (Fig. 2b). During the period of lower TDI concentrations, we observed a sub-peak in TDI concentrations in June. In the lower Delta at ORI Island, the TDI concentrations increased from September to peak concentrations in November, followed by a slight decrease in TDI concentrations from December to March, then increased to May before decreasing markedly to the lowest TDI concentrations in August (Fig. 2c). In Maun, the seasonal TDI concentrations showed peaks in October and January and the TDI concentrations were lower in February and June (Fig. 2d).

The sub-seasonal behavior of the TDI concentrations varied downriver (Fig. 2a, b, c and d). At the Mohembo station, we observe higher frequency variation in the TDI concentration peaks between June and January and very little concentration fluctuation during the period of low TDI concentrations (Fig. 2a). At the Seronga station, there are more sub-seasonal changes in the TDI concentrations near the TDI concentration peaks which make these peaks much broader compared to those observed at the Mohembo station. At the ORI station, the sub-seasonal concentration

changes are small. In Maun, the sub-seasonal TDI concentrations showed much higher frequency and were much broader near the peak TDI concentrations.

4.3. Spatial and temporal variations in air temperature and water temperature

In Mohembo, the air temperature ranged between 0.5 and 46 ℃, with a mean of 23 ± 7 ℃, while the water temperature ranged from 14 to 31 ℃, with a mean of 24 ± 4 ℃ (Table 1). In Seronga, the air temperature ranged between 6 and 41 ℃, with a mean of 23 ± 6 ℃, while the water temperature ranged from 14 to 30 ℃, with a mean of 23 ± 4 ℃ (Table 1). The air temperatures at ORI Island ranged between 6 and 39 ℃ with a mean of 23 ± 7 ℃, while the water temperature ranged from 15 to 29 ℃ with a mean of 24 ± 3 ℃ (Table 1). In Maun, air temperatures ranged between 2 and 43 ℃ with a mean of 23 ± 7 ℃, while water temperature ranged from 13 to 31 ℃ with a mean of 24 ± 4 ℃ (Table 1). Higher air temperatures (Fig. 2e, f, g and h) and water temperatures (Fig. 2i, j, k and l) were observed during the rainy season between September and April and lower air temperatures and water temperatures were observed during the dry season between May and August.

There is little spatial variability in the air and water temperatures across the Okavango Delta as observed at the Mohembo, Seronga, ORI Island and Maun stations (Fig. 3b and c). We observed similar annual, seasonal, and sub-seasonal patterns in air temperatures (Fig. 2e, f, g and h) and water temperatures (Fig. 2i, j, k and l) across the Okavango Delta. The sub-seasonal range in air temperature is much greater than water temperatures.

4.4. Spatial and temporal variations in monthly rain and normalized water levels

4.4.1. Temporal monthly rainfall

The rainy season in the Okavango Delta spanned November to May (Fig. 2m, n, o and p). The dry season spanned June to September. At Mohembo and Seronga, the monthly rainfall ranged from 0 to 143 mm, with a mean of 38 ± 49 mm (Table 1). Peak monthly rainfall occurred in January. In the lower delta, monthly rainfall at ORI Island and Maun ranged from 0 to 213 mm, with a mean of 40 ± 63 mm (Table 1). Monthly rainfall peaked at 213 mm in December 2010. Peak rainfall in the Okavango Delta (Fig. 2m, n, o, and p) is out of phase with peak discharge (Fig. 2q, r, s and t).

4.4.2. Normalized water level

The relationships between solute concentrations and normalized water levels (C-NWL) at the inlet station at Mohembo and at the Delta outlet station in Maun show similar behavior to the relationships observed between solute concentrations and river discharge (C-Q) in the Oromeng et al. (2021) study (supplementary Fig. 2 and 3), indicating that normalized water levels provide good qualitative characterization of hydrologic controls on solute concentrations as river discharge changes. In the Panhandle of the Delta, the normalized water level hydrograph at Mohembo showed rising water levels beginning in November and peaking in May, with sub-peaks occurring in February and April (Fig. 2q). The rising water levels are then followed by a 6- month long recession from June to November, before water levels begin to rise steadily during the next hydrologic year (Fig. 2q). The water level hydrograph in Seronga mimics that of Mohembo and is characterized by a steady increase in water levels from January to May. The rising limb of the hydrograph showed a sub-peak in February (Fig. 2r). The rising water levels are then followed by a 7-month long recession spanning June to December before water levels began to rise steadily marking the beginning of the next flooding cycle (Fig. 2r).

In the lower delta at ORI Island, the hydrograph showed that normalized water levels began increasing in January and peaking in June with minor sub-peaks observed in January (Fig. 2s). The hydro- graph recession spanned July to December (Fig. 2s). The normalized water level hydrograph at Maun showed rising water levels beginning in March and peaking in August with occurrence of a sub-peak in January (Fig. 2t). The peak water levels were followed by decreasing water levels from July to February with a sub-peak in January (Fig. 2t).

5. Discussion

5.1. Spatial and temporal shifts in the river solute concentrations

The results of our investigation of the spatial and temporal changes of the solute concentrations in the Okavango River show downriver enrichment in the TDI concentrations across the Delta (e.g., Fig. 3a) and seasonal and sub-seasonal shifts in solute concentrations observed at the different monitoring stations across the Delta (Fig. 2a, b, c, and d). The spatial and temporal variability in river solute concentrations can be linked to two main processes: (1) climate driven evapotranspiration (ET) characterized by seasonality and (2) sub-seasonal scale hydrologically driven differential solute transfer from the local watershed into the river which is superimposed on the seasonal ET-driven response.

5.2. ET as the persistent driver of the downriver solute increase across the Okavango Delta

The average TDI concentrations progressively increase downriver at a rate of 0.11 mg/L per km based on the linear regression model (mean TDI = (0.11 x distance) + 12.25; $R^2 = 0.89$) of TDI concentrations vs. distance from the Mohembo station to the Maun station (Fig. 3a). Alternatively, we could fit the data with an exponential model and obtain a similar TDI concentration change rate of 0.1 mg/L per km. The mean annual air temperatures do not differ much for the different

stations across the Delta (Fig. 3b), indicating that the local weather conditions were identical across the Delta. Similarly, the mean annual water temperatures do not differ much for the different stations across the Delta (Fig. 3c), indicating that there were no differences in the river water temperature across the Delta. Thus, the downriver increase in the solute concentrations is attributed to ET-driven progressive evapoconcentration (e.g., Sawula and Martins, 1991; McCarthy et al., 1993; Akoko et al., 2013; Atekwana et al., 2016; Mosimane et al., 2017; Mogobe et al., 2018; Oromeng et al., 2021; Letshele et al., 2023), consistent with the 5 months river transit time the flood peak took to travel the ~450 km from the proximal portion of the Delta in Mohembo to the distal portion of the Delta in Maun. The standard deviations from the annual mean TDI concentrations for each of the stations on the linear regression model (Fig. 3a) speak to additional non-evaporative processes causing changes in the river solute concentrations.

On a temporal scale, the effects of ET on TDI concentrations should correspond to seasonality where solute concentration enrichment should be observed during the hot rainy season when ET rates are higher. However, seasonal TDI concentration peaks observed at the 4 stations across the Delta (Fig. 2a, b, c, and d) do not always coincide with peak seasonal high air temperatures (Fig. 2e, f, g, h) and seasonal high water temperatures (Fig. 2i, j, k and l). The poor correspondence of the seasonal and sub-seasonal peaks in the TDI concentrations and water temperatures can be used to argue that other processes besides ET play a role in controlling the temporal solute chemistry of the Okavango River.

5.3. Hydrologically driven modifications of the solute behavior in the Okavango River

Our results of the spatial and temporal variations in the TDI concentrations in the Okavango River (e.g., Fig. 2a, b, c and d and Fig. 3a) show spatial and temporal heterogeneity evident in the distinct signatures of both dilution and solute enrichment across our stations. Spatial and temporal

variations in TDI concentrations can be linked to specific hydrological processes (e.g., Boyer et al., 1997; Ahearn et al., 2004; Dalzell et al., 2007; Liu et al., 2008; Geeraert et al., 2017; Herndon et al., 2018; Rose et al., 2018; Duvert et al., 2020) developing over the large spatial scale of the Delta. The hydrology of the Okavango River is controlled by an annual flood pulse from the upper watershed in Angola which contributes a mean annual inflow of 9.2×10^9 m^3/y to the Delta and by seasonal rains which contribute an additional 6×10^9 m^3/y to the Delta's hydrology (McCarthy and Ellery, 1998; Merron, 1991). Thus, if hydrology drives the temporal perturbations in the river solute behavior, we should observe modifications in the solute concentrations from the pulse flooding spanning March to September (Fig. 2q, r, s and t) and from local rains which span November through March (Fig. 2m, n, o and p). The addition of "fresh" water with low salinity or low dissolved solutes from the annual pulse flooding and seasonal rains is expected to induce dilution in the river solute concentrations (e.g., Ahearn et al., 2004; Herndon et al., 2018; Rose et al., 2018). To understand the role of the pulse flooding and rains in driving the seasonal and sub-seasonal perturbations in the river solute behavior, we utilized the temporal slopes (β) of the relationship between solute concentrations and normalized water levels as a determinant of whether increases in water levels cause solute enrichment or dilution (Godsey et al., 2009; Musolff et al., 2015; Thompson et al., 2011). In addition, we assessed the relationship between solute concentrations and normalized water levels (C- NWL relationship) to get additional insights on discharge timing and solute delivery into the river. We observed that the behavior of solutes was similar during different rising and receding limbs, indicating that similar processes control the solute behavior regardless of the timing of the hydrologic event (Figs. 4, 5, 6 and 7).

5.3.1. Hydrologic controls on the TDI concentration variations in the upper watershed above the Delta

The normalized water level (NWL) hydrographs at our stations are color differentiated based on the rising and falling limbs over time. We show the NWL hydrograph for the Mohembo station (Fig. 4a), the temporal TDI concentrations (Fig. 4b), the temporal slopes (β) (Fig. 4c) and the C-NWL relationships (Fig. 4d) for the rising and falling limbs of the NWL hydrographs. The changes in the TDI concentrations at the Mohembo station are reflective of solute behavior controlled by processes occurring in the upper watershed in Namibia and Angola. The upper watershed above the Mohembo station where all the river flow is sourced from Cubango and Cuito Rivers is dominated by a temperate climate (Peel et al., 2007). Groundwater influx into the river at baseflow (Steudel et al., 2013) causes solute enrichment during low flow conditions in the Okavango River as reflected by the temporal increases in the TDI concentrations (Fig. 4b) and in slope values of >0 (Fig. 4c) at low flow (October to January). The solute enrichment occurring at low flow could also be attributed to wet season storage of floodwaters in the vast floodplains of the Cubango and Cuito Rivers which is released into the river during the dry season (Steudel et al., 2013). The increasing river solute concentrations are also observed on the C-NWL relationships at low flow to ~0.5 NWL during the rising limb of the hydrograph and from ~0.5 NWL to low flow on the receding limb of the hydrograph (Fig. 4d). These observed enrichment episodes at low flow are attenuated by two dilution episodes occurring mid-flow (~0.5 NWL; Fig. 4d) in the rising limb of the discharge hydrograph (February; Fig. 4b) and 0.7 to 0.5 NWL (Fig. 4d) during the falling limb of the discharge hydrograph (May; Fig. 4b). The dilution of TDI concentrations back to baseline solute concentrations between mid-flow and peak flow can be attributed to the supply of runoff from the Cuito and Cubango sub-watersheds in the form of the annual flooding.

5.3.2. Hydrologic controls on the TDI concentration variations in the Panhandle region of the Delta

The variations of the TDI concentrations relative to normalized water levels at the Seronga station (Fig. 5) capture the solute concentration modifications within the Panhandle portion of the Delta. The NWL hydrograph for Seronga (Fig. 5a), the temporal TDI concentrations (Fig. 5b), the temporal slopes (β) (Fig. 5c) and the C-NWL relationships (Fig. 5d) for the rising and falling limbs of the NWL hydrograph are also shown. Unlike at Mohembo, the arrival of the flood pulse at Seronga induces solute dilution during the rising limb of the hydrograph (Fig. 5c and d) as the previously increasing TDI concentrations with decreasing water levels sharply decreases. As the flood recedes, water enriched in solutes drains into the river with decreasing water levels, evidenced by the temporal slopes with $\beta > 0$ (Fig. 5c) during flood recession (October to January) and the solute enrichment between 0.3 NWL to low flow from C-NWL relationships (Fig. 5d). The river water with enriched solutes could be from the drainage of the riparian swamps, delivering dissolved salts sourced from the tree islands and isolated wetland pools in the panhandle to the river as the flood recedes. This explanation is consistent with solute (particularly carbon) delivery into the river in the panhandle during flow recession captured in the Akoko et al. (2013) study.

5.3.3. Hydrologic controls on the TDI concentration variations in the lower delta region

For the ORI Island station, we show the NWL hydrograph (Fig. 6a), the temporal TDI concentrations (Fig. 6b), the temporal slopes (β) (Fig. 6c) and the C-NWL relationships (Fig. 6d) for the rising and falling limbs of the NWL hydrograph. We observe minimal solute response in the river at the ORI island station compared to the Mohembo and Seronga stations as reflected in the temporal slopes plot where $\beta = \sim 0$ (Fig. 6c) and where the TDI concentrations are nearly constant from 0.4 NWL to peak flow (Fig. 6d). However, the TDI concentrations slightly increase

from ~0.4 NWL to low flow on the falling limbs (Fig. 5d). The relatively small change in the solute concentration in the river in this reach where the wetlands are seasonally flooded (Mladenov et al., 2005; Wolski et al., 2006) is indicative of a more homogeneous solute reservoir feeding the river. As river water flows from the confined panhandle to the upper portion of the lower delta, it spreads out into a distributary system. Thus, the minimal change in the solute concentrations as the flood pulse advances and recedes may be because the absolute amount of new water delivered to this portion of the Boro River that flows through the ORI station is a small fraction of the discharge of the Okavango River flowing through the Panhandle. We note that there is a slight decrease in the TDI concentrations in the lower delta during the rainy season (December-February) from low water to about 0.4 NWL during the rising limbs (Fig. 6b and d). The annual flood pulse causes a marked decrease in the TDI concentrations from May to November and between NWL of 0.7 and peak discharge on the rising limb and from peak discharge to 0.4 NWL on the receding limb of the NWL hydrograph. Nevertheless, it appears that the amount of new river water from the annual pulse flooding and seasonal rains cause only limited mixing and dilution of solutes in the river, and that the temporal slopes of ~0 (Fig. 6c) indicate a similar solute source. Alternatively, we hypothesize that the river water flow from the panhandle (confined flow with transverse width of ~12 km) spreads across a much larger portion of the wetland (transverse width of >150 km for distributaries) (Tooth and McCarthy, 2004) in the lower delta. In this scenario, water in the river is a much smaller component compared to water in the wetland that interacts with the river. In addition, since the river near the ORI Island station is close to a tree island, the minimal change in the solute concentrations may be due to the unidirectional ET-driven water flow to- wards the tree island (e.g., McCarthy et al., 1991; Mladenov et al., 2014; Ramberg and Wolski, 2008) which

results in little to no solute transfer from the floodplains into the river along this river reach and similar reaches.

5.3.4. Hydrologic controls on the TDI concentration variations at the outlet of the delta

For the Maun station, we show the NWL hydrograph (Fig. 7a), the temporal TDI concentrations (Fig. 7b), the temporal slopes (β) (Fig. 7c) and the C-NWL relationships (Fig. 7d) for the rising and falling limbs of the hydrograph. At Maun, the river is confined and thus, the water that spread-out from the distributary system and over a much broader wetland area in the lower delta region at the ORI Island reach is channeled through a narrow (~30-100 m width) channel. We observe mostly a dilution-driven solute response in the river characterized by slope values of $\beta < 0$ during flow recession from July November (Fig. 7c). The decreases in the TDI concentrations are observed from ~0.8 NWL to peak flow (Fig. 7d). It is evident that the change in the river morphology and therefore the river water-wetland interaction between the lower delta and the Delta outlet plays a significant role in the differences in the solute response in the lower delta at the ORI Island and the outlet of the Delta in Maun. The river channel at the outlet in Maun is basically a collection system because the river at this location has relatively limited interaction with wetlands compared to the river at the ORI station (Fig. 1). At the Maun station, the TDI concentrations increase during flood recession from July to November and show greater variability compared to the flood recession from October to February or during the flood rise from February to June (Fig. 7b). Although the TDI concentrations (Fig. 7b) increase during the flood recession (Fig. 7a), the slopes are < 0 and indicate a source of water with lower solute concentrations consistent with dilution during this period (Fig. 7c). Additionally, the effect of seasonal rains is observable in the hydrograph from December to March (Fig. 7a) accompanied by TDI concentration decreases (Fig. 7b), yet the slope values ($\beta \sim 0$) indicate no change in solute source

(7c). The C-NWL is relatively flat from 0.4 NWL to low flow (Fig. 7d). It therefore appears that during the rainy season, the falling rains which may have interacted with the solute reservoirs in the Delta wetland (precipitates on the floodplain and on the islands and the isolated evaporated wetland pools) and the broader watershed may not have transferred enough solutes into the river to cause significant enrichment in the river solutes. Alternatively, since our monitoring period was during the transition from the drought and flood period, the Delta was significantly flooded, and several intermittent channels flowed after >15 y of no-flow. Therefore, the dilution response in the Okavango River at the outlet may be due to the contribution of additional fresh water from the newly flowing channels in the lower delta.

5.4. Implications of the variable solute responses across endorheic basins

Our results show spatial and temporal heterogeneity in the river solute response driven by hydrologic processes, ET and the changing river morphology across the endorheic Okavango River Basin. Our findings demonstrate that in endorheic basins where river flow is highly variable and ET rates are high, water movement and solute processing in rivers are strongly governed by hydrology and ET which causes salt accumulation on the basin surface (Yapiyev et al., 2017) and evapoconcentration of solutes in the river and in wetlands. In addition, the diverse morphology of rivers draining endorheic basins modifies river flow and solute behavior across the basin and typically transitions from (1) channel systems in the headwaters originating from mountains or highlands (e.g., Upper Okavango River Basin; Fig. 8), to (2) a well- defined and confined channel dominated by advective transport (Panhandle; Fig. 8) then (3) a dispersal system forming a lower delta area (Lower delta region; Fig. 8) and (4) an outlet channel (Delta outlet; Fig. 8) through which water is exported from the delta area to a terminal lake (e.g., Lake Ngami). Similar to the Okavango River, several other river systems in endorheic basins exhibit changing river

morphology, for instance, the Helmand River drains the transboundary endorheic Helmand basin occupying parts of Afghanistan, Pakistan and Iran. The Helmand River transitions from the upper delta in the headwaters to the lower delta comprised of wetlands then flow towards the lowest part ending in a hypersaline lake named Gowd-e-Zareh (Vekerdy et al., 2006; Yapiyev et al., 2017). This diverse morphology of rivers in endorheic basins that modifies water flow and solute transport has implications for the characterization of spatial solute dynamics, the design of water quality monitoring regimes and water management decision making across endorheic basins.

The upper watershed section (segment 1; Fig. 8) is characterized by variable solute responses in the channel system driven by episodic solute enrichment from river connectivity to groundwater and river-floodplain interaction involving the release of solute enriched water "packages" from floodplains into the river during low flow, and dilution from flooding at high flow. Unlike the upper watershed, the lower watershed area hosting segments 2, 3 and 4 (Fig. 8) are characterized by groundwater recharge by the river and solute enrichment from river interaction with solute stores in the local watershed. The difference in the river- groundwater-wetland interaction between the upper watershed and lower watershed area is typical of river basins transcending different climatic conditions. For instance, the Okavango River Basin spans from temperate climate in the upper watershed to semi-arid climate within the lower watershed area and thus, providing interesting insights on the hydrologic controls of solute behavior in settings with both effluent and influent rivers draining an endorheic basin.

The water exiting the upper watershed flows within a well-defined and confined channel in the middle section of the basin (segment 2; Fig. 8) which transports solutes to the lower delta area. Owing to the channel confinement and associated faster flow, the flowing water in the channel has a shorter residence time resulting mostly in advection dominating over the effects of ET in the

river channel. In this river segment, the river interacts with riparian swamps which drain solute enriched water into the river at low flow and flooding induces dilution in the river at high flow. The solute responses in the middle segment of basins are crucial for determining solute cycling and solute transport rates in faster flowing confined channels with episodic solute input from riparian wetlands.

Upon reaching the terminus of an endorheic basin, the river spreads out into distributary channels forming the lower delta region (segment 3, Fig. 8). The lower delta is dominated by dispersive transport of water and solutes (Gooseff et al., 2008) which allows for extensive river-floodplain-wetland-island interaction. Due to the water dispersion in the lower delta, water depths are shallow and river flow is slower (Gooseff et al., 2008), thereby increasing the residence time of water in the lower delta which predisposes the water to pronounced effects of ET in endorheic basins. Although one would expect high solute variability in the lower delta area from river-floodplain-wetland-island interaction and ET, the occurrence of location specific solute response of minimal solute variability can be observed in the distributary channels depending on the amount of water and solutes delivered from the upper delta to the different river reaches in the lower delta area and the extent of river-floodplain-wetland-island interaction along the river reaches. The location specific solute responses in the lower delta region of endorheic basins have implications for constraining solute behavior in lower delta areas as it may be highly variable both in space and time.

The outlet of the delta area (segment 4, Fig. 8) acts as a collection system where water exported out of the delta area is channeled through a narrow river channel. The solute dynamics at the delta outlet is dependent on the solute concentrations of the exported water from the lower delta such that if the water from the lower delta region did not accumulate solutes to cause significant solute

enrichment in the river, the outlet will show a dilution-driven response. Thus, the delta outlet is a good point to monitor solute load and outflux from the delta area of endorheic basins which has implications for quantifying salt contribution of inland deltas to downstream lakes and salt pans. The variable solute responses in the different segments of a river in an endorheic basin show that river systems in endorheic basins can be complex and it may be misleading to describe them as single hydrochemical response river systems.

The river connectivity to solute stores (salt precipitates and isolated wetland pools) in the local watershed (e.g., Covino, 2017) observed across the different segments of the river geometry mostly at lower flow (e.g., Figs. 4, 6 and 7) highlights the existence of hydro-geochemical "hot moments" created by hydrology and "hotspots" within flood- plains, salt islands and isolated wetland pools in endorheic basins. The hot moments in rivers in endorheic basins are characterized by solute enrichments occurring mostly at low flow which are attenuated to baseline river chemistry by pulse flooding and storm events. We propose that the "hydrologic reset" of hot moments in the river to baseline river chemistry helps maintain the surface water resources fresh in endorheic basins by diluting river solutes and evapoconcentrated solutes in wetland water, and by facilitating the "flushing" of solutes out of the delta area via "Hydrologic solute flushing", as suggested for the Okavango Delta by Ramatlapeng et al. (2021). Under the ongoing climate change which is projected to significantly affect river inflow by reducing precipitation, while simultaneously increasing ET in endorheic basins such as the Okavango River Basin (Milzow et al. 2010), the main mechanisms (ie., hydrologic reset in the river and hydrologic solute flushing from the Delta) maintaining surface waters fresh are under great threat. The projected increasing aridity in most endorheic basins will impact the hydrochemical status of the rivers by enhancing salinization and thereby affecting the river's ecological functioning and water quality status.

6. Conclusions

A high frequency time series investigation of solutes conducted in the Okavango River across the Okavango Delta in the middle Kalahari Desert in Botswana showed marked spatial and temporal variability in solute concentrations. The variations in river solute concentrations are controlled by two main processes that modify solute behavior: (1) sea sonal climate driven evapotranspiration (ET) and (2) hydrologically driven differential solute transfer from the local wetlands into the Okavango River. At the spatial scale, ET causes progressive downriver enrichment in TDI concentrations at 0.1 mg/L per km of river flow. At a temporal scale, the TDI concentrations increase from evapoconcentration during the hot rainy season and decrease from an annual pulse flooding. Additionally, superimposed on the seasonal solute behavior are sub-seasonal solute transfer from the floodplains, salt islands and isolated evaporated wetland pools initiated by hydrologic piston flow during rising flooding and drainage into the river during flood recession. The influx of solutes into the river by pulse flooding helps maintain the Delta in pristine freshwater conditions by facilitating solute "flushing" and export out of the Delta. Our findings indicate that the temporal hydrology, river connectivity to solute stores in the local watershed and evapotranspiration jointly control the solute behavior at variable spatial and temporal scales in rivers in arid watersheds, and that concentration-normalized water levels (C-NWL) relationships constructed from high resolution time series data are useful in characterizing solute dynamics in ungauged rivers in arid watersheds.

7. Figures

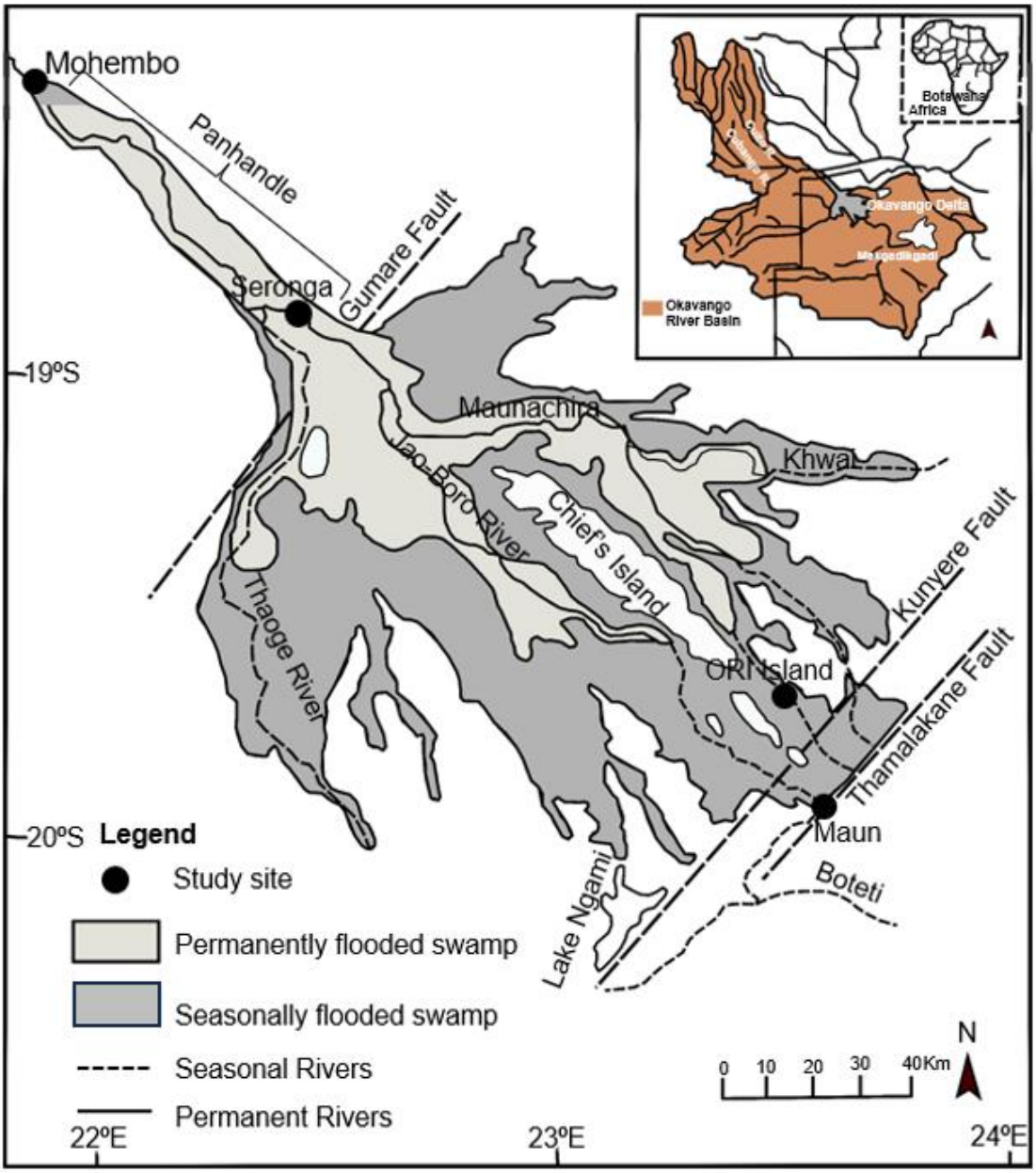

Figure 1: Map of the Okavango Delta, showing the Panhandle, the lower delta region, seasonal and permanent rivers and some islands (Modified from Ellery et al., 2003). The monitoring stations used in this study are shown as filled black circles. The insert shows the location of the Okavango Delta in Africa and the Okavango River Basin (Modified from Kgathi et al., 2006).

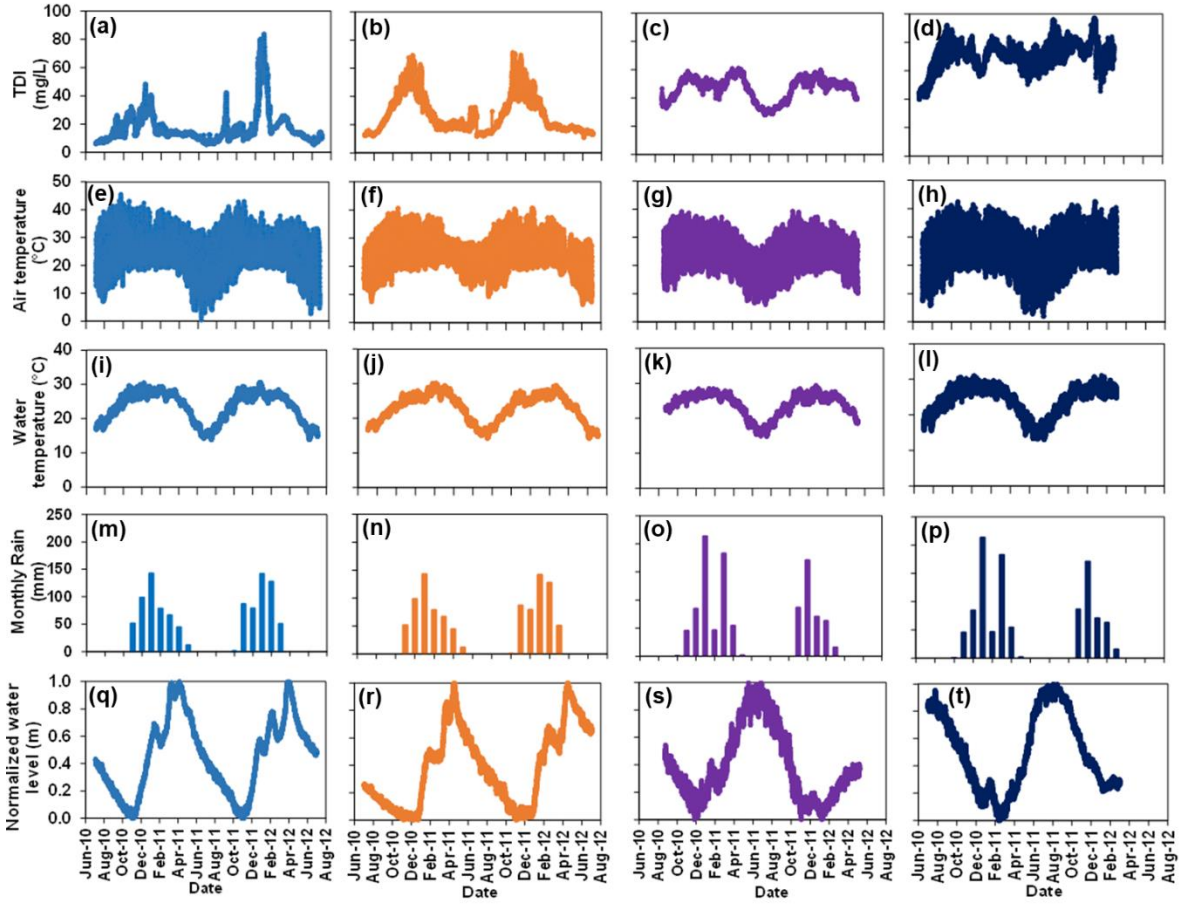

Figure 2: Temporal plots of the total dissolved ions (TDI) concentrations (a, b, c and d), air temperature (e, f, g and h), water temperature (i, j, k and l), monthly rain (m, n, o and p) and normalized water levels (q, r, s and t) measured from the Mohembo, Seronga, ORI Island and Maun stations along the Okavango River.

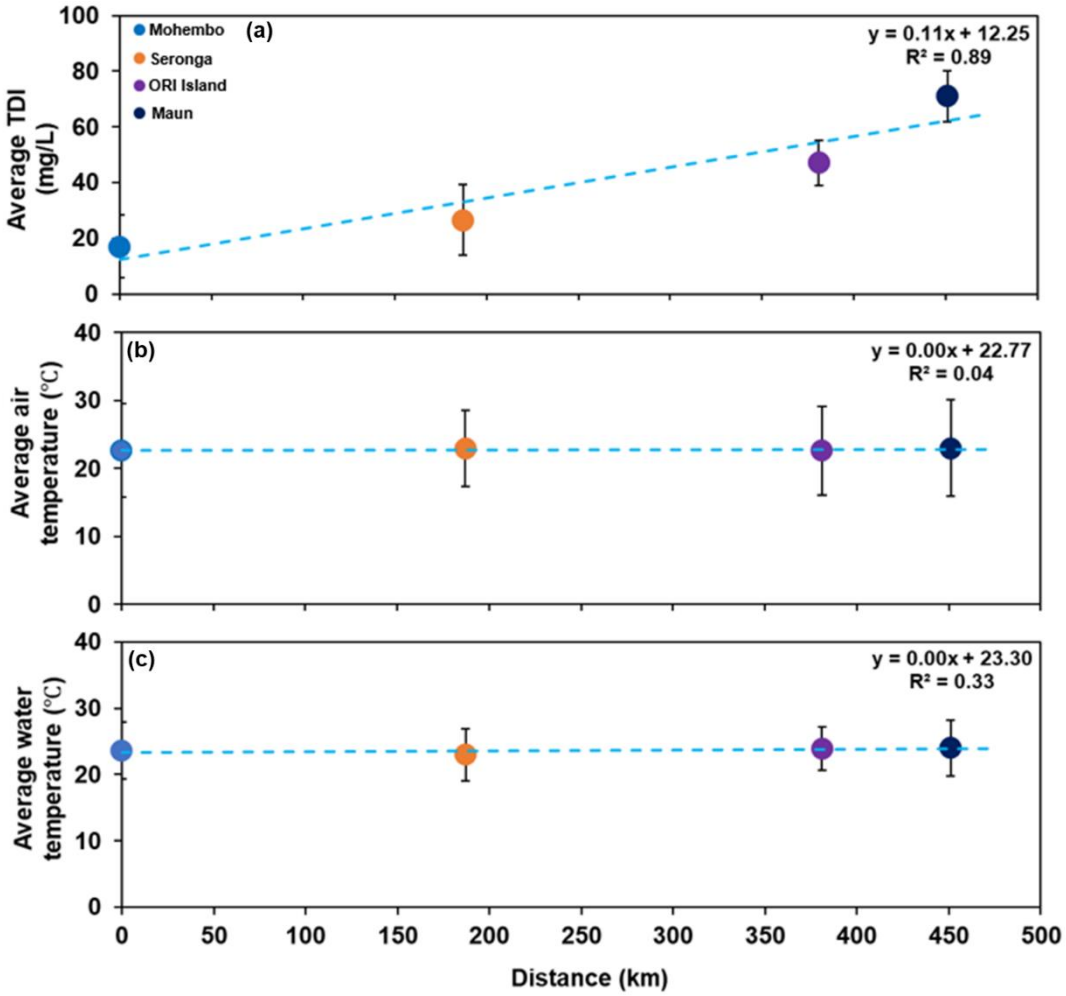

Figure 3: Plots of river distance vs the average total dissolved ions (TDI) concentrations (a), air temperature (b) and water temperature (c) measured from the Mohembo, Seronga, ORI Island and Maun stations along the Okavango River.

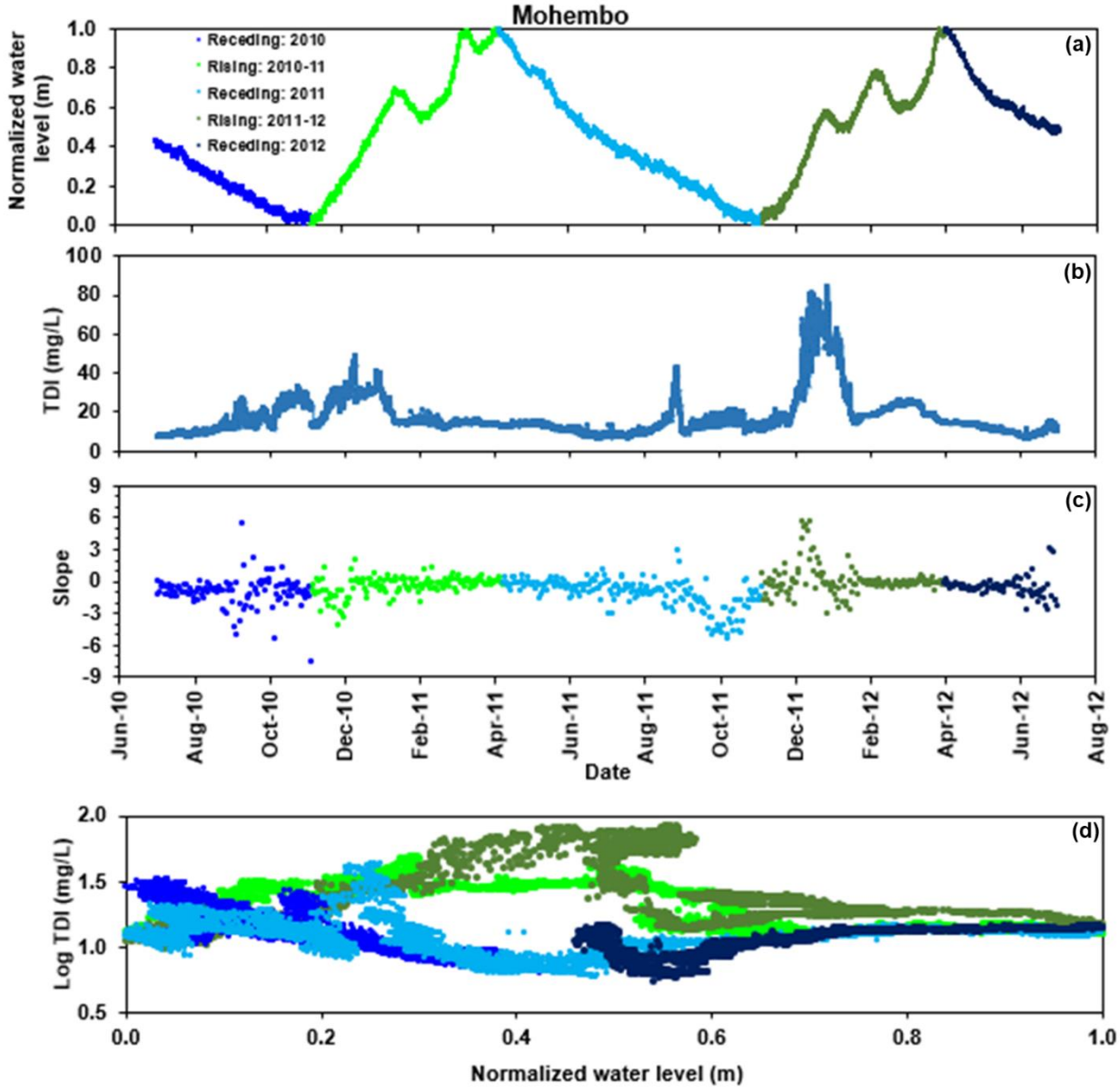

Figure 4: Normalized water level hydrograph (a) at the Mohembo station, color differentiated based on rising and receding water levels. Also shown are the temporal plots of the total dissolved ions (TDI) concentrations (b) and the slopes of the relationship between TDI concentrations and normalized water level (c), and the relationship between normalized water level and Log TDI concentrations during rising and receding flow (d) at Mohembo.

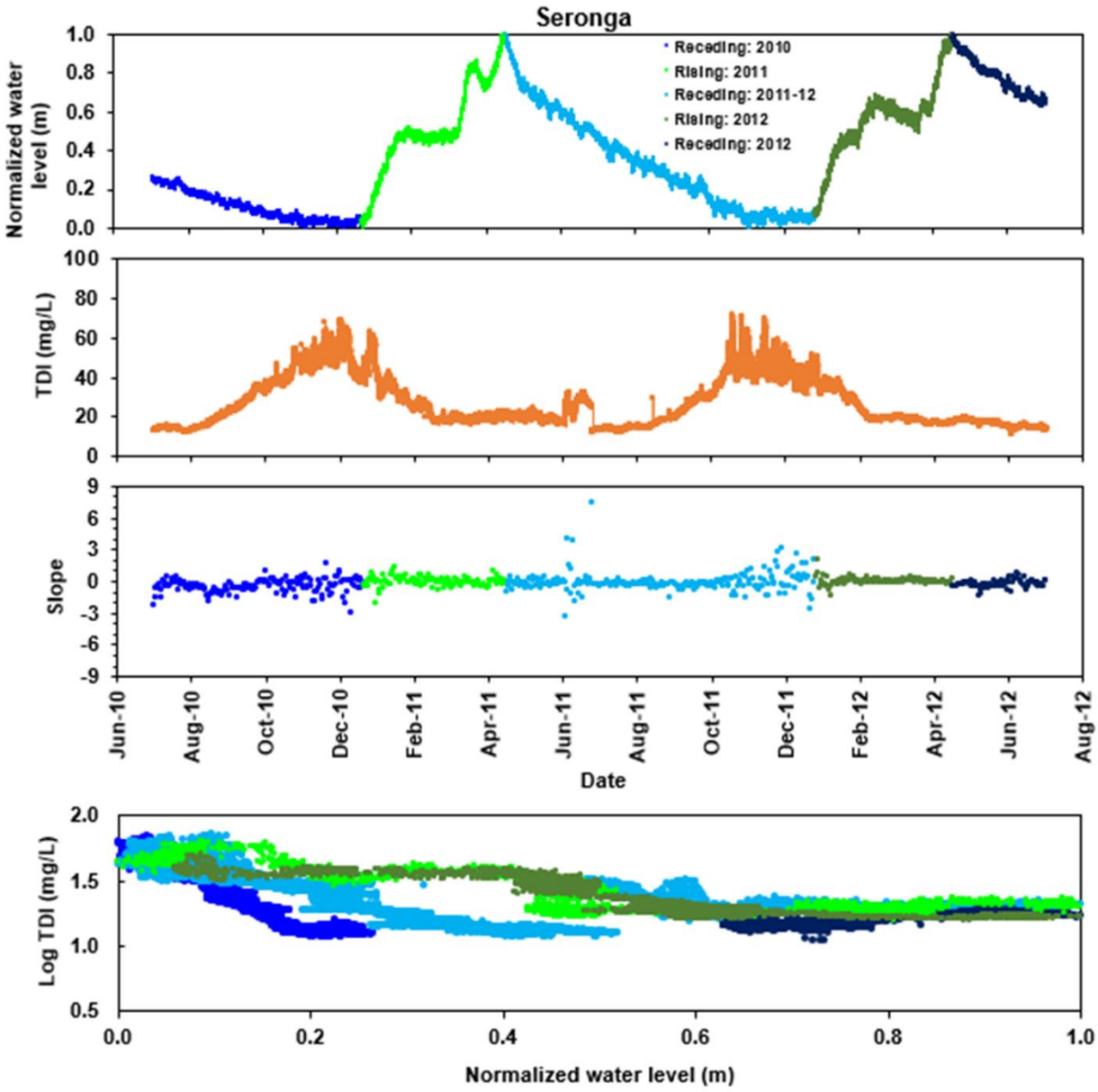

Figure 5: Normalized water level hydrograph (a) at the Seronga station, color differentiated based on rising and receding water levels. Also shown are the temporal plots of the total dissolved ions (TDI concentrations (b) and the slopes of the relationship between TDI concentrations and normalized water level (c), and the relationship between normalized water level and Log TDI concentrations during rising and receding flow (d) at Seronga.

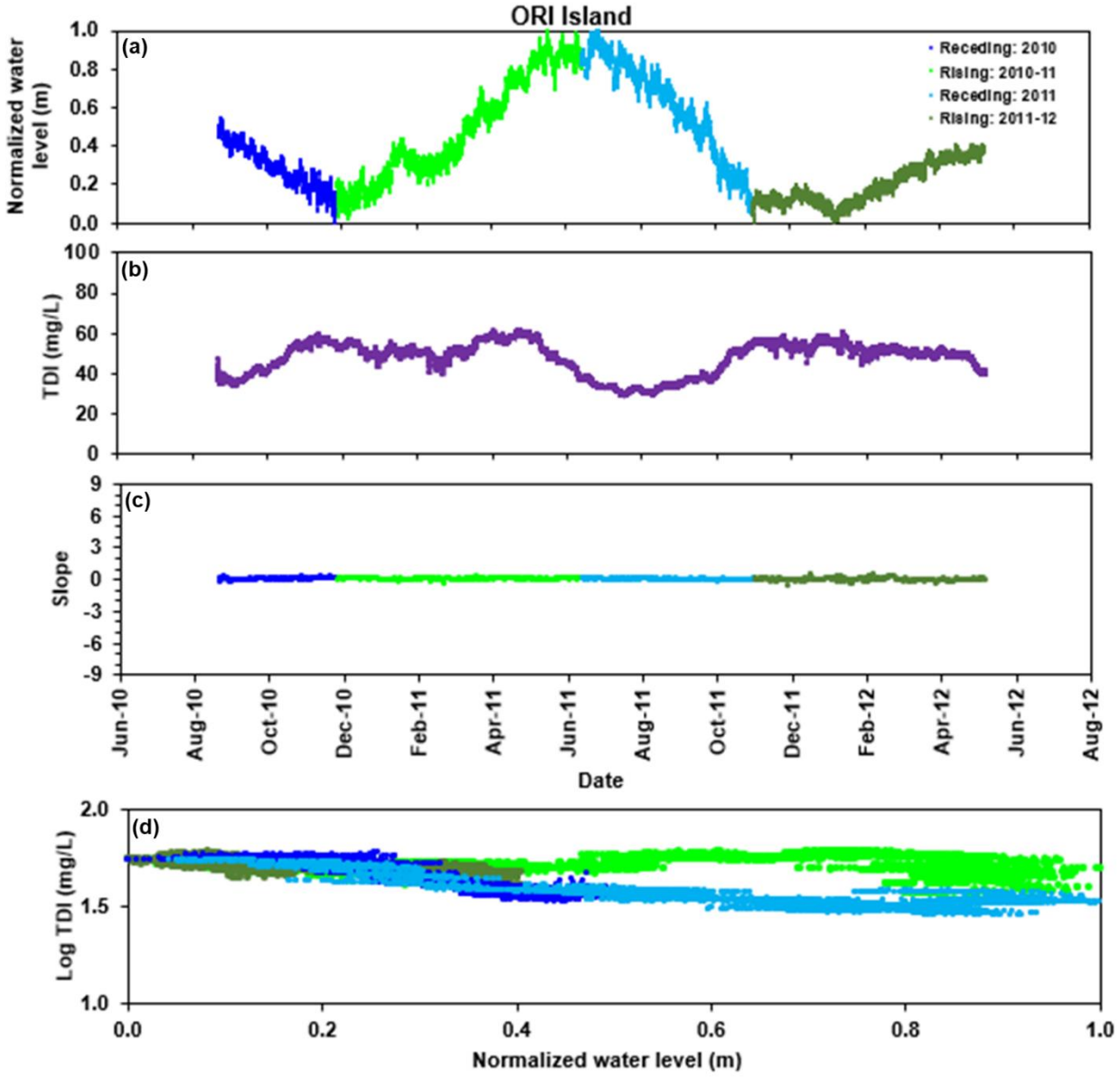

Figure 6: Normalized water level hydrograph (a) at the ORI Island station, color differentiated based on rising and receding water levels. Also shown are the temporal plots of the total dissolved ions (TDI) concentrations (b) and the slopes of the relationship between the TDI concentrations and normalized water level (c), and the relationship between normalized water level and Log TDI concentrations during rising and receding flow (d) at ORI Island.

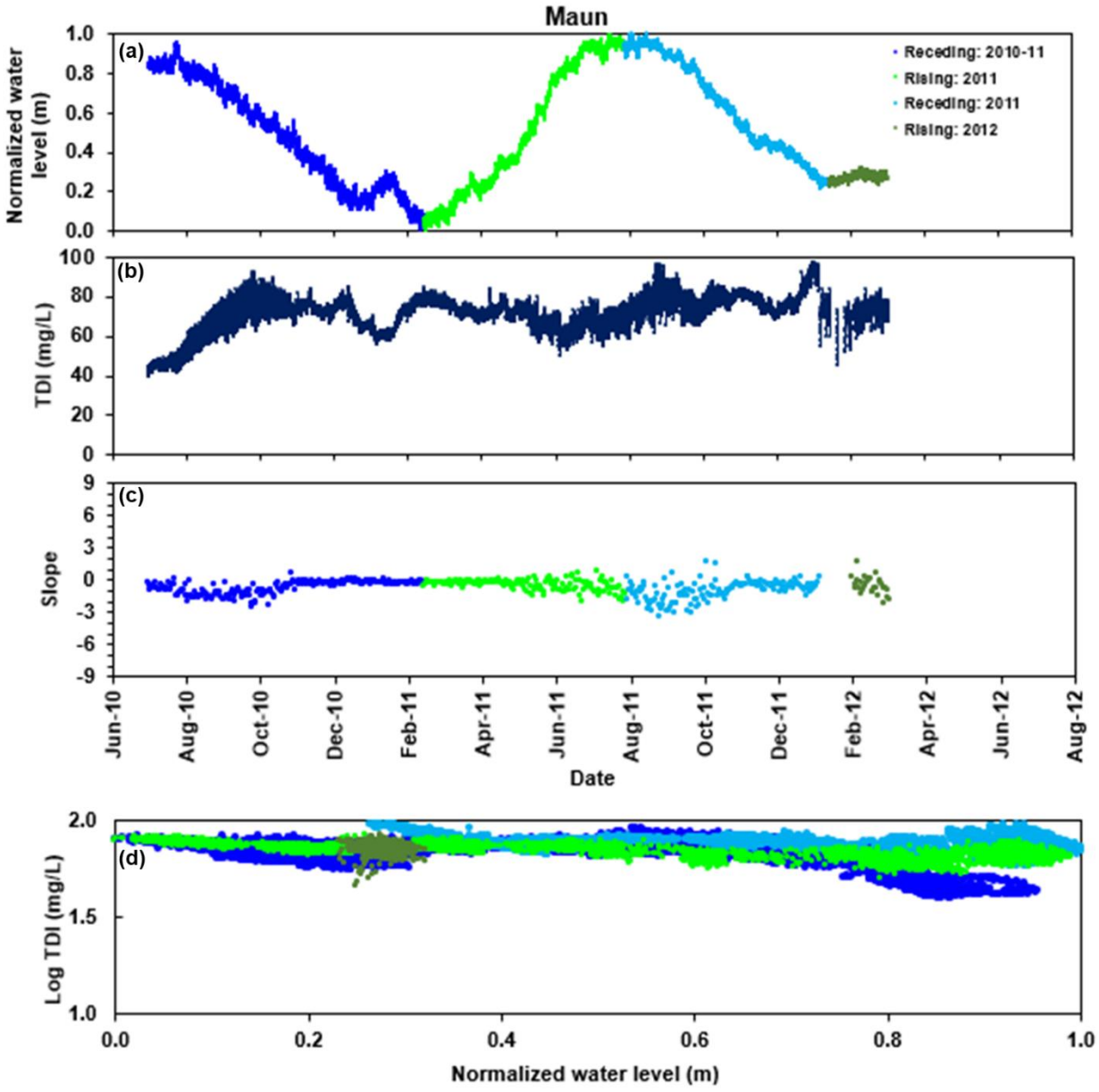

Figure 7: Normalized water level hydrograph (a) at the Maun station, color differentiated based on rising and receding water levels. Also shown are the temporal plots of total dissolved ions (TDI) concentrations (b) and the slopes of the relationship between TDI concentrations and normalized water level (c), and the relationship between normalized water level and Log TDI concentrations during rising and receding flow (d) at Maun.

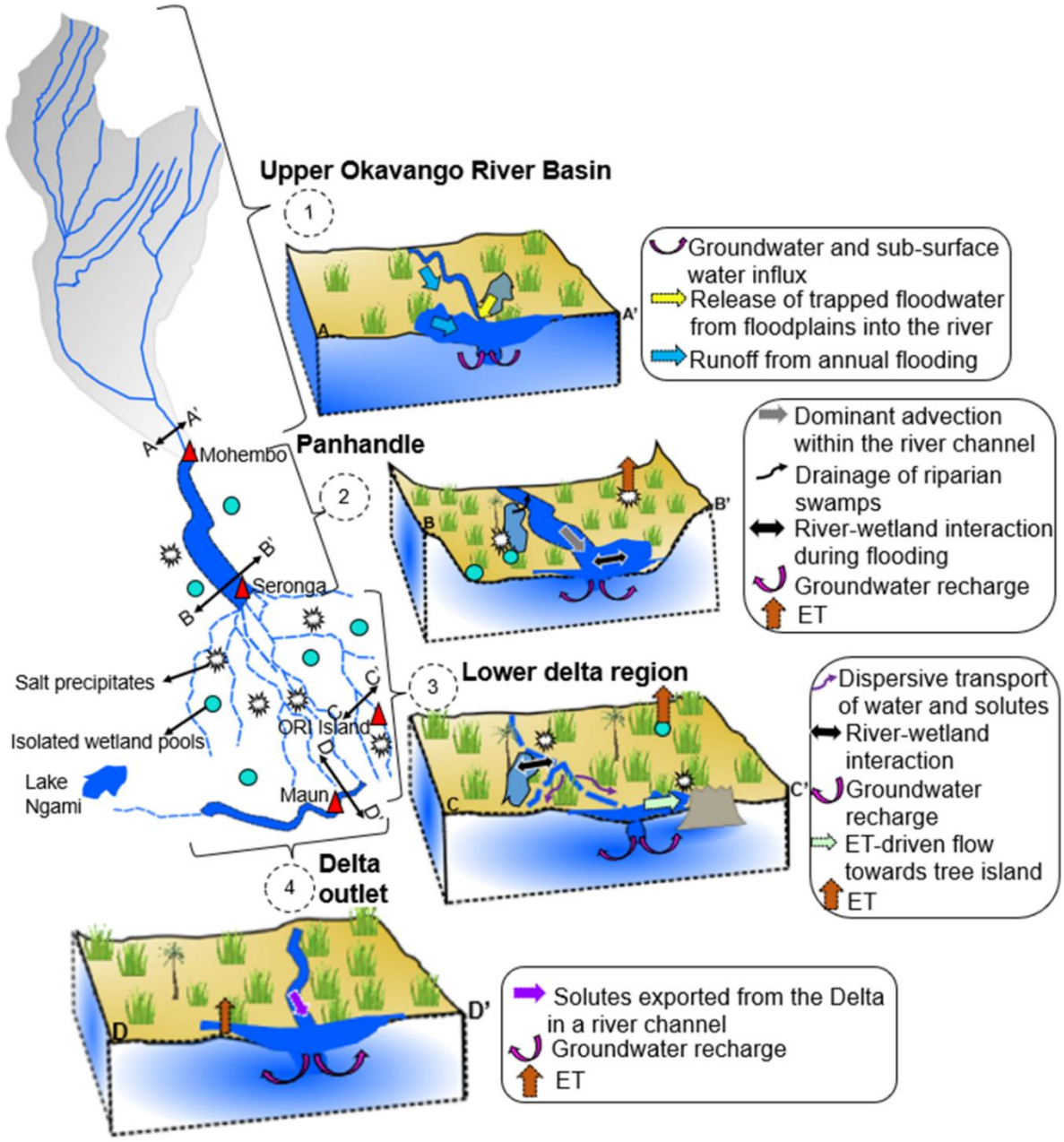

Figure 8: Conceptual model illustrating processes driving changes in the solute concentrations across the Okavango Delta. The role of hydrologic processes and ET in controlling solute dynamics is shown in cross sections A-A' for the upper watershed above the Mohembo station, at B-B' for the Panhandle region above the Seronga station, at C-C' for the lower delta above the Okavango Research Institute (ORI) Island station and D-D' for the river segment at the exit of the Delta above the Maun station.

8. Supplementary figures

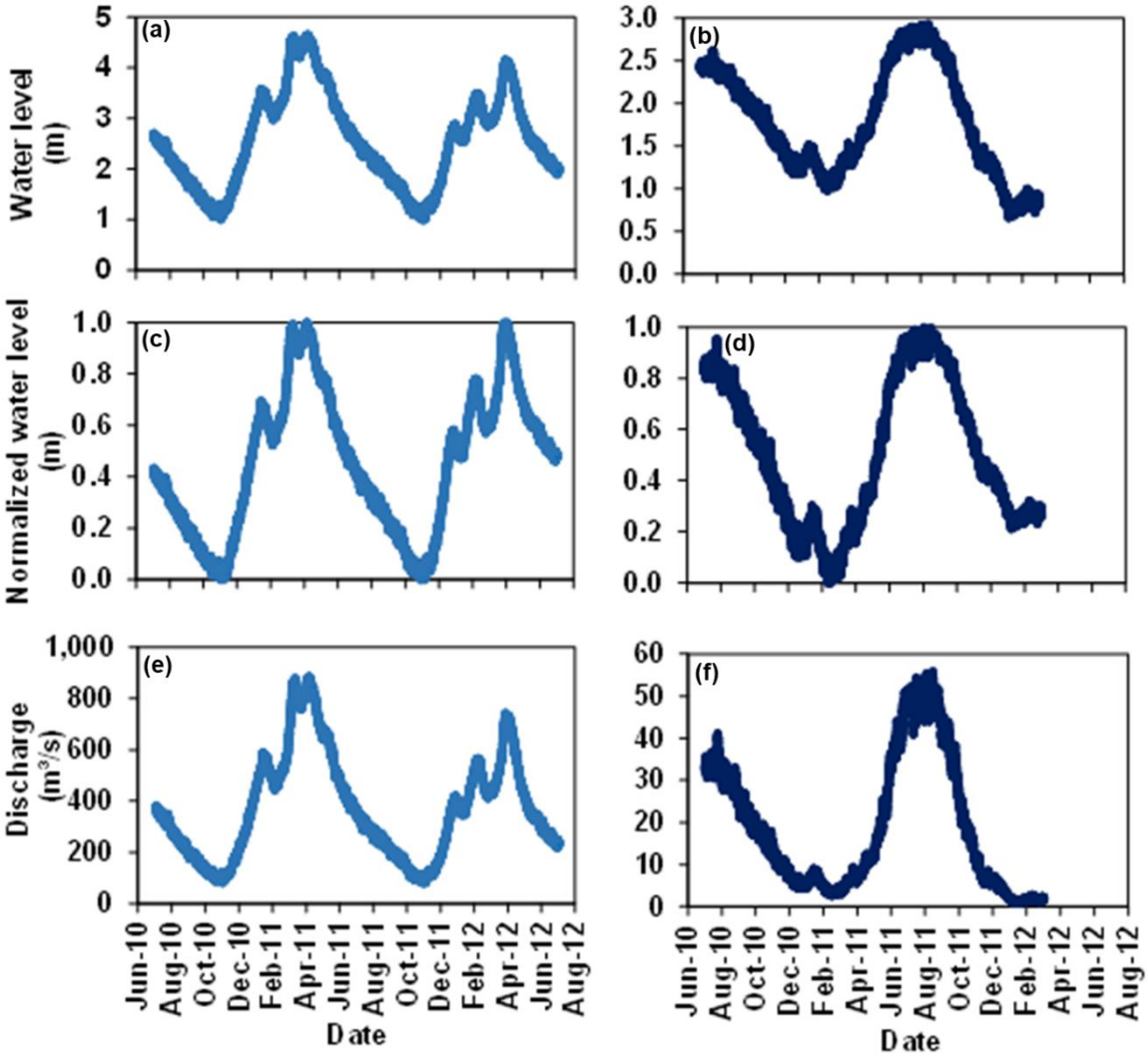

Supplementary figure 1: Temporal plots of water level (a and b), normalized water level (c and d) and river discharge (e and f) measured from the Mohembo and Maun stations in the Okavango River in the Okavango Delta, Botswana

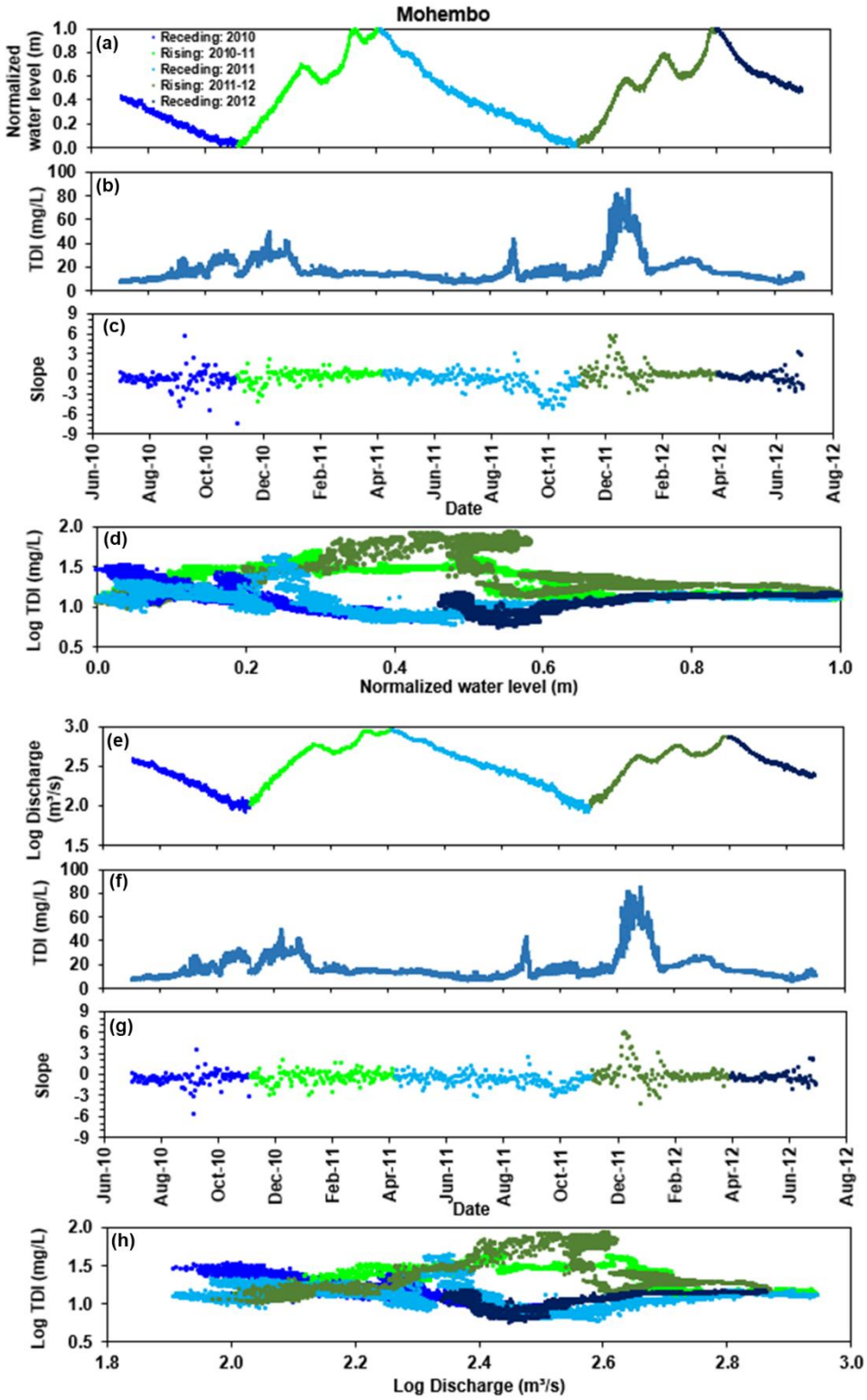

Supplementary figure 2: Normalized water level (a) and discharge (e) hydrographs at the Mohembo station, color differentiated based on receding and rising water levels or discharge. The

plots of TDI (b and f), slope of the relationship between Log TDI and Normalized water level (c), the relationship between Log TDI and normalized water level (d), the slope of the relationship between Log TDI and Log discharge (g) and the relationship between Log TDI and Log Discharge (h) during receding and rising water levels and discharge are also shown.

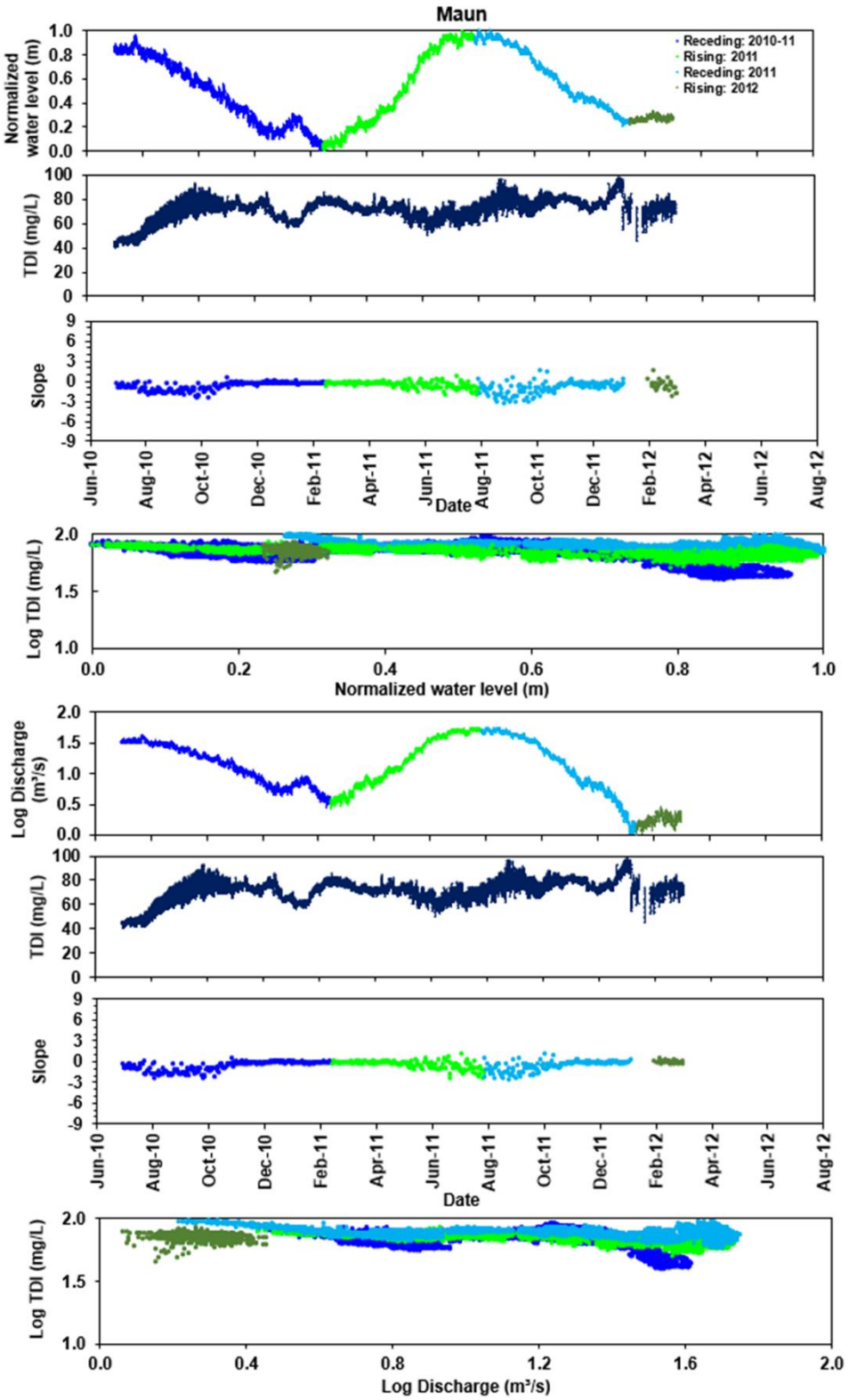

Supplementary figure 3: Normalized water level (a) and discharge (e) hydrographs at the Maun station, color differentiated based on receding and rising water levels or discharge. The plots of

TDI (b and f), slope of the relationship between Log TDI and Normalized water level (c), the relationship between Log TDI and normalized water level (d), the slope of the relationship between Log TDI and Log discharge (g) and the relationship between Log TDI and Log Discharge (h) during receding and rising water levels and discharge are also shown.

8. **Table 1:** Descriptive statistics for measured parameters. Min = minimum; Max = maximum; SD = Standard deviation; n = Number of data; TDI = total dissolved ions

Parameter	Mean	Min.	Max.	SD	n
TDS (mg/L) in Mohembo	17.1	5.5	83.6	11.4	17250
TDS (mg/L) in Seronga	26.6	11.0	71.2	12.6	17300
TDS (mg/L) in ORI Island	47.1	28.3	61.1	8.1	14759
TDS (mg/L) in Maun	71.0	39.9	97.2	9.2	14427
Air temperature (°C) in Mohembo	22.7	0.5	45.6	6.9	17250
Air temperature (°C) in Seronga	23.0	6.4	40.7	5.6	17300
Air temperature (°C) in ORI Island	22.6	6.2	39.3	6.5	14759
Air temperature (°C) in Maun	23.0	2.0	42.6	7.1	14427
Water temperature (°C) in Mohembo	23.6	13.8	30.6	4.3	17250
Water temperature (°C) in Seronga	23.0	14.3	30.2	3.9	17300
Water temperature (°C) in ORI Island	23.9	14.9	29.4	3.3	14759
Water temperature (°C) in Maun	24.0	13.0	31.1	4.2	14427
Monthly rain (mm) in Mohembo	37.6	0	142.7	49.4	17250
Monthly rain (mm) in Seronga	37.6	0	142.7	49.4	17300
Monthly rain (mm) in ORI Island	39.8	0	213.3	62.6	14759
Monthly rain (mm) in Maun	39.8	0	213.3	62.6	14427
Normalized water level (m) in Mohembo	0.5	0	1.0	0.3	17250
Normalized water level (m) in Seronga	0.4	0	1.0	0.3	17300
Normalized water level (m) in ORI Island	0.4	0	1.0	0.3	14759
Normalized water level (m) in Maun	0.5	0	1.0	0.3	14427

9. Citations

Ahearn, D.S., Sheibley, R.W., Dahlgren, R.A. and Keller, K.E., 2004. Temporal dynamics of stream water chemistry in the last free-flowing river draining the western Sierra Nevada, California. Journal of Hydrology, 295(1-4), pp.47-63.

Akoko, E., Atekwana, E.A., Cruse, A.M., Molwalefhe, L. and Masamba, W.R., 2013. River-wetland interaction and carbon cycling in a semi-arid riverine system: the Okavango Delta, Botswana. Biogeochemistry, 114(1-3), pp.359-380.

Akondi, R.N., Atekwana, E.A. and Molwalefhe, L., 2019. Origin and chemical and isotopic evolution of dissolved inorganic carbon (DIC) in groundwater of the Okavango Delta, Botswana. Hydrological sciences journal, 64(1), pp.105-120.

Atekwana, E.A., Molwalefhe, L., Kgaodi, O. and Cruse, A.M., 2016. Effect of evapotranspiration on dissolved inorganic carbon and stable carbon isotopic evolution in rivers in semi-arid climates: The Okavango Delta in North West Botswana. Journal of Hydrology: Regional Studies, 7, pp.1-13.

Basu, N.B., Thompson, S.E. and Rao, P.S.C., 2011. Hydrologic and biogeochemical functioning of intensively managed catchments: A synthesis of top-down analyses. Water Resources Research, 47(10).

Baumberg, V., Helmschrot, J., Steudel, T., Göhmann, H., Fischer, C. and Flügel, W.A., 2014. Assessing basin heterogeneities for rainfall–runoff modelling of the Okavango River and its transboundary management. Proceedings of the International Association of Hydrological Sciences, 364, pp.320-325.

Bereslawski, E., 1997. Geohydrology, Geology, and Soils of the Cubango River Basin (Angolan Sector). OKACOM Okavango River Basin Preparatory Assessment Study, Specialist's Report.

Boyer, E.W., Hornberger, G.M., Bencala, K.E. and McKnight, D.M., 1997. Response characteristics of DOC flushing in an alpine catchment. Hydrological processes, 11(12), pp.1635-1647.

Bufford, K.M., Atekwana, E.A., Abdelsalam, M.G., Shemang, E., Atekwana, E.A., Mickus, K., Moidaki, M., Modisi, M.P. and Molwalefhe, L., 2012. Geometry and faults tectonic activity of the Okavango Rift Zone, Botswana: Evidence from magnetotelluric and electrical resistivity tomography imaging. Journal of African Earth Sciences, 65, pp.61-71.

Catuneanu, O., Wopfner, H., Eriksson, P.G., Cairncross, B., Rubidge, B.S., Smith, R.M.H. and Hancox, P.J., 2005. The Karoo basins of south-central Africa. Journal of African Earth Sciences, 43(1-3), pp.211-253.

Clow, D.W. and Mast, M.A., 2010. Mechanisms for chemostatic behavior in catchments: Implications for CO2 consumption by mineral weathering. Chemical Geology, 269(1-2), pp.40-51.

Covino, T., 2017. Hydrologic connectivity as a framework for understanding biogeochemical flux through watersheds and along fluvial networks. Geomorphology, 277, pp.133-144.

Dalzell, B.J., Filley, T.R. and Harbor, J.M., 2007. The role of hydrology in annual organic carbon loads and terrestrial organic matter export from a midwestern agricultural watershed. Geochimica et Cosmochimica Acta, 71(6), pp.1448-1462.

Dawam, S.R. and Ku-Mahamud, K.R., 2019. Reservoir water level forecasting using normalization and multiple regression. Indonesian Journal of Electrical Engineering and Computer Science, 14(1), pp.443-449.

Dincer, T., Hutton, L.G. and Kupee, B.B.J., 1979. Study, using stable isotopes, of flow distribution, surface-groundwater relations and evapotranspiration in the Okavango Swamp, Botswana. In Isotope hydrology 1978.Duvert, C., Hutley, L.B., Birkel, C., Rudge, M., Munksgaard, N.C., Wynn, J.G., Setterfield, S.A., Cendón, D.I. and Bird, M.I., 2020. Seasonal shift from biogenic to geogenic fluvial carbon caused by changing water sources in the wet-dry tropics. Journal of Geophysical Research: Biogeosciences, 125(2).

Ellery, W.N., McCarthy, T.S. and Smith, N.D., 2003. Vegetation, hydrology, and sedimentation patterns on the major distributary system of the Okavango Fan, Botswana. Wetlands, 23(2), pp.357-375.

Evans, C., Davies, T.D., 1998. Causes of concentration/discharge hysteresis and its potential as a tool for analysis of episode hydrochemistry. Water Resour. Res. 34 (1), 129–137.

Fovet, O., Humbert, G., Dupas, R., Gascuel-Odoux, C., Gruau, G., Jaffrézic, A., Thelusma, G., Faucheux, M., Gilliet, N., Hamon, Y. and Grimaldi, C., 2018. Seasonal variability of stream water quality response to storm events captured using high-frequency and multi-parameter data. Journal of Hydrology, 559, pp.282-293.

Geeraert, N., Omengo, F.O., Borges, A.V., Govers, G. and Bouillon, S., 2017. Shifts in the carbon dynamics in a tropical lowland river system (Tana River, Kenya) during flooded and non-flooded conditions. Biogeochemistry, 132(1-2), pp.141-163.

Godsey, S.E., Kirchner, J.W. and Clow, D.W., 2009. Concentration–discharge relationships reflect chemostatic characteristics of US catchments. Hydrological Processes: An International Journal, 23(13), pp.1844-1864.

Gooseff, M.N., Bencala, K.E. and Wondzell, S.M., 2008. Solute transport along stream and river networks. River confluences, tributaries and the fluvial network, pp.395-417.

Gumbricht, T. and McCarthy, T.S., 2003. Spatial patterns of islands and salt crusts in the Okavango Delta, Botswana. South African Geographical Journal, 85(2), pp.164-169.

Gumbricht, T., McCarthy, J. and McCarthy, T.S., 2004. Channels, wetlands and islands in the Okavango Delta, Botswana, and their relation to hydrological and sedimentological processes. Earth Surface Processes and Landforms: The Journal of the British Geomorphological Research Group, 29(1), pp.15-29.

Gumbricht, T., McCarthy, T.S. and Merry, C.L., 2001. The topography of the Okavango Delta, Botswana, and its tectonic and sedimentological implications. South African Journal of Geology, 104(3), pp.243-264.

Herndon, E.M., Steinhoefel, G., Dere, A.L. and Sullivan, P.L., 2018. Perennial flow through convergent hillslopes explains chemodynamic solute behavior in a shale headwater catchment. Chemical Geology, 493, pp.413-425.

Humphries, M.S., McCarthy, T.S., Cooper, G.R.J., Stewart, R.A. and Stewart, R.D., 2014. The role of airborne dust in the growth of tree islands in the Okavango Delta, Botswana. Geomorphology, 206, pp.307-317.

Huntsman-Mapila, P., Kampunzu, A.B., Vink, B. and Ringrose, S., 2005. Cryptic indicators of provenance from the geochemistry of the Okavango Delta sediments, Botswana. Sedimentary Geology, 174(1-2), pp.123-148.

Jones, M.J., 2010. The groundwater hydrology of the Okavango basin. OKACOM Okavango River Basin Transboundary Diagnostical Analysis Technical Report.

Kgathi, D.L., Kniveton, D., Ringrose, S., Turton, A.R., Vanderpost, C.H.M., Lundqvist, J. and Seely, M., 2006. The Okavango; a river supporting its people, environment and economic development. Journal of Hydrology, 331(1-2), pp.3-17.

Kinabo, B.D., Atekwana, E.A., Hogan, J.P., Modisi, M.P., Wheaton, D.D. and Kampunzu, A.B., 2007. Early structural development of the Okavango rift zone, NW Botswana. Journal of African Earth Sciences, 48(2-3), pp.125-136.

Kinabo, B.D., Hogan, J.P., Atekwana, E.A., Abdelsalam, M.G. and Modisi, M.P., 2008. Fault growth and propagation during incipient continental rifting: Insights from a combined aeromagnetic and Shuttle Radar Topography Mission digital elevation model investigation of the Okavango Rift Zone, northwest Botswana. Tectonics, 27(3).

Letshele, K.P., Atekwana, E.A., Molwalefhe, L., Ramatlapeng, G.J. and Masamba, W.R., 2023. Stable hydrogen and oxygen isotopes reveal aperiodic non-river evaporative solute enrichment in the solute cycling of rivers in arid watersheds. Science of the Total Environment, 856, p.159113.

Liu, F., Parmenter, R., Brooks, P.D., Conklin, M.H. and Bales, R.C., 2008. Seasonal and interannual variation of streamflow pathways and biogeochemical implications in semi-arid, forested catchments in Valles Caldera, New Mexico. Ecohydrology: Ecosystems, Land and Water Process Interactions, Ecohydrogeomorphology, 1(3), pp.239-252.

Liu, J., Chen, B., Xu, Z.Y., Wei, Y., Su, Z.H., Yang, R., Ji, Y.X., Wang, X.D., Zhang, L.L., An, N. and Yang, F., 2020. Tracing solute sources and carbon dynamics under various hydrological conditions in a karst river in southwestern China. Environmental Science and Pollution Research, pp.1-12.

Lloyd, J.W. and Heathcote, J.A.A., 1985. Natural inorganic hydrochemistry in relation to ground water.

McCarthy, T.S. and Ellery, W.N., 1994. The effect of vegetation on soil and ground water chemistry and hydrology of islands in the seasonal swamps of the Okavango Fan, Botswana. Journal of Hydrology, 154(1-4), pp.169-193.

McCarthy, T.S. and Ellery, W.N., 1998. The okavango delta. Transactions of the Royal Society of South Africa, 53(2), pp.157-182.

McCarthy, T.S. and Metcalfe, J., 1990. Chemical sedimentation in the semi-arid environment of the Okavango Delta, Botswana. Chemical geology, 89(1-2), pp.157-178.

McCarthy, T.S., 2006. Groundwater in the wetlands of the Okavango Delta, Botswana, and its contribution to the structure and function of the ecosystem. Journal of hydrology, 320(3-4), pp.264-282.

McCarthy, T.S., Barry, M., Bloem, A., Ellery, W.N., Heister, H., Merry, C.L., Röther, H. and Sternberg, H., 1997. The gradient of the Okavango fan, Botswana, and its sedimentological and tectonic implications. Journal of African Earth Sciences, 24(1-2), pp.65-78.

McCarthy, T.S., Bloem, A. and Larkin, P.A., 1998. Observations on the hydrology and geohydrology of the Okavango Delta. South African Journal of Geology, 101(2), pp.101-117.

McCarthy, T.S., Ellery, W.N. and Ellery, K., 1993. Vegetation-induced, subsurface precipitation of carbonate as an aggradational process in the permanent swamps of the Okavango (delta) fan, Botswana. Chemical geology, 107(1-2), pp.111-131.

McCarthy, T.S., Ellery, W.N. and Stanistreet, I.G., 1992. Avulsion mechanisms on the Okavango fan, Botswana: the control of a fluvial system by vegetation. Sedimentology, 39(5), pp.779-795.

McCarthy, T.S., McIver, J.R. and Verhagen, B.T., 1991. Groundwater evolution, chemical sedimentation and carbonate brine formation on an island in the Okavango Delta swamp, Botswana. Applied Geochemistry, 6(6), pp.577-595.

McCarthy, TS, Cooper, GRJ, Tyson, PD &Ellery, W., 2000. Seasonal flooding in the Okavango Delta, Botswana-recent history and future prospects. South African Journal of Science, 96(1), pp.25-33.

Mendelsohn, J., el Obeid, S., 2004. Okavango River: The Flow of a Lifeline. Struik.

Merron, G.S., 1991. The ecology and management of the fishes of the Okavango Delta, Botswana, with particular reference to the role of the seasonal floods (Doctoral dissertation, Rhodes University).

Milzow, C., Burg, V. and Kinzelbach, W., 2010. Estimating future ecoregion distributions within the Okavango Delta Wetlands based on hydrological simulations and future climate and development scenarios. Journal of Hydrology, 381(1-2), pp.89-100.

Milzow, C., Kgotlhang, L., Bauer-Gottwein, P., Meier, P. and Kinzelbach, W., 2009. Regional review: the hydrology of the Okavango Delta, Botswana—processes, data and modelling. Hydrogeology Journal, 17(6), pp.1297-1328.

Mladenov, N., McKnight, D.M., Wolski, P. and Ramberg, L., 2005. Effects of annual flooding on dissolved organic carbon dynamics within a pristine wetland, the Okavango Delta, Botswana. Wetlands, 25(3), pp.622-638.

Mladenov, N., Wolski, P., Hettiarachchi, G.M., Murray-Hudson, M., Enriquez, H., Damaraju, S., Galkaduwa, M.B., McKnight, D.M. and Masamba, W., 2014. Abiotic and biotic factors influencing the mobility of arsenic in groundwater of a through-flow island in the Okavango Delta, Botswana. Journal of Hydrology, 518, pp.326-341.

Moatar, F., Abbott, B.W., Minaudo, C., Curie, F. and Pinay, G., 2017. Elemental properties, hydrology, and biology interact to shape concentration-discharge curves for carbon, nutrients, sediment, and major ions. Water Resources Research, 53(2), pp.1270-1287.

Modie, B.N., 2000. Geology and mineralisation in the Meso-to Neoproterozoic Ghanzi-Chobe Belt of northwest Botswana. Journal of African Earth Sciences, 30(3), pp.467-474.

Modisi, M.P., Atekwana, E.A., Kampunzu, A.B. and Ngwisanyi, T.H., 2000. Rift kinematics during the incipient stages of continental extension: Evidence from the nascent Okavango rift basin, northwest Botswana. Geology, 28(10), pp.939-942.

Mogobe, O., Mosimanyana, E., Masamba, W.R.L. and Mosepele, K., 2018. Monitoring water quality of the Upper Okavango Delta. Climate Change and Adaptive Land Management in Southern Africa—Assessments, Changes, Challenges, and Solutions. Biodiversity and Ecology, 6, pp.106-111.

Mosepele, K., Moyle, P.B., Merron, G.S., Purkey, D.R. and Mosepele, B., 2009. Fish, floods, and ecosystem engineers: aquatic conservation in the Okavango Delta, Botswana. Bioscience, 59(1), pp.53-64.

Mosepele, K., Ngwenya, B.N. and Bernard, T., 2006. Artisanal fishing and food security in the Okavango Delta, Botswana. World Sustainable Development Outlook: Global and Local Resources in Achieving Sustainable Development, Inderscience, Geneva, pp.159-168.

Moses, O. and Gondwe, M., 2019. Simulation of changes in the twenty-first century maximum temperatures using the statistical downscaling model at some stations in Botswana. Modeling Earth Systems and Environment, 5(3), pp.843-855.

Mosimane, K., Struyf, E., Gondwe, M.J., Frings, P., van Pelt, D., Wolski, P., Schoelynck, J., Schaller, J., Conley, D.J. and Murray-Hudson, M., 2017. Variability in chemistry of surface and soil waters of an evapotranspiration-dominated flood-pulsed wetland: solute processing in the Okavango Delta, Botswana. Water SA, 43(1), pp.104-115.

Musolff, A., Schmidt, C., Selle, B. and Fleckenstein, J.H., 2015. Catchment controls on solute export. Advances in Water Resources, 86, pp.133-146.

Nichols, G., 2007. Fluvial systems in desiccating endorheic basins. Sedimentary processes, environments and basins: a tribute to Peter Friend, pp.569-589.

Nyberg, B., Gawthorpe, R.L. and Helland-Hansen, W., 2018. The distribution of rivers to terrestrial sinks: Implications for sediment routing systems. Geomorphology, 316, pp.1-23.

Obakeng, O.T. and Gieske, A.S.M., 1997. Hydraulic conductivity and transmissivity of a water-table aquifer in the Boro River system, Okavango Delta. Botswana Geological Survey Department bulletin series, 46.

Oromeng, K.V., Atekwana, E.A., Molwalefhe, L. and Ramatlapeng, G.J., 2021. Time-series variability of solute transport and processes in rivers in semi-arid endorheic basins: The Okavango Delta, Botswana. Science of The Total Environment, 759, p.143574.

Peel, M.C., Finlayson, B.L. and McMahon, T.A., 2007. Updated world map of the Köppen-Geiger climate classification.

Pombo, S., de Oliveira, R.P. and Mendes, A., 2015. Validation of remote-sensing precipitation products for Angola. Meteorological Applications, 22(3), pp.395-409

Ramatlapeng, G.J., Atekwana, E.A., Molwalefhe, L. and Oromeng, K.V., 2021. Intermittent hydrologic perturbations control solute cycling and export in the Okavango Delta. Journal of Hydrology, 594, p.125968.

Ramberg, L. and Wolski, P., 2008. Growing islands and sinking solutes: processes maintaining the endorheic Okavango Delta as a freshwater system. Plant Ecology, 196(2), pp.215-231.

Ringrose, S., Harris, C., Huntsman-Mapila, P., Vink, B.W., Diskins, S., Vanderpost, C. and Matheson, W., 2009. Origins of strandline duricrusts around the Makgadikgadi Pans (Botswana Kalahari) as deduced from their chemical and isotope composition. Sedimentary Geology, 219(1-4), pp.262-279.

Rose, L.A., Karwan, D.L. and Godsey, S.E., 2018. Concentration–discharge relationships describe solute and sediment mobilization, reaction, and transport at event and longer timescales. Hydrological processes, 32(18), pp.2829-2844.

Sawula, G. and Martins, E., 1991. Major ion chemistry of the lower Boro River, Okavango Delta, Botswana. Freshwater Biology, 26(3), pp.481-493.

Steudel, T., Göhmann, H., Flügel, W.A. and Helmschrot, J., 2013. Assessment of hydrological dynamics in the upper Okavango River Basins. Biodiversity and Ecology, 5, pp.247-262.

Thompson, S.E., Basu, N.B., Lascurain Jr, J., Aubeneau, A. and Rao, P.S.C., 2011. Relative dominance of hydrologic versus biogeochemical factors on solute export across impact gradients. Water resources research, 47(10).

Tooth, S. and McCarthy, T.S., 2004. Controls on the transition from meandering to straight channels in the wetlands of the Okavango Delta, Botswana. Earth Surface Processes and Landforms: The Journal of the British Geomorphological Research Group, 29(13), pp.1627-1649.

Vekerdy, Z., Dost, R.J.J., Reinink, G. and Partow, H., 2006. History of environmental change in the Sistan Basin based on satellite image analysis: 1976-2005.

Wilson, B.H. and Dincer, T., 1976, August. An introduction to the hydrology and hydrography of the Okavango Delta. In Symposium on the Okavango Delta (pp. 33-48). Botswana Soc. Gaborone Botswana.

Wolski, P., Murray-Hudson, M., Savenije, H. and Gumbricht, T., 2005. Modeling of the hydrology of the Okavango Delta. Publication of the Water and Ecosystem Resources for Regional Development (WERRD) project, HOORC, Maun, Botswana.

Wolski, P., Savenije, H.H., Murray-Hudson, M. and Gumbricht, T., 2006. Modelling of the flooding in the Okavango Delta, Botswana, using a hybrid reservoir-GIS model. Journal of Hydrology, 331(1-2), pp.58-72.

Wymore, A.S., Leon, M.C., Shanley, J.B. and McDowell, W.H., 2020. Hysteretic response of solutes and turbidity at the event scale across forested tropical montane watersheds. Critical Zone (CZ) Export to Streams as Indicator for CZ Structure and Function.

Yapiyev, V., Sagintayev, Z., Inglezakis, V.J., Samarkhanov, K. and Verhoef, A., 2017. Essentials of endorheic basins and lakes: A review in the context of current and future water resource management and mitigation activities in Central Asia. Water, 9(10), p.798.

Zhi, W., Li, L., Kaye, J.P., Dong, W., Brown, W., Steefel, C.I., Williams, K.H., 2018. Understanding contrasting concentration-discharge (CQ) behaviors in a seasonally snow-covered watershed. AGUFM 2018, EP11C-2077.

Chapter 3: Flow intermittency controls the temporal behavior of solutes in rivers in arid watersheds: The Okavango River, NW Botswana

Abstract

I measured the concentrations of the total dissolved ions (TDI), dissolved silica, major cations and anions and the stable water isotopes (δD and $\delta^{18}O$) at sub-weekly to daily intervals for five years in the Okavango River at the outlet of the Okavango Delta (Delta) in semi-arid Botswana. The study objectives were to (1) document the temporal variability of the solute concentrations in a river in an arid watershed and (2) determine the role of flow intermittency in controlling the temporal changes in the solute concentrations in the river. At the seasonal scale, I found out that the TDI and major ion concentrations in the river were enriched during the beginning of the hot rainy season and during the arrival of the flood pulse from Angola. The river solute concentrations increased from the dissolution and transfer of precipitated salts stored on the floodplains and on hundreds of thousands of tree islands scattered across the Okavango Delta wetlands, as well as from the 'flushing' of solute enriched evaporated water in isolated wetland pools. Seasonal rains in the Delta and the annual flood pulse connect the river to solutes stored in the local Delta watershed consisting of floodplains, tree islands and isolated wetland pools, and facilitate solute transfer into the river. The 2019-2020 drought punctuated the annual flood pulse and rain induced overland transport of solutes to the river which allowed for solute accumulation in the local Delta watershed. Post drought rewetting re-established river connectivity to solute stores in the local Delta watershed which resulted in enhanced solute transfer into the river, particularly during the 2021-2022 flood post drought. Of the total estimated solute load (143,565 tons) exported during this study, ~64% was exported during the 2021-2022 flood. The 2021-22 flood is the largest flood during this study, and it appears to have been sufficiently high to access more solutes in the local

Delta watershed including solutes that had accumulated during drought. Our findings demonstrate that intermittent and variable flow from rains and flooding drives river connectivity to solutes stored in the local Delta watershed, and that drought play a crucial role in ceasing this connectivity of the river to solutes in the local Delta watershed and thereby allowing for the accumulation of solutes in the local Delta watershed which are then accessed and transferred into the river during rewetting post drought. These findings highlight the significance of both seasonal and drought-driven flow intermittency in controlling solute transport and export in the Okavango Delta and other rivers in arid watersheds.

1. Introduction

The transport and cycling of solutes in rivers are highly dependent on the river hydrology and the connection of rivers to solute stores in their local watersheds often consisting of floodplains and wetlands. River connectivity to solute stores in local watersheds is initiated by flow pathways (e.g., overland flow, shallow subsurface flow and groundwater flow) activated during hydrologic events (e.g., rains and flooding) (Gooseff et al., 2008; Liu et al., 2008; Covino, 2017; Geeraert et al., 2017; Fovet et al., 2018; Duvert et al., 2020; Ramatlapeng et al., 2021; 2023; Oromeng et al., 2021). However, the occurrence of flow intermittency in rivers significantly alters the hydrologic connectivity between rivers and solute sources/stores in watersheds (Boulton et al., 2017). Flow intermittency in rivers is typically characterized by flow cessation during the dry season and during droughts, and subsequent resurgence of flow during the rainy season and flooding (Boulton et al., 2017; Costigan et al., 2017; Datry et al., 2017; Tramblay et al., 2021). During flow cessation, the river becomes disconnected from its watershed sources of solutes (e.g., Boulton et al., 2017). Subsequent resurgence of flow from rains and flooding restores river connectivity to solute sources/stores in the watershed and facilitate solute transfer to rivers (Boulton et al., 2017). This

variable river connectivity to solute sources/stores driven by river flow intermittency controls the timing and magnitude of solute delivery into rivers (Boyer et al., 1997; Dalzell et al., 2007; Gooseff et al., 2008; Liu et al., 2008; Boulton et al., 2017; Covino, 2017; Geeraert et al., 2017; Fovet et al., 2018; Duvert et al., 2020; Ramatlapeng et al., 2021; 2023; Oromeng et al., 2021). Although flow intermittency occurs in rivers in both humid and arid watersheds, its occurrence is prevalent in rivers in arid watersheds due to severed groundwater to river connection and sporadic precipitation (Parsons et al., 1999; Tooth, 2000; Costa et al., 2012; Nanson et al., 2002). In contrast, rivers in humid environments are sustained by groundwater at base flow and receive inflow from the higher precipitation (e.g., Godsey et al., 2009; Rose et al., 2018). Because the rivers in humid watersheds are supported by groundwater, flow intermittency changes river solute concentrations by delivering non-groundwater derived solutes from the watershed and/or through dilution of groundwater solutes in the river. However, groundwater significantly buffers river chemistry such that the relative effect of flow intermittency in changing river solute behavior in humid watersheds diminishes with increasing downriver discharge supported by groundwater (e.g., Godsey et al., 2009; Rose et al., 2018). In arid watersheds, river chemistry is not buffered by groundwater and is highly variable due to intermittent flow that modulates river connectivity to solute stores and solute transfer into rivers (e.g., Oromeng et al., 2021; Ramatlapeng et al., 2021; 2023). This high variability in the river solute behavior needs to be investigated to better assess the connection between intermittent river flow and river solute behavior in arid watersheds. Despite the significance of flow intermittency in rivers in arid watersheds, there is still a lack of understanding of how flow cessation, drying, rewetting and episodic flow and the accompanying variable river-watershed connectivity control the temporal behavior of river solutes.

The ongoing climate change is exacerbating aridity in arid regions by reducing precipitation and increasing air temperatures (Zarch et al., 2017; Cherlet et al., 2018). The increased aridity has intensified the occurrence of flow cessation during the dry season and from droughts, and caused greater variability in episodic surface flows into rivers (e.g., Zeroual et al., 2013). Thus, understanding how the intensifying flow intermittency in rivers in arid watersheds govern solute behavior is crucial for forming the framework for adapting solute cycling models to account for these rivers' unique hydrochemical behavior under a changing climate. The insights derived from the connection between intermittent hydrology and river solute behavior are also important for the design of river water quality monitoring efforts and pollution control, and for making water management decisions in arid regions with limited freshwater resources. In addition, knowledge on flow intermittency control on solute behavior in rivers in arid watersheds will contribute insights to the temporal dimension of the trigger-transfer-reserve-pulse (TTRP) model proposed by Ludwig and Tongway (1997) and by Belnap et al. (2005). Within this TTRP framework, hydrology triggers the transport of solutes across watersheds and the solutes may either be retained in the river and its local watershed (reserve) or exported out of the system (pulse). Flow intermittency may add a dimension of unpredictable temporal variability in the solute transport, retention and export that needs to be constrained and well understood.

Understanding the role of intermittent flow in controlling the temporal solute transfer into rivers in arid watersheds requires the evaluation of long-term river discharge, solutes (total dissolved ions, silica and major ions) and stable water isotopes (δD and δ^{18}O). The temporal river discharge provides insights on the variability of river flow, while water source partitioning techniques (i.e., solutes and stable water isotopes) are crucial for characterizing solute behavior and the different sources of water transported and transferred into the river during different time

periods (e.g., Koeniger et al., 2009; Ala-Aho et al., 2018; Horgby et al., 2019; Duvert et al., 2020). The evaluation of the temporal river discharge and water source partitioning techniques at the outlet of the basin allows for the assessment of major catchment-wide processes affecting the hydrochemical behavior of the river and enables us to capture the response of the river chemistry to seasonal and climatic event-based (e.g., drought) flow intermittency.

We investigated the role of flow intermittency driven by intermittent and variable rains during the rainy season, annual pulse flooding (rising and receding flood) during the dry season, and drought in controlling the long-term behavior of solutes in the Okavango River in northwestern Botswana (Fig. 1). The Okavango River flows through the Okavango Delta (hereafter referred to as the Delta; Fig. 1) in Botswana. The Okavango Delta is the largest freshwater wetland in southern Africa (McCarthy and Ellery, 1998) and is a Ramsar World Heritage site (Secretariat of the Convention on Wetlands, 2017). The Okavango Delta lies in the middle Kalahari Desert near the terminus of the endorheic Okavango River Basin (ORB). The ORB is a transboundary basin covering Angola in its headwaters to the north, and Namibia and Botswana in its lower drainage area to the south. The ORB transcends climatic gradients from a higher rainfall temperate climate in Angola to a semi-arid climate in Botswana (Peel et al., 2007). Near the terminus of the ORB in Botswana where the Okavango Delta is located, the hydrology is highly intermittent and primarily controlled by annual flood pulses initiated by rains from the upper ORB in Angola and by local rains (Wolski et al., 2005). However, in late 2019-early 2020, the Delta experienced drought. This drought coincided with the lowest precipitation record of 550 mm in the upper ORB since 1981 (Lourenco and Woodborne, 2023). River flow in the Okavango River in the lower delta (the region with distributary channels between the Gumare and Thamalakane Faults shown in Fig. 1) ceased for about 10 months.

The Delta is characterized by high evapotranspiration (ET) rates (McCarthy and Ellery, 1998) which induce precipitation of salts on the floodplains and on hundreds of thousands of tree islands, and evapo-concentrate solutes in isolated wetland pools scattered across the Delta (Dincer et al., 1979; McCarthy et al., 1991). Previous studies on solute transport in the Delta revealed that the Okavango River periodically connects with solute stores (salt precipitates on floodplains and tree islands, and solute enriched wetland pools) via overland flow during rains and rising and receding floods, resulting in episodic transfer of solutes into the river (Oromeng et al., 2021; Ramatlapeng et al., 2021; 2023; Letshele et al., 2023). However, there is still a lack of understanding of how this river-floodplain-wetland interaction and solute transfer into the river is modulated by flow intermittency driven by a combination of seasonal rains, annual flood pulse and the occurrence of a drought. In the absence of drought, the seasonal rains and annual flood pulse will cause repetitive and predictable river-floodplain-wetland interaction (e.g., Ramatlapeng et al., 2021). However, the occurrence of a drought will punctuate the flood pulse and rain induced river-floodplain-wetland connectivity and allow for the accumulation of solutes in the local watershed which may be transferred into the river during rewetting events post drought (e.g., Clark et al., 2017). Yet, this river-floodplain-wetland connectivity and solute transport remains poorly understood. Thus, the role of river flow, drying and rewetting in altering the long-term river solute behavior remain enigmatic. As a freshwater river system that provides potable water and food (fish and tswii) to the riparian communities and sustains a vibrant but fragile ecosystem (Mosepele et al., 2006; 2009; Kgathi et al., 2006), it is imperative to know how the Okavango River chemistry behaves under varying flow conditions, as this has implications on the temporal river water quality and ecosystem health.

In this study, I made temporal measurements of river discharge, total dissolved ions (TDI), silica, major cations (sodium, potassium, magnesium and calcium) and anions (chloride, alkalinity, sulfate, nitrate and phosphate), and stable water isotopes (δD and $\delta^{18}O$) in the Okavango River at the outlet of the Okavango Delta in Maun (Fig. 1). The objectives were to (1) document the temporal variability of the solute concentrations in the Okavango River and (2) determine the role of flow intermittency in driving the temporal changes in the solute concentrations in the river. The placement of the station at the outlet of the Delta for this investigation enables me to capture the integration of processes governing the behavior of solutes that affect the Okavango Delta and its wetlands, and to assess the response of the river chemistry to seasonal and drought-driven flow intermittency. The findings from this study will provide insights on the role of flow intermittency on the variability of solute behavior which is crucial for the assessment of the temporal river salinity status and ecological sustainability in rivers in arid watersheds.

2. The Okavango Delta

2.1. Location

The study site is located in the Okavango River at the outlet of the Okavango Delta in Maun (Fig. 1). The Okavango Delta is made up of two distinct regions: the Panhandle and the lower delta region (Fig. 1). The Panhandle is a ~6000 km^2 narrow valley with a topographic gradient of 1:5500 through which the Okavango River meanders before splitting into numerous distributary channels that forms the lower delta region (McCarthy et al., 1997). The lower delta region is a low gradient (1:3400) alluvial fan with a surface area of ~22,000 km^2 (McCarthy et al., 1992) lying in the Quaternary half-graben of the Okavango Rift Zone (McCarthy et al., 1993; Modisi et al., 2000; Kinabo et al., 2007; Kinabo et al., 2008; Bufford et al., 2012). The Delta's topography is relatively

flat with the local relief rarely exceeding 2 m except for areas with termite mounds and tree islands (McCarthy et al., 1998; Gumbricht et al., 2001; McCarthy, 2006).

2.2. Geology

The Cuito and Cubango sub-basins in the upper ORB lie on the Precambrian Congo Craton made up of crystalline metamorphic gneisses, quartzites and migmatites (Bereslawski, 1997; Steudel et al., 2013). These metamorphic rocks are covered by sedimentary rocks of the Karoo Supergroup and thick layers of unconsolidated sands, clays, lime rock and lateritic layers of the Kalahari Superior Formation (Bereslawski, 1997; Catuneanu et al., 2005; Jones, 2010). The bedrock geology of the lower ORB around the Okavango Delta consists of Precambrian crystalline rocks of the Damara and Ghanzi-Chobe orogenic belt (Modie, 2000; Milzow et al., 2009). The superficial geology is made up of Quaternary Kalahari alluvium and recent swamp sediments (Ringrose et al., 2009) that overlies ~40 m of sands, and 105-175 m of lacustrine and fluvio-deltaic sediments (Kalscheuer et al., 2015). The lacustrine and fluvio-deltaic sediments are the remnants of Paleo Lake Makgadikgadi and the Paleo Okavango Megafan sedimentary units (Podgorski et al., 2013; 2015; Kalscheuer et al., 2015).

2.3. Climate

The climate in the ORB transitions from a temperate climate in the Angolan highlands to the steppe arid climate in the middle Kalahari Desert in Botswana (Peel et al., 2007). In both the upper watershed in Angola and lower watershed in the Delta, the climate is characterized by wet and dry seasons (McCarthy and Ellery, 1994; Milzow et al., 2009; Steudel et al., 2013). The wet season spans from November to March, while the dry season span from April to October. The mean annual rainfall during the wet season in the upper ORB is ~1100 mm (Pombo et al., 2015). The maximum daily temperatures range from 22 and 24 ºC during the rainy season and decrease to 15-17 ºC

during the dry season (Steudel et al., 2013). The lower watershed in the Delta receives an average annual rainfall of ~450 mm during the rainy season (Milzow et al., 2009). The highest mean monthly maximum temperatures during the rainy season range from 32 to 35 ºC and the lowest mean monthly minimum temperatures during the dry season range between 2 and 7 ºC (Moses and Gondwe, 2019). The estimated potential evapotranspiration in the Delta is ~2172 mm/y, which is 4 times greater than the rainfall received in the Delta (Wilson and Dincer, 1976).

2.4. Hydrology

The hydrology of the Okavango River is driven by an annual flood pulse derived from the Angolan highlands in the upper ORB and by local seasonal rains. The mean annual inflow of water from the Cubango and Cuito Rivers in the upper ORB to the Delta is 9.2 x 10^9 m^3/y and the local seasonal rains augment the river flow with ~6 x 10^9 m^3/y (McCarthy and Ellery, 1998; Merron, 1991). The Cuito and Cubango Rivers in the upper ORB contribute about 45% and 55% of the discharge, respectively, to the Okavango River as it flows into the Delta (Mendelsohn and el Obeid, 2004). The water from the Cuito and Cubango Rivers is derived from the precipitation that falls in the Angolan highlands around October. This water reaches the northwestern part of the Delta in Botswana as a flood pulse via the Okavango River around February-May (McCarthy and Ellery, 1998; McCarthy et al., 2003; Wolski et al., 2006). Upon reaching the entrance to the Delta in northwestern Botswana, the flood pulse slowly expands out and travels ~450 km through the Okavango Delta as a progressive wave from the proximal portion of the Delta in Mohembo to the distal portion in Maun in about 4-6 months (McCarthy and Ellery, 1998). As the flood wave progresses across the Delta, the area inundated by the floodwaters gradually increases from an annual low of 4500-6000 km^2 to an annual high of 9000-12,000 km^2 (Ramberg and Wolski, 2008). The annual variations in the inundation extent in the Delta are due to varying flood magnitude and

major global climatic factors such as the El Niño Southern Oscillation (ENSO) phenomenon that cause droughts (McCarthy et al., 2000; McCarthy et al., 2003). Owing to the high hydraulic conductivity (10-30 m/day) and porosity (30 %) of the Kalahari sands on the surface of the Delta (Obakeng and Gieske, 1997), and the relatively slow movement of the floodwaters across the Delta, the flood inundation is accompanied by the recharge of the shallow unconfined aquifer (McCarthy, 2006). Therefore, the Okavango River recharges groundwater during flooding, and this is evidenced by the deepening of the groundwater table away from the Delta and its wetlands (McCarthy et al., 1997; Ellery et al., 2003; McCarthy, 2006; Akondi et al., 2019).

The highly variable flooding in the Delta creates unique hydro-ecotones. The Panhandle region is in a permanently flooded ecotone with water depths average of 1.5 m (Wilson and Dincer, 1976), average river gradient of 1:5500 (Gumbricht et al., 2004), and river velocity of 0.4-0.8 m/s within the channel (Wolski et al., 2006). The lower delta region has seasonally flooded ecotones and occasionally flooded ecotones, and the water depths generally decrease downriver and average 1 m in the lower delta portion (Wilson and Dincer, 1976). The Okavango River's gradient in the lower Delta averages 1:3400 (Gumbricht et al., 2004), and the river velocities average 0.01 m/s (Wolski et al., 2006). The spreading out of water into the numerous distributary channels forming the delta, and vegetation in the lower Delta slow down river flow velocities.

There are ~150,000 tree island complexes scattered across the different ecotones in the Delta. These islands vary in their morphology and size from a few square meters to ~700,000 m^2 and cover 5% of the area of the permanently flooded ecotone, 25% of seasonally flooded ecotone and 50% of the occasionally flooded ecotone (McCarthy and Metcalfe, 1990; Gumbricht et al., 2004; Humphries et al., 2014). These islands are dominated by trees and halophytic grasses on their fringes which facilitate evapotranspiration-driven flow of water from the Okavango River towards

the islands (Gumbricht and McCarthy, 2003; Ramberg and Wolski, 2008). The evaporation of floodwaters occurring in this hot desert setting and transpiration by the vegetation on island fringes enhance the accumulation of salt precipitates on island fringes and centers (Gumbricht and McCarthy, 2003; Ramberg and Wolski, 2008).

During periods of no flooding in the rainy season, the seasonally and occasionally flooded ecotones of the Delta host isolated surface water pools (McCarthy et al., 1998) formed by trapped water from summer rains and the previous year's flood. Owing to the hot climate and the accompanying high evaporation rates in the Delta, the water in the isolated wetland pools show enriched $\delta^{18}O$ (0.1-7.5‰) caused by evaporation (Dincer et al., 1979; McCarthy et al., 1991; 1998).

3. Methodology

3.1. Sample collection and analyses

This study was conducted between November 2017 and July 2022 in the Okavango River (23º28′48.99″E, 19º57′16.77″S) in Maun. We collected river samples by the grab technique into 20 ml glass scintillation vials at sub-weekly (2017-2018) and daily (2019-2022) intervals. The samples were protected from sunlight and kept in a cool storage. The samples were transported to the University of California, Davis (USA), where they were filtered through 0.45 μM nylon syringe filters and refrigerated until analyses. Aliquots of the samples were analyzed for anions and cations using an Ion Chromatography System (Dionex ICS-6000). Total dissolved ions (TDI) were measured using a benchtop micro-conductivity/TDS meter calibrated according to the manufacturer's instructions. Silica concentrations were measured by spectrophotometry on a CHEMetrics (V-3000 series) photometer. The alkalinity was measured using the Apollo SciTech

Alkalinity Titrator (AS-ALK2). The $\delta^{18}O$ and δD were measured using the Picarro (L2140-i) Cavity Ringdown Spectrometer Water Isotope Analyzer. The Picarro L2140-i performed 6 injections per sample and the last 3 injections were averaged for the sample's isotope value. Each batch run was calibrated with the Vienna Standard Mean Ocean Water (VSMOW) standard and machine drift was verified by running a test standard and select standards (USGS 46, USGS 47 and USGS 48) in between samples. The isotope ratios are reported in delta notation (δ) in per mil (‰):

$$\delta\ (‰) = ((R_{sample} - R_{standard})/ R_{standard}) \times 1000$$

where R is the ratio of D/H, or $^{18}O/^{16}O$ in the sample and standard. The δD and $\delta^{18}O$ are reported relative to VSMOW. The precision (1σ standard deviation) of the Picarro Water Isotope Analyzer isotopic measurement is better than ± 1 ‰ for δD and ± 0.1‰ for $\delta^{18}O$.

3.2. River discharge and rainfall

River discharge data measured at the Maun (Thamalakane) station (23º25′35.09″E, 20º0′17.04″S) were obtained from the Botswana Department of Water Affairs. Hourly rainfall data measured at the Sexaxa station were obtained from the archives of the Okavango Research Institute (ORI). The hourly rainfall data were averaged every 24 h in R Studio to obtain mean daily rainfall.

3.3. Air temperature

Hourly air temperature measured at the Sexaxa weather station were obtained from the archives of the Okavango Research Institute (ORI). The hourly air temperature data were averaged every 24 h in R Studio to obtain mean daily air temperatures.

4. Results

4.1. Summary statistics

The descriptive statistics (mean, minimum, maximum and the standard deviations) of the river discharge, mean daily rainfall, mean daily air temperature, δD of river water, D-excess and solute concentrations (TDI, silica, anions and cations) are shown in Table 1.

4.2. Temporal hydrology (river discharge and rainfall)

The hydrograph constructed from the relationship between discharge and water level data is shown in Fig 2a. The temporal river discharge shown by the hydrograph ranged between 0 and 48 m^3/s and averaged 11 ± 13 m^3/s, with lower river discharge occurring in 2018 and the highest river discharge occurring in 2021. The hydrograph shows peaks of varying magnitudes that correspond to the rainy season (e.g., in March 2018) and the annual flooding of the Okavango Delta (e.g., in August 2018, July 2020 and June 2021). River flow ceased during the late 2019-early 2020 drought period (brown shaded region; Fig. 2a). During the beginning of the rainy season, the hydrograph receded as river discharge decreased between November and February. River discharge rise occurred towards the end of the rainy season in March, albeit smaller in 2018 compared to 2021. The river discharge gradually increased and peaked in August during the dry season due to pulse flooding. The peak discharge during flooding was followed by recession from late August through December.

Rainfall amount during the study period ranged from 0 to 48 mm/d and averaged 1.9 ± 6 mm/d. The temporal rainfall distribution shows that more rain fell from mid-rainy season (February and March) to the end of the rainy season in 2017/2018 and 2019 (Fig. 2b).

4.3. Temporal variations in air temperature

The mean daily air temperatures ranged from 12 to 32 ℃ and averaged 23 ± 4 ℃ with clear seasonal and sub-seasonal patterns (Fig. 2c). Higher air temperatures were observed during the rainy season between September and April and lower air temperatures were observed during the dry season between May and August (Fig. 2c). The rapid sub-seasonal changes in the air temperature were superimposed on the seasonal air temperature variations. The minimum (troughs) and maximum (peaks) air temperatures did not differ much over the 5 years of our study.

4.4. Temporal variations in the stable isotopic composition (δD) of river water

The temporal δD variations in river water is shown in Fig. 2d. The δD ranged between -43‰ and 39‰ with an average of 8 ± 24‰. The δD was enriched during the beginning of the rainy season to mid-rainy season in 2017-18 and 2020-21 (Fig. 2d). This enrichment in the δD was followed by a precipitous decrease in the δD in February 2018, and December 2020. The δD remained lower to the end of the rainy season in April. The dry season was marked by a progressive increase in the δD in 2018-19 prior to the drought and 2021-22 after the drought, when the δD reached a high of 39‰. In contrast, the 2019 dry season that precedes the drought was characterized by highly fluctuating δD.

4.5. Temporal variations in solute concentrations (TDI, cations and anions)

The TDI concentrations (Fig. 2f) ranged between 53 and 211 mg/L and averaged 100 ± 34 mg/L. On a temporal basis, the concentrations of TDI increased at the beginning of the rainy season during the 2017-18 and 2020-21 rainy seasons and increased consistently into the 2022 rainy season when the solute concentrations suddenly increased to the highest value of 211 from the mid-rainy season to the end of the rainy season. The enrichment in the TDI concentrations was followed by a sudden decrease in the concentrations at the end of the rainy season. The beginning of the dry season in May is marked by a rapid increase in the TDI concentrations which remained

high until June, after which the TDI concentrations decreased through end of the dry season in 2018, 2020, 2021 and 2022. In contrast, the 2019 dry season that precedes the 2019-2020 drought is characterized by highly fluctuating TDI concentrations. The Na^+ concentrations (Fig. 2g) ranged between 7 and 42 mg/L, with an average of 22 ± 11 mg/L. Mg^{2+} concentrations (Fig. 2h) ranged between 1 and 8 mg/L with an average of 2 ± 1 mg/L. On a temporal basis, the behavior of the cations (Na^+, K^+, Mg^{2+} and Ca^{2+}) mimicked the behavior of the TDI concentrations before and shortly after the drought shown by increased concentrations at the beginning of the 2018 and 2020 rainy season and dry seasons (e.g., Fig. 2f, g and h). The cations concentration increase was followed by decrease in the concentrations. Similar to TDI concentrations, the 2019 dry season was characterized by fluctuating concentrations of cations (e.g., Fig. 2g, and h). Although Na^+ concentrations progressively increased between 2021 and 2022, Mg^{2+} concentrations stayed relatively constant between 2021 and 2022. The temporal behavior of the ratio of Na^+/Ca^{2+} show higher ratios between late January 2021 and late July 2022 with a slow decrease between late January 2021 and May 2021 (Fig. 2i). During other times, the Na^+/Ca^{2+} ratios remained low, fluctuating around 2.

The Cl^- concentrations (Fig. 3b) ranged between nondetectable (we assigned 0 mg/L) and 12 mg/L, averaged 2 ± 2 mg/L and mimicked the behavior of the temporal TDI concentrations. Alkalinity ranged from 53 to 222 mg/L and averaged 90 ± 20 mg/L. Alkalinity mimicked the temporal behavior of Na^+ concentrations with elevated concentrations during the start of the rainy season and dry season during flooding, and sustained elevated concentrations between 2021 and 2022 (Fig. 3c). SO_4^{2-} concentrations ranged between 0.1 and 7 and averaged 1 ± 2 mg/L. The SO_4^{2-} concentrations remained low during our study and increased between the 2022 rainy season into the dry season, reaching the highest concentration of 7.1 mg/L (Fig. 3d). NO_{3-} concentrations

ranged from 0.1 to 14 and averaged 3 ± 2 mg/L. The NO_{3-} concentrations were higher during the beginning of the rainy season in 2020-21, middle of the rainy season in 2018 and 2022, and during the start of the dry season (Fig. 3e). The PO_4^{3-} concentrations ranged between 0 and 2, and averaged 0.2 ± 0.2 mg/L. The PO_4^{3-} concentrations were relatively low during our study and only increased at the beginning of the 2021 dry season between May and June. This increase was followed by a sudden decrease in the PO_4^{3-} concentrations in July (Fig. 3f).

5. Discussion

5.1. Temporal shifts in the river solute behavior

The results of our investigation of the temporal variations of river solute concentrations in the Okavango River show sub-seasonal, seasonal, and inter-annual variations (Fig. 2f, g and h; Fig. 3). At seasonal and sub-seasonal scales, the general behavior of the solute concentrations in the river is characterized by episodic solute enrichment at the beginning of the rainy season (November-February of 2017-18 and 2020-21) and at the end of the rainy season in 2022. The solute concentrations were also enriched during the initial phase of the arrival of the flood waters from the upper watershed in Angola (May-June of 2018, 2019, 2020 and 2022) during the dry season (Fig. 2f, g and h; Fig. 3). These elevated solute concentrations during the rainy and dry seasons are followed by dilution as the rainy season and flooding progress. Although the seasonal and sub-seasonal solute responses dominate the annual behavior of solutes, we observe inter-annual variations in the river solute behavior. For instance, months (May, June, July and August) leading up to the drought in 2019 showed unique solute responses of highly fluctuating solute concentrations throughout the dry season (e.g., Fig. 2f; Fig. 3b-c). Furthermore, the response of solutes (e.g., TDI, sodium and chloride) following the 10-month long drought between 2021 and 2022 exhibit a distinct behavior of continuous and steady increase in concentrations (Fig. 2f and

g; Fig. 3b). This steady increase in the river solute concentrations is observed regardless of the occurrence of the largest flood pulse and discharge during this study (Fig. 2a) post-drought. The observed temporal behavior of the different solutes in the river can be linked to a strong influence of seasonal and drought-driven flow intermittency on solute transport in this arid environment. Flow in rivers in arid environments is highly intermittent due to low and variable seasonal rains, and episodic flooding (Nanson et al., 2002). At the seasonal scale, flow intermittency in these rivers is primarily driven by the intermittent and variable seasonal rains, episodic flooding, and flow cessation during the dry season. The overland flow generated during seasonal hydrologic events such as rains and flooding is likely to establish connectivity between the rivers and solute sources/stores in their local watersheds and facilitate solute transfer to rivers (e.g., Ramatlapeng et al., 2021). The occurrence of a drought leads to prolonged flow cessation which is likely to punctuate the rain and flood induced overland transport of solutes to rivers, and thereby allowing for the accumulation of solutes in the watershed. These solutes can then be accessed and transferred to the river during rewetting events post drought, resulting in enhanced solute transfer to rivers (e.g., Clark et al., 2017). Thus, the role of both seasonal and drought-driven flow intermittency in controlling temporal solute transport and solute behavior in rivers in arid environments needs to be constrained.

5.2. Flow intermittency as a major driver of the temporal solute behavior in the river

5.2.1. Control of seasonal flow intermittency on the temporal solute behavior in the river

The seasonal flow intermittency in the Okavango River is primarily driven by the annual flood pulse derived from the Angolan highlands in the upper Okavango River Basin which inundates the Delta during the dry season (McCarthy et al., 2000) (unshaded portions of the plot; Fig. 2a) and seasonal rains occurring in the Delta region during the rainy season (blue-shaded portions of the

plot; Fig. 2b). Flow from the annual flood pulse constitutes two major changing flow regimes; (1) rising flood occurring when floodwaters from Angola inundate the Delta and increase flow from low flow to peak flow conditions, and (2) flood recession occurring when flow decreases from peak flow to low flow conditions (Fig. 2a). The magnitude of the annual flood pulses from Angola varies over time (Fig. 2a). Seasonal rains in the Delta are also variable and highly intermittent (Fig. 2a). Thus, if seasonal flow intermittency from pulse flooding and rains controls the temporal behavior in the river solute behavior, we should observe modifications in the river solute concentrations from pulse flooding during the dry season between March and September, and from seasonal rains which span November through March (Fig. 2a and b). The arrival of "fresh" floodwaters with low dissolved solutes from the annual flood pulse from Angola in the Delta and seasonal rains is expected to induce a dilution response in the river solute concentrations (e.g., Ahearn et al., 2004; Herndon et al., 2018; Rose et al., 2018). However, we note that the arrival of the flood pulse from Angola in the Delta and the beginning of local rains is associated with solute enrichment in the river (Fig. 2f, g and h; Fig. 3). It is also noteworthy that the beginning of the rainy season in the Delta coincides with the tail end of the recession of the previous year's flood (Fig. 2a).

Since the river solute concentrations are anomalously high during the beginning of flooding and rains, we assess the role of hydrologic connectivity between the river and watershed-derived solutes in causing enrichment in the river solutes. We developed a conceptual model that illustrates how solutes can be accessed and transferred from the local watershed consisting of floodplains, wetlands, and tree islands to the river, and from groundwater (Fig. 4). This conceptual model considers solute accumulation from the high evapotranspiration (ET) rates in the Delta and the role of hydrologic connectivity between the river and watershed solute stores in mobilizing and

transferring solutes from the local watershed into the river during rains and flooding. The solute stores in the local Delta watershed include (1) salt precipitates on floodplains and on tree islands (Gumbricht et al., 2004) (2) solute enriched evaporated water in isolated wetland pools and evaporated wetland water (Dincer et al., 1979) (3) saline groundwater (Ramberg and Wolski, 2008). The overland flow generated by rains (Fig. 4a), the initial floodwaters (Fig. 4b) and receding flood (Fig. 4c) connect the river to the solute stores in the local Delta watershed and initiates the transfer of the solutes into the river (e.g., Ramatlapeng et al., 2021; 2023; Oromeng et al., 2021; Akoko et al., 2013). This mass transfer of solutes from the local watershed into the river during flooding and rains occurs through chemically distinct water sources that are either dominated by evapoconcentration and/or dissolution of salt precipitates from floodplains and tree islands in the Delta watershed. Groundwater discharge to rivers is also an important source of solutes (Godsey et al., 2009). In the Okavango Delta, the surface water-groundwater interaction has not been investigated extensively. However, the hydraulic gradient of the groundwater table steepens away from the Delta (McCarthy et al., 1993; 1998), suggesting that the Okavango River is a potential source of groundwater recharge. In addition, a study by Akondi et al. (2019) indicated that the stable hydrogen and oxygen isotopic composition of groundwater shows enrichment and lie along the Okavango Delta Evaporation Line (ODEL), which is consistent with groundwater recharge by evaporated river water. Although these previous studies showed absence of groundwater influx into the river, it is possible to have influx of groundwater with similar chemistry to the river which further complicates surface water-groundwater interaction dynamics. Therefore, the role of groundwater in modifying river chemistry during hydrologic events still needs to be explored and constrained. Our study is not able to constrain this role of groundwater in changing river chemistry during different hydrologic regimes.

We tested our conceptual model using the relationship between stable water isotopes (δD vs. $\delta^{18}O$) (Fig. 5), the relationship between solute (TDI) concentrations and the isotopic composition (δD) of river water (Fig. 6) and the relationship between individual ions (Fig. 7) during rising and receding flow regimes. The stable water isotopes and ions from rising and receding flow provide insights on the different water "packages" transferred from the local watershed into the river during major changing flow regimes in the Delta (e.g., Koeniger et al., 2009; Ala-Aho et al., 2018; Horgby et al., 2019; Duvert et al., 2020). In our evaluation, we also show an evaporation model line (black dashed line in Figure 6 and 7) derived from the Okavango River water collected in Maun and evaporated over time (Atekwana et al., 2016). In principle, the water packages dominated by evapoconcentration should show evidence of evaporative effects from the relationship between δD and $\delta^{18}O$ (e.g., Craig, 1961), and follow the trajectory of the evaporation model line which show a positive relationship between TDI vs. δD. The δD and $\delta^{18}O$ of the Okavango River water co-vary (Fig. 5) and the river samples plot below the Global Meteoric Water Line (GMWL) and mostly along the Okavango Delta Evaporation Line (ODEL), consistent with evaporation of the river water during transit through the Delta (Dincer et al., 1979; Atekwana et al., 2016). The samples from the 2019 drying period prior to the 2019-2020 drought deviated from the ODEL due to greater evaporation extent (Fig. 5) (e.g., Atekwana et al., 2016). We also note that the river samples from the rising and receding flow regimes plot differentially along the ODEL (Fig. 5), signifying different evaporation extents likely influenced by varying water residence times in the Delta, mixing of different waters (e.g., floodwaters, rainwater and wetland water) and/or changing flow magnitude modulated by seasonal flow intermittency.

The high evaporation in the Delta induces evapoconcentration of solutes in the Delta and its wetlands (Fig. 4) (Dincer et al., 1979; Ramberg and Wolski, 2008; Letshele et al., 2023). During

seasonal rains (Fig. 4a) and rising flood when the floodwaters inundate the Delta (Fig. 4b), the initiated overland flow establish both longitudinal hydrologic connectivity within the river channel and lateral hydrologic connectivity between the river and the Delta wetlands, resulting in the "flushing" of the solute enriched evaporated water from the Delta wetlands and isolated wetland pools into the river. Similarly, the return flow during flood recession flushes the solute enriched wetland water into the river (Fig. 4c). This transfer of solute enriched evaporated water packages into the Okavango River is evidenced by data from different flow regimes that follow the trajectory of the evaporation model line showing a positive relationship between TDI vs. δD (Fig. 6c, d, e, f, i, k, l and m). However, during other times (e.g., the 2018 rising and receding flood), the floodwaters deliver distinct water packages that do not follow the trajectory of the evaporation model line and show a wide range in the isotopic composition (δD) with little to no changes in the TDI concentrations (e.g., Fig. 6g and h). These water packages are likely sourced from evaporated wetland water with similar proportions of ions to river water (e.g., Ramatlapeng et al., 2021). The differences in the chemistry of the wetland water accessed and transferred into the river during seasonal rains and flooding highlight the hydrochemical heterogeneity of the Delta's wetland water and the important role of seasonal flow intermittency in modulating the accessing, mobilization, and delivery of the wetland water into the river.

The other water packages transferred into the river during rains and flooding show dominance of the dissolution of salt precipitates (i.e., sodium carbonate) (e.g., Ramatlapeng et al., 2021). As the rain and flood waters flush evaporated wetland water into the river, salt precipitates on the floodplains and tree islands in the Delta are also accessed, dissolved, and transferred into the Okavango River (Fig. 4a-c). However, the temporal dominance of salt dissolution and the magnitude of the transfer of dissolved salts from the local watershed into the river are primarily

contingent on the flood magnitude which controls the extents of longitudinal connectivity of the river water and solutes within the river channel, lateral connectivity between the river and watershed-derived solutes, and vertical accessibility of solutes in their stores. In this study, the predominance of salt dissolution is particularly evident during the 2021-22 flood, as indicated by the sustained higher sodium concentrations (Fig. 2g), Na^+/Ca^+ (Fig. 2i) and alkalinity (Fig. 3c). The transfer of the dissolved sodium carbonate salts into the river during the 2021-22 flood is further supported by the increasing TDI concentrations with minimal changes in the δD (Fig. 6m) and the positive relationship between sodium and alkalinity (Fig. 7). The 2021-22 flood is the largest flood during this study (Fig. 2a) and it appears to have been sufficiently high to establish significant longitudinal connectivity between the river water and salts along the river channel, lateral connectivity between the river and salts on floodplains and tree islands, and vertical connectivity between the river water and salt precipitates stored on the elevated tree islands in the Delta watershed. The vertical interception of salts on the tree islands might not have occurred if the flood magnitude had been lower due to the higher elevation of tree islands as most of the islands are formed around and on termite mounds (Gumbricht et al., 2004). Alternatively, the enhanced dissolved salts transfer into the river by the 2021-22 flood can be explained by the accessing of salts that accumulated during the 2019-20 drought. Our findings underscore the critical role of intermittent seasonal flow from rains and flooding in governing river connectivity to watershed-derived solutes and in dictating the type of solutes accessed and the magnitude of solute transfer into rivers in arid environments.

5.2.2. Control of the temporal solute behavior in the river from flow cessation by drought

Although seasonal flow intermittency strongly governs the temporal behavior of the river solute behavior, major global climatic factors such as the El Niño Southern Oscillation (ENSO)

phenomenon can cause significant interannual shifts in the river hydrology and chemistry by decreasing precipitation and causing droughts (Dahm and Molles, 1992). Alemaw (2022) showed the existence of a strong positive linear correlation between seasonal and annual rainfall depths in southern Africa and the warm seasonal ENSO indices, which explains the lower rainfall and recent drought events of 2019/2020. Drought-driven flow intermittency from the 2019-20 drought and subsequent rewetting events significantly altered the river-floodplain-wetland interaction in the Delta (e.g., Fig. 4d, e and f). For instance, the months of May, June, July and August leading up to the drought in 2019 exhibit highly fluctuating solute concentrations throughout the 2019 dry season. This fluctuation in the solute concentrations of the river (e.g., TDI, magnesium, chloride and alkalinity; Fig. 2f and h; 3b and c) is consistent with water sourced from remnant wetland pools formed during the flow contraction-fragmentation-drying phase (e.g., Fig. 4d) that typically occur at the beginning of a drought (Boulton et al., 2017; Gómez et al., 2017). The absence of flow in the river during this period (Fig. 2a) supports the occurrence of the flow contraction-fragmentation-drying phase in the river at the onset of the drought that typically result in the formation of isolated pools in the floodplains and within the river channel (e.g., Fig. 4d). These isolated wetland pools were subjected to the high evaporation rates in the Delta as shown by the samples from this drying period plotting below the Okavango Delta Evaporation Line (ODEL; Fig 5) indicating greater evaporation extent. Evapo-concentration of solutes in these isolated pools is reflected by the positive relationship between TDI vs. the isotopic composition (δD) (Fig. 6i). Because the isolated wetland pools usually host water of different isotopic and chemical compositions (Gómez et al., 2017; Bonada et al., 2020), the water from the isolated wetland pools can cause the observed variable solute responses in the river as they differentially drain water into the river (Gómez et al., 2017).

Post drought, the Okavango River gradually transitions from longitudinal hydrologic connectivity where solute transport is confined to the river channel to lateral hydrologic connectivity where the river interacts with the local watershed (e.g., Boulton et al., 2017). During the drought when there is severed connectivity between the river and solute stores in the local watershed, solutes accumulated within the river channel and in solute stores on floodplains and tree islands in the Delta (Fig. 4e) (e.g., Clark et al., 2017). The initial rewetting event in the Okavango River after the drought, which is the arrival of the flood pulse from Angola in May 2020 (Fig. 2a), established longitudinal hydrologic connectivity within the river channel and flushed out solutes within the river channel as shown by the solute enriched front of these initial floodwaters that is followed by fresh floodwaters (e.g., Fig. 2f, g and h; Fig. 3; Fig. 4f). As the annual flood expands and inundates the Delta, the antecedent moisture condition of the local watershed improves such that during the first rainy season that follows the May-November 2020 flooding period, overland flow is generated and re-establishes the lateral hydrologic connectivity of the Okavango River to its local watershed. The overland flow generated by rains and the 2020-2021 rising floodwaters during this period intercepts solute stores in the Delta and delivers solutes to the river at the beginning of the rainy season (Fig. 2d, f, g and h; Fig. 3). The solute enrichment is then followed by dilution, consistent with pre-drought solute behavior observed during the rainy season and flooding. However, after the first rainy season post drought, the largest flood since 2017 occurred (Fig. 2a) and accessed solutes that had accumulated in the watershed during the drought, resulting in the sustained higher magnitude of solute transfer to the river (e.g., Fig. 2f and g; Fig. 3) between 2021 and 2022 (e.g., Murphy et al., 2018). About 64% of the total estimated solute load (143,565 tons) during this study was exported from the Delta (Fig. 10a and b) during this period. This ~64% solute export between 2021 and 2022 is significantly higher than the ~9%

of solutes exported during the 2018 flood and ~19% during the 2020 flood. This flood dissolved salt precipitates (i.e., sodium carbonate minerals trona ($Na_3(CO_3)(HCO_3)\cdot 2H_2O$) or thermonatrite ($Na_2CO_3\cdot H_2O$)) on floodplains and salt islands (e.g., McCarthy et al., 1991, McCarthy and Ellery, 1995) as indicated by the corresponding significant increase in sodium concentrations and alkalinity (Fig. 2g and Fig. 3c), increased Na^+/Ca^{2+} during this post drought period (Fig. 2i) and the positive relationship between alkalinity and sodium concentrations (Fig. 7). In addition to salts, the flood mobilized and transferred chloride, nitrate and phosphate from the watershed into the river (Fig. 3b, e and f). The transfer of nitrate and phosphate into the river has implications on nutrient cycling in the river and ecosystem health. The 2021-2022 interval highlights a prolonged "hot moment" that deviates from the annual solute behavior of the Okavango River, putting emphasis on the significance of drought-driven flow intermittency in controlling the interplay between solute accumulation and solute transport and export in arid watersheds.

6. Conclusions and Implications

Total dissolved ions, dissolved silica, major ions concentrations, river discharge and the δD and $\delta^{18}O$ of river water were used to investigate the role of flow intermittency in controlling the temporal behavior of solutes in the Okavango River in the semi-arid Botswana. Our investigation reveal that seasonal and drought-driven flow intermittency strongly control the temporal variability of solute concentrations in the river. The seasonal flow intermittency is driven by rains during the rainy season and annual pulse flooding during the dry season. The rains and flood generate overland flow that facilitates the transfer of solutes (dissolved salts on floodplains and tree islands, and evaporated water in isolated wetland pools) from the watershed into the river. This mass transfer of solutes into the river occurs through chemically different water packages that induce varying solute regimes in the river. The occurrence of drought ceases the river-floodplain-wetland

connectivity and promotes solute accumulation in the river channel and watershed. The re-establishment of solute transport by rewetting events after the drought show a gradual transition from longitudinal hydrologic connectivity where solute transport is confined to the river channel to lateral hydrologic connectivity where the river interacts with the local watershed. The lateral connectivity of the river to solute stores in the watershed during the largest flood since 2017 intercepted solutes that accumulated in the watershed during drought, resulting in enhanced solute transfer from the watershed into the river between 2021 and 2022. This interplay between solute transport during hydrologic events and solute accumulation during drought provides insights to the temporal dimension of the trigger-transfer-reserve-pulse (TTRP) model proposed by Ludwig and Tongway (1997) and by Belnap et al. (2005) for transport in arid environments. In this TTRP model, hydrology triggers the transport of materials and solutes across watersheds and the materials/solutes may either be retained in the watersheds (*reserve*) or exported out of the system (*pulse*). Our findings demonstrate that while seasonal flow drives solute transport and export, droughts play a significant role in promoting the accumulation of solutes in the river and watershed by punctuating solute transport and thereby enhancing the *"reserve"* component of the TTRP model. The accumulated solutes are then accessed and transferred into the river during rewetting events post drought, resulting in enhanced solute transfer to rivers and solute export (*pulse*). This drought-driven enhanced solute accumulation and solute export should be considered as an important component that modulates the temporal dimension of the "reserve" and "pulse" aspects of the TTRP model for rivers in arid watersheds.

Our solute load estimates (Fig. 8) reveal that from the total estimated solute load (143,565 tons) exported from the Delta during our study, ~9% was exported during the 2018 flood (with maximum river discharge of ~13 m^3/s), ~19% during the 2020 flood (with maximum river

discharge of ~29 m^3/s) and ~64% during the 2021-22 flood (with maximum river discharge of ~48 m^3/s). The remaining solutes were exported during the rainy season. Our findings on the solute load and export from the Delta demonstrate the importance of higher magnitude flow (e.g., 2021-22 flood) in "flushing" out substantial amounts of solutes from rivers in arid watersheds, and thereby helping keep the rivers "fresh". With the ongoing climate change that will reduce precipitation and increase evaporation in arid regions, the need for flow to keep rivers in arid environments pristine and their ecosystems vibrant, is an awakening call for continued efforts geared towards understanding the controls of intermittent flow in changing river water chemistry.

7. Figures

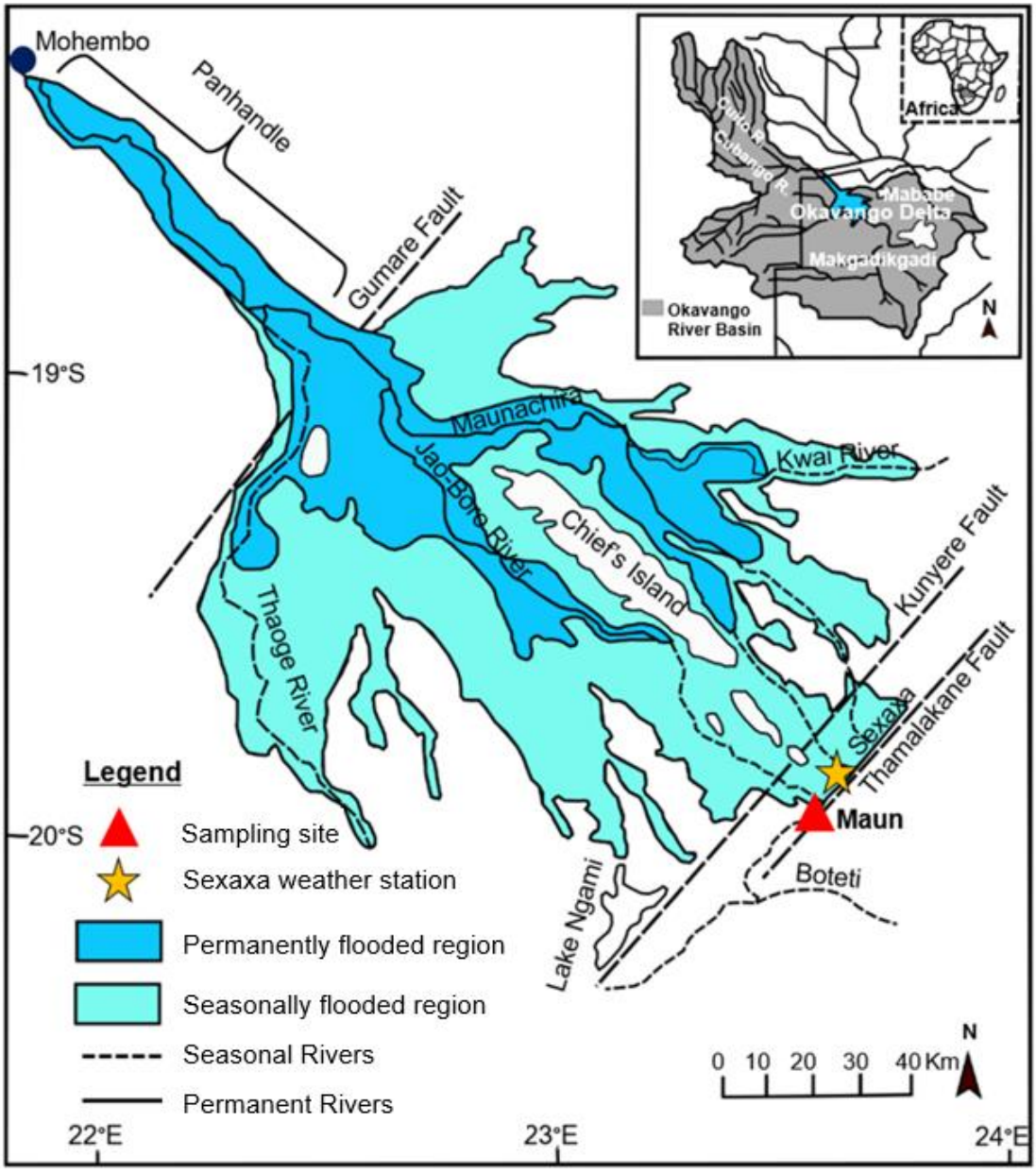

Figure 1: Map of the Okavango Delta, showing the Panhandle, the Delta region, seasonal and permanent rivers and select islands (Modified from Ellery et al., 2003). The river water sampling location and the weather station used in this study are shown as a filled red triangle and orange star, respectively. The insert shows the location of the Okavango Delta in Africa and the Okavango River catchment (Modified from Kgathi et al., 2006).

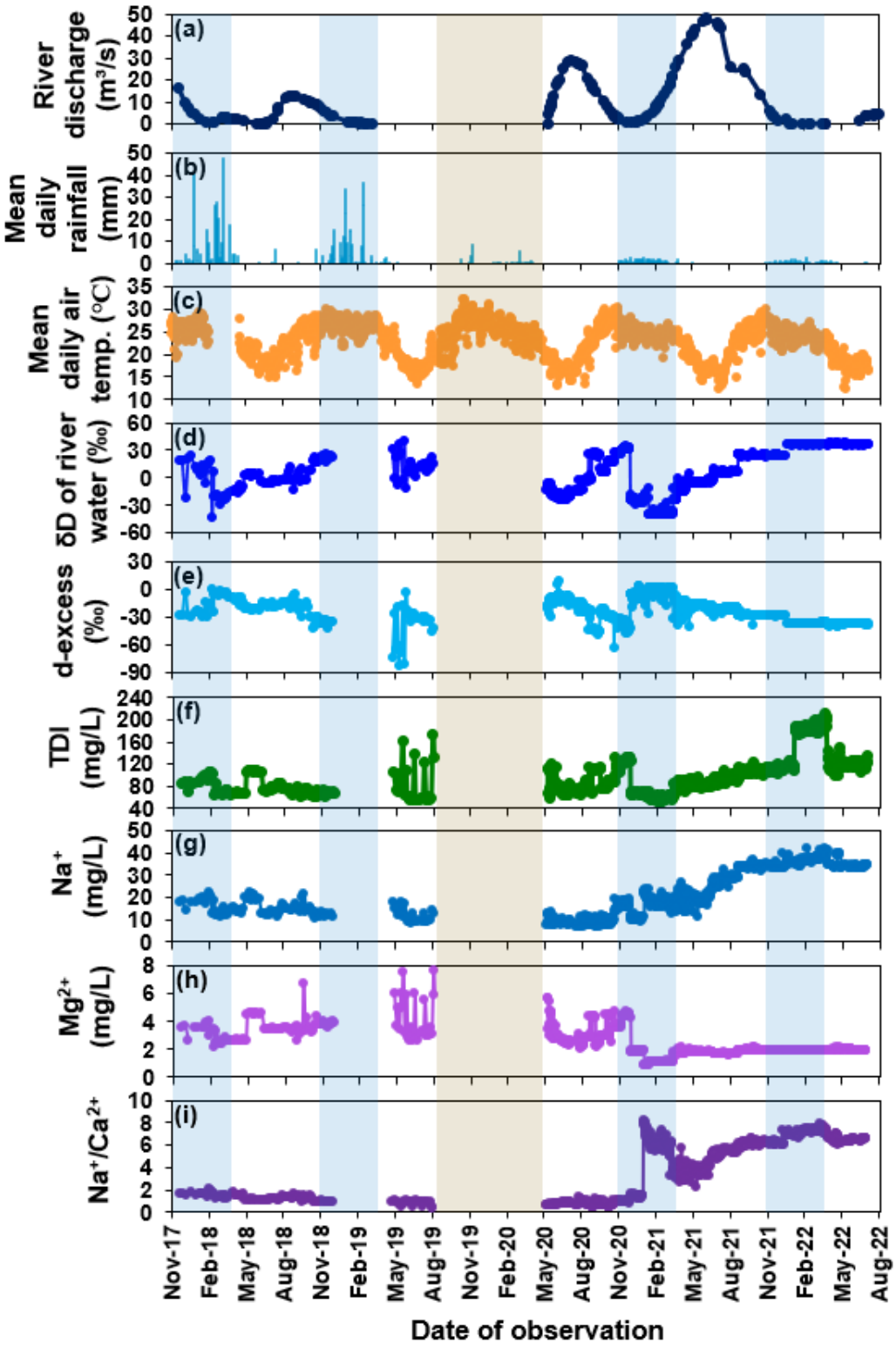

Figure 2: Temporal plots of (a) river discharge, (b) mean daily rainfall, (c) mean daily air temperature, (d) δD and (e) d-excess of river water, (f) total dissolved ions (TDI), (g) Na^{+}, (h) Mg^{2+}

and (i) Na^{+}/Ca^{2+} measured at the distal portion of the Okavango Delta in Maun. The blue shade represents the rainy season, the brown shade represents the drought period and the unshaded portion is the seasonal dry period.

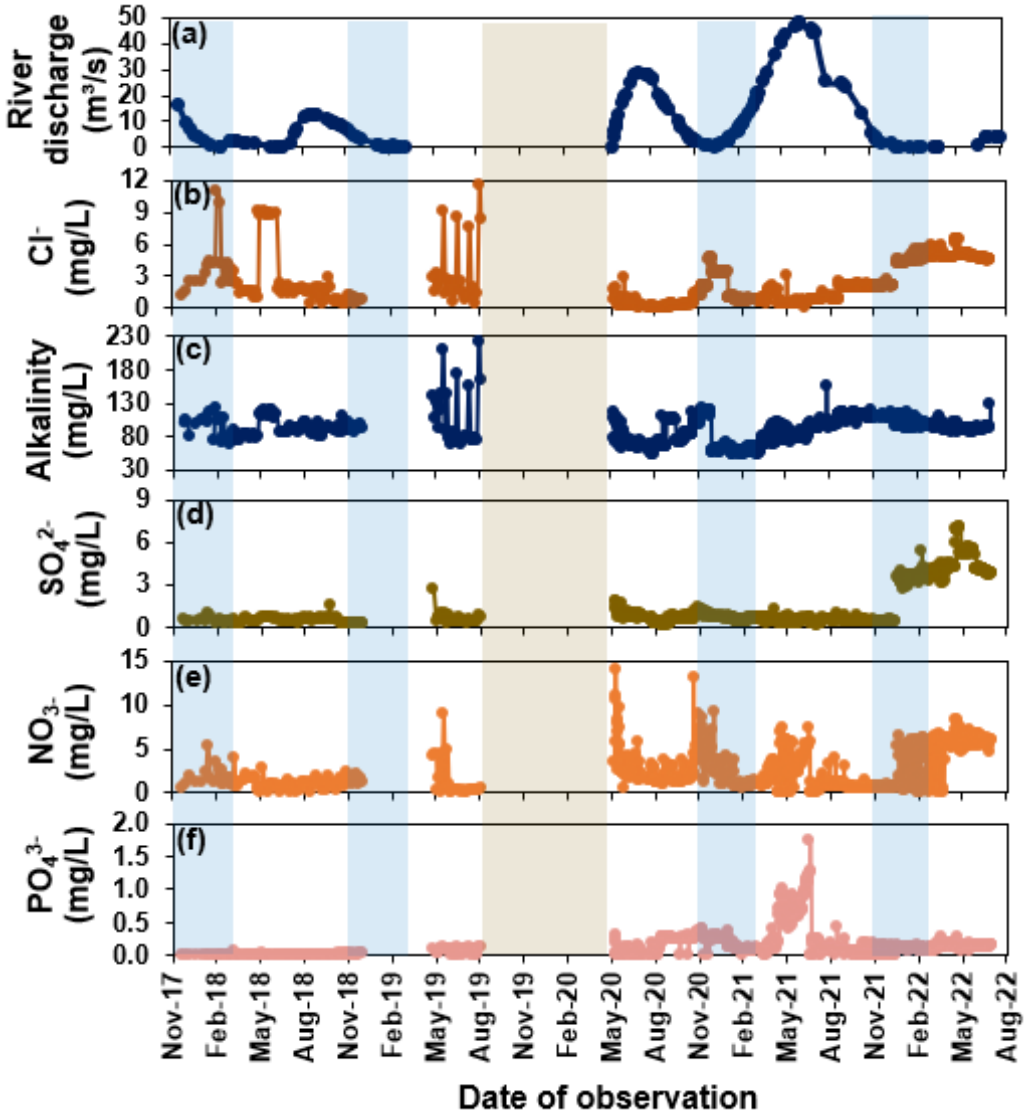

Figure 3: Temporal plots of (a) river discharge, (b) chloride, (c) alkalinity, (d) sulfate, (e) nitrate and (f) phosphate measured from the Okavango River water collected at the distal portion of the Okavango Delta in Maun. The blue shade represents the rainy season, the brown shade represents the drought period and the unshaded portion is the seasonal dry period.

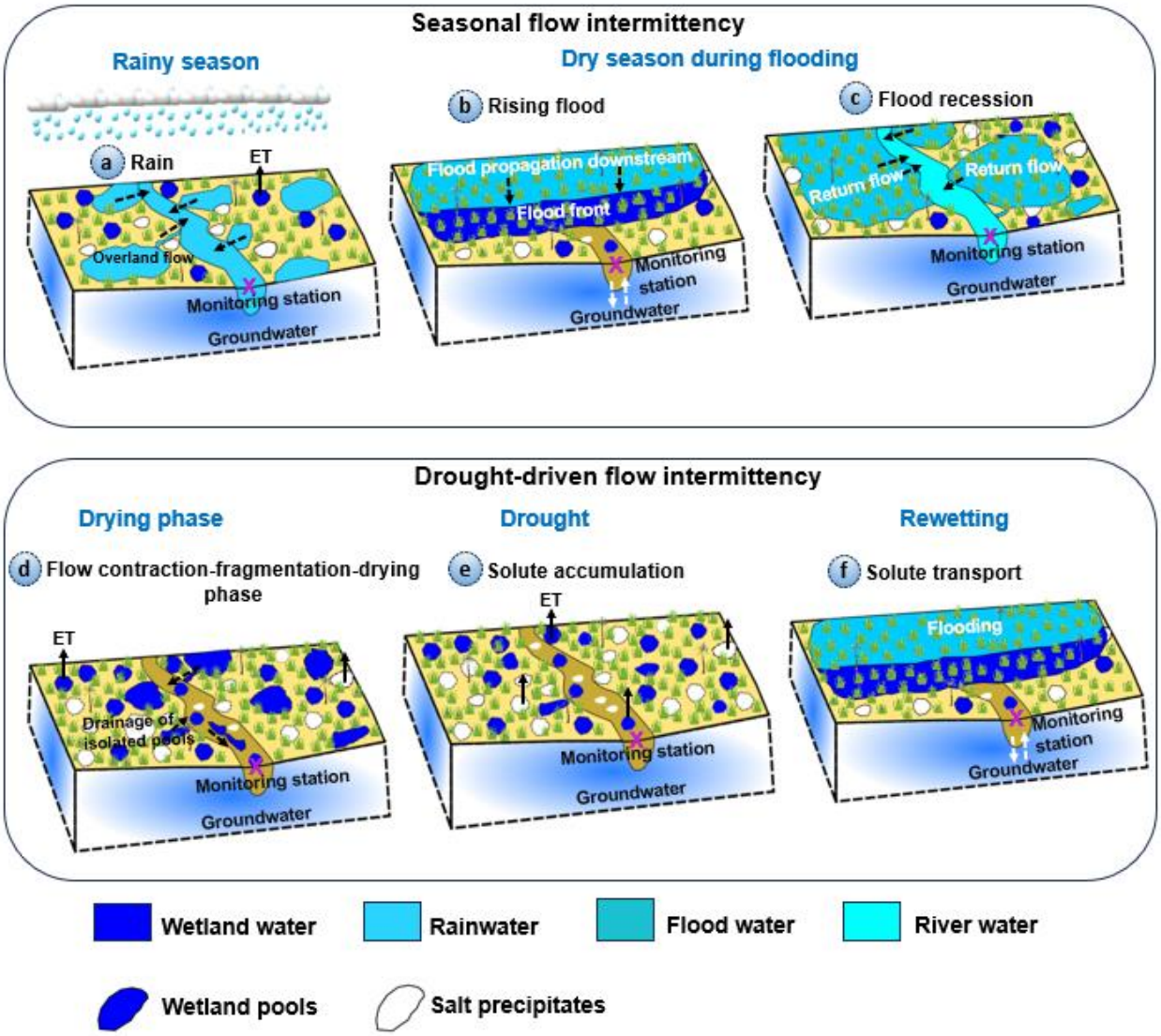

Figure 4: Conceptual model showing the role of seasonal flow intermittency in driving solute transfer from the local watershed into the river during (a) the rainy season and (b) rising flood and (c) receding flood. Also illustrated in the conceptual model is the role of drought-driven flow intermittency in controlling solute transport during (d) the drying phase before drought when flow contraction-fragmentation-drying phase occurs, (e) drought when solute accumulation is enhanced and (f) rewetting when solute transport is re-established.

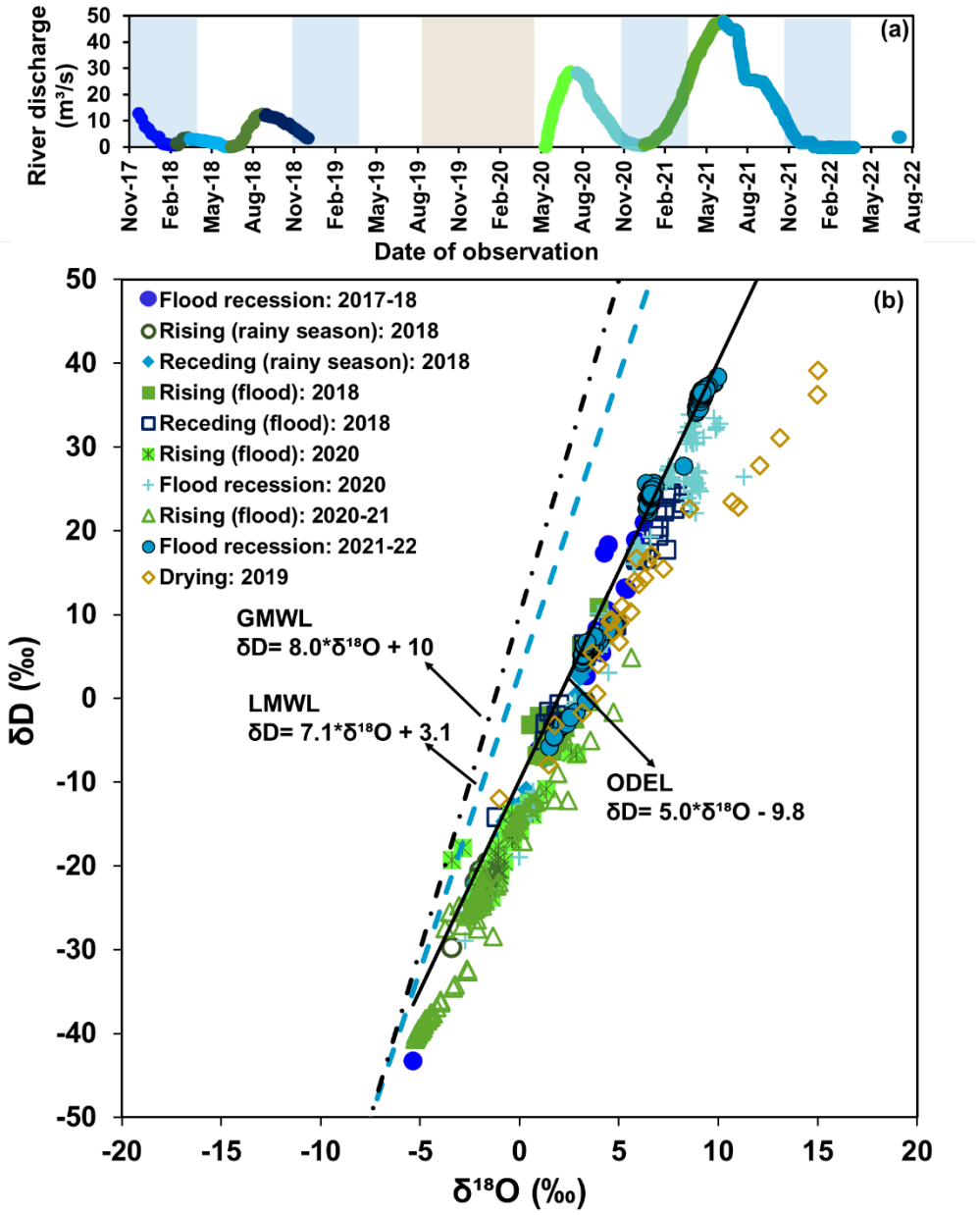

Figure 5: (a) River discharge hydrograph from the outlet of the Delta in Maun, color differentiated based on rising and receding discharge. The blue shade on the hydrograph represents the rainy season, the brown shade represents the drought period and the unshaded portion is the seasonal dry period. Also shown is the (b) plot of the stable oxygen isotopic composition ($\delta^{18}O$) vs. the stable hydrogen isotope (δD) for the Okavango River samples measured at the Delta outlet in

Maun. The river samples are color differentiated based on rising and receding discharge. The global meteoric water line (GMWL; Craig, 1961), local meteoric water line from Maun rain (LMWL) from Akondi et al. (2019) and the Okavango Delta evaporation line (ODEL) of Atekwana et al. (2016) are included.

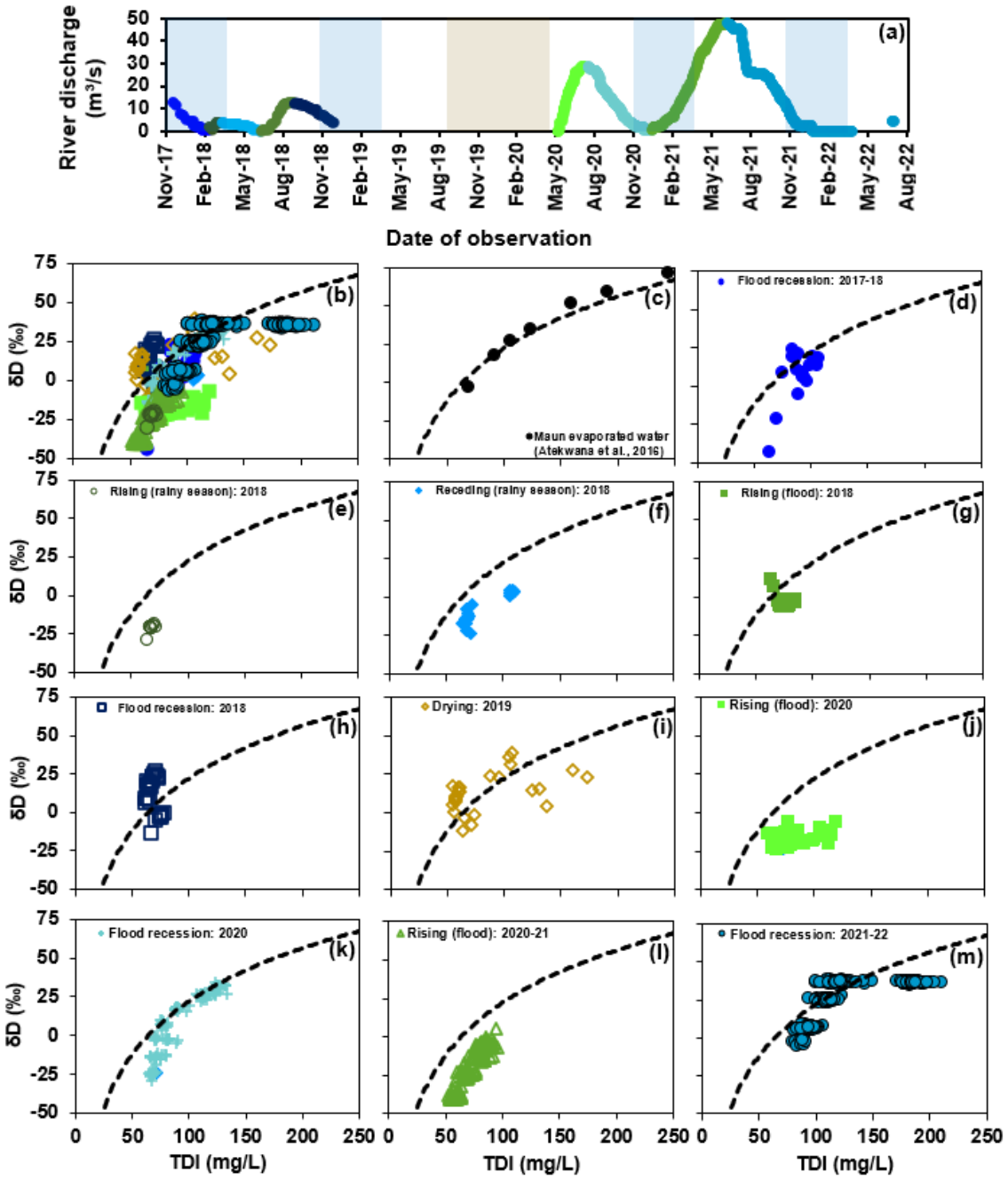

Figure 6: (a) River discharge hydrograph from the outlet of the Delta in Maun, color differentiated based on rising and receding discharge. The blue shade on the hydrograph represents the rainy season, the brown shade represents the drought period and the unshaded portion is the seasonal dry period. Also shown are the cross plots TDI vs. δD during rising and receding flood in the

Okavango River at Maun. The cross plots are color differentiated based on rising and receding discharge.

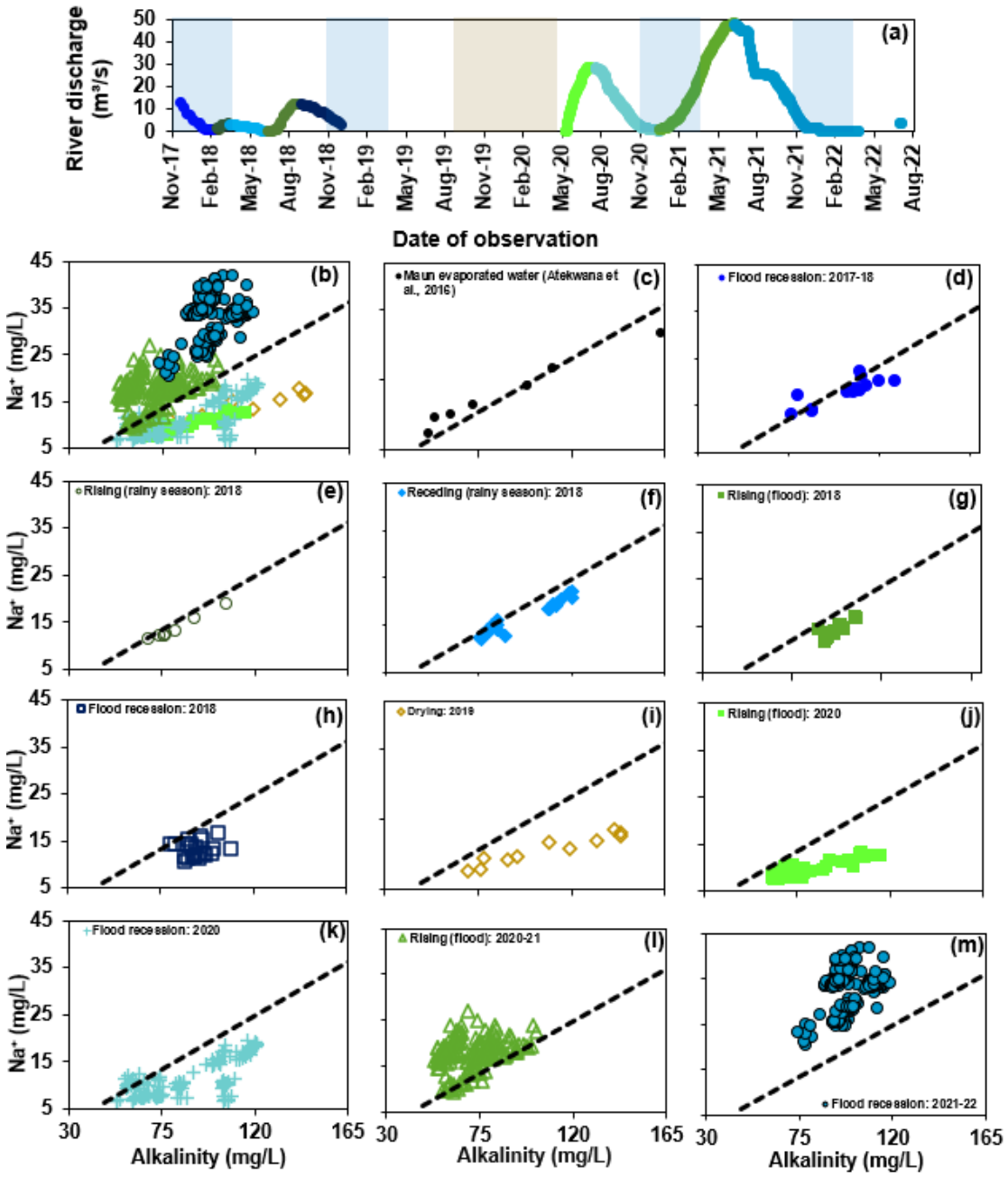

Figure 7: (a) River discharge hydrograph from the outlet of the Delta in Maun, color differentiated based on rising and receding discharge. The blue shade on the hydrograph represents the rainy

season, the brown shade represents the drought period and the unshaded portion is the seasonal dry period. Also shown are the cross plots of Alkalinity vs. Na^+ measured in the Okavango River at Maun. The cross plots are color differentiated based on rising and receding discharge.

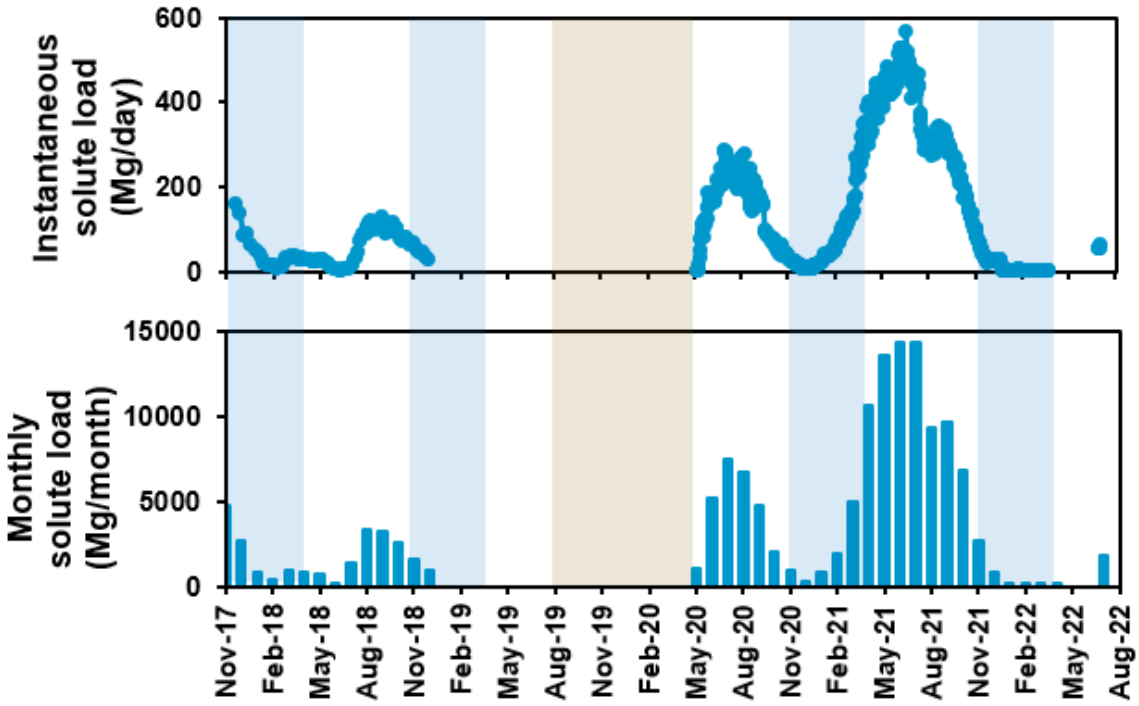

Figure 8: Temporal variations of (a) instantaneous solute load and (b) the monthly solute load measured in the Okavango River at the outlet of the Okavango Delta in Maun.

8. **Table 1:** Descriptive statistics for measured parameters. Min = minimum; Max = maximum; SD = Standard deviation; n = Number of data; TDI = total dissolved ions

Parameter	Mean	Min.	Max.	SD	n
River discharge (m^3/s)	11.0	0.02	48.21	13.0	556
Mean daily rainfall (mm)	1.9	0.0	48.0	5.8	1661
Mean daily air temperature (°C)	22.7	12.2	32.2	4.0	1645
δD of river water (‰)	8.1	-43.3	39.2	23.8	895
d-excess (‰)	-24.6	-83.7	7.9	13.0	895
TDI (mg/L)	99.8	52.5	211.1	34	895
Silica (mg/L)	35.2	12.6	63.4	8.5	895
Na^+ (mg/L)	22.3	6.6	41.9	10.5	895
K^+ (mg/L)	4.6	1.7	19.6	2.5	895
Mg^{2+} (mg/L)	2.4	0.9	7.7	1.0	895
Ca^{2+} (mg/L)	8.0	2.8	42.6	4.9	895
Cl^- (mg/L)	2.2	0.0	11.6	2.0	895
Alkalinity (mg/L)	89.6	52.8	221.6	19.6	894
SO_4^{2-} (mg/L)	1.4	0.1	7.1	1.6	895
NO_{3-} (mg/L)	2.6	0.1	14.1	2.2	895
PO_4^{3-} (mg/L)	0.2	0.0	1.8	0.2	895

9. Citations

Ahearn, D.S., Sheibley, R.W., Dahlgren, R.A. and Keller, K.E., 2004. Temporal dynamics of stream water chemistry in the last free-flowing river draining the western Sierra Nevada, California. Journal of Hydrology, 295(1-4), pp.47-63.

Akoko, E., Atekwana, E.A., Cruse, A.M., Molwalefhe, L. and Masamba, W.R., 2013. River-wetland interaction and carbon cycling in a semi-arid riverine system: the Okavango Delta, Botswana. Biogeochemistry, 114(1-3), pp.359-380.

Akondi, R.N., Atekwana, E.A. and Molwalefhe, L., 2019. Origin and chemical and isotopic evolution of dissolved inorganic carbon (DIC) in groundwater of the Okavango Delta, Botswana. Hydrological sciences journal, 64(1), pp.105-120.

Ala-Aho, P., Soulsby, C., Pokrovsky, O.S., Kirpotin, S.N., Karlsson, J., Serikova, S., Vorobyev, S.N., Manasypov, R.M., Loiko, S., Tetzlaff, D., 2018. Using stable isotopes to assess surface water source dynamics and hydrological connectivity in a highlatitude wetland and permafrost influenced landscape. J. Hydrol. 556, 279–293

Alemaw, B.F. 2022. The Recent Droughts of 2019/20 in Southern Africa and Its Teleconnection with ENSO Events. Atmospheric and Climate Sciences, 12, 246-263.

Atekwana, E.A., Molwalefhe, L., Kgaodi, O. and Cruse, A.M., 2016. Effect of evapotranspiration on dissolved inorganic carbon and stable carbon isotopic evolution in rivers in semi-arid climates: The Okavango Delta in North West Botswana. Journal of Hydrology: Regional Studies, 7, pp.1-13.

Belnap, J., Welter, J.R., Grimm, N.B., Barger, N. and Ludwig, J.A., 2005. Linkages between microbial and hydrologic processes in arid and semiarid watersheds. Ecology, 86(2), pp.298-307.

Bereslawski, E., 1997. Geohydrology, Geology, and Soils of the Cubango River Basin (Angolan Sector). OKACOM Okavango River Basin Preparatory Assessment Study, Specialist's Report.

Bonada, N., Cañedo-Argüelles, M., Gallart, F., von Schiller, D., Fortuño, P., Latron, J., Llorens, P., Múrria, C., Soria, M., Vinyoles, D. and Cid, N., 2020. Conservation and management of isolated pools in temporary rivers. Water, 12(10), p.2870.

Boulton, A.J., Rolls, R.J., Jaeger, K.L. and Datry, T., 2017. Hydrological connectivity in intermittent rivers and ephemeral streams. In Intermittent rivers and ephemeral streams (pp. 79-108). Academic Press.

Boyer, E.W., Hornberger, G.M., Bencala, K.E. and McKnight, D.M., 1997. Response characteristics of DOC flushing in an alpine catchment. Hydrological processes, 11(12), pp.1635-1647.

Bufford, K.M., Atekwana, E.A., Abdelsalam, M.G., Shemang, E., Atekwana, E.A., Mickus, K., Moidaki, M., Modisi, M.P. and Molwalefhe, L., 2012. Geometry and faults tectonic activity of the Okavango Rift Zone, Botswana: Evidence from magnetotelluric and electrical resistivity tomography imaging. Journal of African Earth Sciences, 65, pp.61-71.

Catuneanu, O., Wopfner, H., Eriksson, P.G., Cairncross, B., Rubidge, B.S., Smith, R.M.H. and Hancox, P.J., 2005. The Karoo basins of south-central Africa. Journal of African Earth Sciences, 43(1-3), pp.211-253.

Cherlet, M., Hutchinson, C., Reynolds, J., Hill, J., Sommer, S. and von Maltitz, G., 2018. World atlas of desertification. Luxembourg: Publication office of the european union.

Clark, K.E., Shanley, J.B., Scholl, M.A., Perdrial, N., Perdrial, J.N., Plante, A.F. and McDowell, W.H., 2017. Tropical river suspended sediment and solute dynamics in storms during an extreme drought. Water Resources Research, 53(5), pp.3695-3712.

Costa, A.C., Bronstert, A., de Araujo, J.C., 2012. A channel transmission losses model for different dryland rivers. Hydrol. Earth Syst. Sci. 16 (4), 1111–1135

Costigan, K.H., Kennard, M.J., Leigh, C., Sauquet, E., Datry, T. and Boulton, A.J., 2017. Flow regimes in intermittent rivers and ephemeral streams. In Intermittent rivers and ephemeral streams (pp. 51-78). Academic Press.

Covino, T., 2017. Hydrologic connectivity as a framework for understanding biogeochemical flux through watersheds and along fluvial networks. Geomorphology, 277, pp.133-144.

Craig, H., 1961. Isotopic variations in meteoric waters. Science 133 (3465), 1702–1703

Dahm, C.N. and Molles Jr, M.C., 1992. Streams in semiarid regions as sensitive indicators of global climate change. In Global climate change and freshwater ecosystems (pp. 250-260). New York, NY: Springer New York.

Dalzell, B.J., Filley, T.R. and Harbor, J.M., 2007. The role of hydrology in annual organic carbon loads and terrestrial organic matter export from a midwestern agricultural watershed. Geochimica et Cosmochimica Acta, 71(6), pp.1448-1462.

Datry, T., Singer, G., Sauquet, E., Capdevilla, D.J., Von Schiller, D., Subbington, R., Magrand, C., Paril, P., Milisa, M., Acuña, V. and Alves, M.H., 2017. Science and management of intermittent rivers and ephemeral streams (SMIRES). Research Ideas and Outcomes, 3, pp.23-p.

Dincer, T., Hutton, L.G. and Kupee, B.B.J., 1979. Study, using stable isotopes, of flow distribution, surface-groundwater relations and evapotranspiration in the Okavango Swamp, Botswana. In Isotope hydrology 1978.

Duvert, C., Hutley, L.B., Birkel, C., Rudge, M., Munksgaard, N.C., Wynn, J.G., Setterfield, S.A., Cendón, D.I. and Bird, M.I., 2020. Seasonal shift from biogenic to geogenic fluvial carbon caused

by changing water sources in the wet-dry tropics. Journal of Geophysical Research: Biogeosciences, 125(2).

Ellery, W.N., McCarthy, T.S. and Smith, N.D., 2003. Vegetation, hydrology, and sedimentation patterns on the major distributary system of the Okavango Fan, Botswana. Wetlands, 23(2), p.357.

Fovet, O., Humbert, G., Dupas, R., Gascuel-Odoux, C., Gruau, G., Jaffrézic, A., Thelusma, G., Faucheux, M., Gilliet, N., Hamon, Y. and Grimaldi, C., 2018. Seasonal variability of stream water quality response to storm events captured using high-frequency and multi-parameter data. Journal of Hydrology, 559, pp.282-293.

Geeraert, N., Omengo, F.O., Borges, A.V., Govers, G. and Bouillon, S., 2017. Shifts in the carbon dynamics in a tropical lowland river system (Tana River, Kenya) during flooded and non-flooded conditions. Biogeochemistry, 132(1-2), pp.141-163.

Godsey, S.E., Kirchner, J.W. and Clow, D.W., 2009. Concentration–discharge relationships reflect chemostatic characteristics of US catchments. Hydrological Processes: An International Journal, 23(13), pp.1844-1864.

Gómez, R., Arce, M.I., Baldwin, D.S. and Dahm, C.N., 2017. Water physicochemistry in intermittent rivers and ephemeral streams. In Intermittent rivers and ephemeral streams (pp. 109-134). Academic Press.

Gooseff, M.N., Bencala, K.E. and Wondzell, S.M., 2008. Solute transport along stream and river networks. River confluences, tributaries and the fluvial network, pp.395-417.

Gumbricht, T. and McCarthy, T.S., 2003. Spatial patterns of islands and salt crusts in the Okavango Delta, Botswana. South African Geographical Journal, 85(2), pp.164-169.

Gumbricht, T., McCarthy, J. and McCarthy, T.S., 2004. Channels, wetlands and islands in the Okavango Delta, Botswana, and their relation to hydrological and sedimentological processes.

Earth Surface Processes and Landforms: The Journal of the British Geomorphological Research Group, 29(1), pp.15-29.

Gumbricht, T., McCarthy, T.S. and Merry, C.L., 2001. The topography of the Okavango Delta, Botswana, and its tectonic and sedimentological implications. South African Journal of Geology, 104(3), pp.243-264.

Herndon, E.M., Steinhoefel, G., Dere, A.L. and Sullivan, P.L., 2018. Perennial flow through convergent hillslopes explains chemodynamic solute behavior in a shale headwater catchment. Chemical Geology, 493, pp.413-425.

Horgby, Å., Boix Canadell, M., Ulseth, A.J., Vennemann, T.W., Battin, T.J., 2019. HighResolution Spatial Sampling Identifies Groundwater as Driver of CO2 Dynamics in an Alpine Stream Network. J. Geophys. Res. Biogeosci. 124 (7), 1961–1976.

Humphries, M.S., McCarthy, T.S., Cooper, G.R.J., Stewart, R.A., Stewart, R.D., 2014. The role of airborne dust in the growth of tree islands in the Okavango Delta, Botswana. Geomorphology 206, 307–317.

Jones, M.J., 2010. The groundwater hydrology of the Okavango basin. OKACOM Okavango River Basin Transboundary Diagnostical Analysis Technical Report.

Kalscheuer, T., Blake, S., Podgorski, J.E., Wagner, F., Green, A.G., Maurer, H., Jones, A. G., Muller, M., Ntibinyane, O., Tshoso, G., 2015. Joint inversions of three types of electromagnetic data explicitly constrained by seismic observations: results from the central Okavango Delta, Botswana. Geophys. J. Int. 202 (3), 1429–1452.

Kgathi, D.L., Kniveton, D., Ringrose, S., Turton, A.R., Vanderpost, C.H.M., Lundqvist, J. and Seely, M., 2006. The Okavango; a river supporting its people, environment and economic development. Journal of Hydrology, 331(1-2), pp.3-17.

Kinabo, B.D., Atekwana, E.A., Hogan, J.P., Modisi, M.P., Wheaton, D.D. and Kampunzu, A.B., 2007. Early structural development of the Okavango rift zone, NW Botswana. Journal of African Earth Sciences, 48(2-3), pp.125-136.

Kinabo, B.D., Hogan, J.P., Atekwana, E.A., Abdelsalam, M.G. and Modisi, M.P., 2008. Fault growth and propagation during incipient continental rifting: Insights from a combined aeromagnetic and Shuttle Radar Topography Mission digital elevation model investigation of the Okavango Rift Zone, northwest Botswana. Tectonics, 27(3).

Koeniger, P., Leibundgut, C., Stichler, W., 2009. Spatial and temporal characterisation of stable isotopes in river water as indicators of groundwater contribution and confirmation of modelling results; a study of the Weser River, Germany. Isot. Environ. Health Stud. 45 (4), 289–302.

Letshele, K.P., Atekwana, E.A., Molwalefhe, L., Ramatlapeng, G.J. and Masamba, W.R., 2023. Stable hydrogen and oxygen isotopes reveal aperiodic non-river evaporative solute enrichment in the solute cycling of rivers in arid watersheds. Science of the Total Environment, 856, p.159113.

Liu, F., Parmenter, R., Brooks, P.D., Conklin, M.H. and Bales, R.C., 2008. Seasonal and interannual variation of streamflow pathways and biogeochemical implications in semi-arid, forested catchments in Valles Caldera, New Mexico. Ecohydrology: Ecosystems, Land and Water Process Interactions, Ecohydrogeomorphology, 1(3), pp.239-252.

Lourenco, M. and Woodborne, S., 2023. Defining the Angolan Highlands Water Tower, a 40 plus-year precipitation budget of the headwater catchments of the Okavango Delta. Environmental Monitoring and Assessment, 195(7), p.859.

Ludwig, J.A., and Tongway, D.J. 1997. A landscape approach to rangeland ecology. In Landscape ecology, function and management: principles from Australia's rangelands, eds J.A. Ludwig, D.J.

Tongway, D.O. Freudenberger, J.C. Noble, and K.C. Hodgkinson, pp. 1–12. Melbourne: CSIRO Publishing.

McCarthy, J.M., Gumbricht, T., McCarthy, T., Frost, P., Wessels, K. and Seidel, F., 2003. Flooding patterns of the Okavango wetland in Botswana between 1972 and 2000. Ambio: A journal of the human environment, 32(7), pp.453-457.

McCarthy, T.S. and Ellery, W.N., 1994. The effect of vegetation on soil and ground water chemistry and hydrology of islands in the seasonal swamps of the Okavango Fan, Botswana. Journal of Hydrology, 154(1-4), pp.169-193.

McCarthy, T.S. and Ellery, W.N., 1995. Sedimentation on the distal reaches of the Okavango Fan, Botswana, and its bearing on calcrete and silcrete (ganister) formation. Journal of Sedimentary Research, 65(1a), pp.77-90.

McCarthy, T.S. and Ellery, W.N., 1998. The okavango delta. Transactions of the Royal Society of South Africa, 53(2), pp.157-182.

McCarthy, T.S. and Metcalfe, J., 1990. Chemical sedimentation in the semi-arid environment of the Okavango Delta, Botswana. Chemical geology, 89(1-2), pp.157-178.

McCarthy, T.S., 2006. Groundwater in the wetlands of the Okavango Delta, Botswana, and its contribution to the structure and function of the ecosystem. Journal of hydrology, 320(3-4), pp.264-282.

McCarthy, T.S., Barry, M., Bloem, A., Ellery, W.N., Heister, H., Merry, C.L., Röther, H. and Sternberg, H., 1997. The gradient of the Okavango fan, Botswana, and its sedimentological and tectonic implications. Journal of African Earth Sciences, 24(1-2), pp.65-78.

McCarthy, T.S., Bloem, A. and Larkin, P.A., 1998. Observations on the hydrology and geohydrology of the Okavango Delta. South African Journal of Geology, 101(2), pp.101-117.

McCarthy, T.S., Ellery, W.N. and Ellery, K., 1993. Vegetation-induced, subsurface precipitation of carbonate as an aggradational process in the permanent swamps of the Okavango (delta) fan, Botswana. Chemical geology, 107(1-2), pp.111-131.

McCarthy, T.S., Ellery, W.N. and Stanistreet, I.G., 1992. Avulsion mechanisms on the Okavango fan, Botswana: the control of a fluvial system by vegetation. Sedimentology, 39(5), pp.779-795.

McCarthy, T.S., McIver, J.R. and Verhagen, B.T., 1991. Groundwater evolution, chemical sedimentation and carbonate brine formation on an island in the Okavango Delta swamp, Botswana. Applied Geochemistry, 6(6), pp.577-595.

McCarthy, TS, Cooper, GRJ, Tyson, PD &Ellery, W., 2000. Seasonal flooding in the Okavango Delta, Botswana-recent history and future prospects. South African Journal of Science, 96(1), pp.25-33.

Mendelsohn, J., el Obeid, S., 2004. Okavango River: The Flow of a Lifeline. Struik.

Merron, G.S., 1991. The ecology and management of the fishes of the Okavango Delta, Botswana, with particular reference to the role of the seasonal floods (Doctoral dissertation, Rhodes University).

Milzow, C., Kgotlhang, L., Bauer-Gottwein, P., Meier, P. and Kinzelbach, W., 2009. Regional review: the hydrology of the Okavango Delta, Botswana—processes, data and modelling. Hydrogeology Journal, 17(6), pp.1297-1328.

Modie, B.N., 2000. Geology and mineralisation in the Meso-to Neoproterozoic Ghanzi-Chobe Belt of northwest Botswana. Journal of African Earth Sciences, 30(3), pp.467-474.

Modisi, M.P., Atekwana, E.A., Kampunzu, A.B. and Ngwisanyi, T.H., 2000. Rift kinematics during the incipient stages of continental extension: Evidence from the nascent Okavango rift basin, northwest Botswana. Geology, 28(10), pp.939-942.

Mosepele, K., Moyle, P.B., Merron, G.S., Purkey, D.R. and Mosepele, B., 2009. Fish, floods, and ecosystem engineers: aquatic conservation in the Okavango Delta, Botswana. Bioscience, 59(1), pp.53-64.

Mosepele, K., Ngwenya, B.N. and Bernard, T., 2006. Artisanal fishing and food security in the Okavango Delta, Botswana. World Sustainable Development Outlook: Global and Local Resources in Achieving Sustainable Development, Inderscience, Geneva, pp.159-168.

Moses, O. and Gondwe, M., 2019. Simulation of changes in the twenty-first century maximum temperatures using the statistical downscaling model at some stations in Botswana. Modeling Earth Systems and Environment, 5(3), pp.843-855.

Murphy, S.F., McCleskey, R.B., Martin, D.A., Writer, J.H. and Ebel, B.A., 2018. Fire, flood, and drought: extreme climate events alter flow paths and stream chemistry. Journal of Geophysical Research: Biogeosciences, 123(8), pp.2513-2526.

Nanson, G.C., Tooth, S.T., Knighton, A.D., Bull, L.J., Kirkby, M.J., 2002. A global perspective on dryland rivers: perceptions, misconceptions and distinctions. Dryland rivers: hydrology and geomorphology of semi-arid channels 17–54.

Obakeng, O.T. and Gieske, A.S.M., 1997. Hydraulic conductivity and transmissivity of a water-table aquifer in the Boro River system, Okavango Delta. Botswana Geological Survey Department bulletin series, 46.

Oromeng, K.V., Atekwana, E.A., Molwalefhe, L. and Ramatlapeng, G.J., 2021. Time-series variability of solute transport and processes in rivers in semi-arid endorheic basins: The Okavango Delta, Botswana. Science of The Total Environment, 759, p.143574.

Parsons, A.J., Wainwright, J., Stone, P.M., Abrahams, A.D., 1999. Transmission losses in rills on dryland hillslopes. Hydrol. Process. 13 (17), 2897–2905.

Peel, M.C., Finlayson, B.L. and McMahon, T.A., 2007. Updated world map of the Köppen-Geiger climate classification.

Podgorski, J.E., Green, A.G., Kalscheuer, T., Kinzelbach, W.K., Horstmeyer, H., Maurer, H., Rabenstein, L., Doetsch, J., Auken, E., Ngwisanyi, T., Tshoso, G., 2015. Integrated interpretation of helicopter and ground-based geophysical data recorded within the Okavango Delta, Botswana. J. Appl. Geophys. 114, 52–67.

Podgorski, J.E., Green, A.G., Kgotlhang, L., Kinzelbach, W.K., Kalscheuer, T., Auken, E., Ngwisanyi, T., 2013. Paleo-megalake and paleo-megafan in southern Africa. Geology 41 (11), 1155–1158.

Pombo, S., de Oliveira, R.P. and Mendes, A., 2015. Validation of remote-sensing precipitation products for Angola. Meteorological Applications, 22(3), pp.395-409

Ramatlapeng, G.J., Atekwana, E.A. and Molwalefhe, L., 2023. Spatial and temporal controls on the solute behavior of rivers in arid watersheds: The Okavango River, NW Botswana. Journal of Hydrology, 618, p.129141.

Ramatlapeng, G.J., Atekwana, E.A., Molwalefhe, L. and Oromeng, K.V., 2021. Intermittent hydrologic perturbations control solute cycling and export in the Okavango Delta. Journal of Hydrology, 594, p.125968.

Ramberg, L. and Wolski, P., 2008. Growing islands and sinking solutes: processes maintaining the endorheic Okavango Delta as a freshwater system. Plant Ecology, 196(2), pp.215-231.

Ringrose, S., Harris, C., Huntsman-Mapila, P., Vink, B.W., Diskins, S., Vanderpost, C., Matheson, W., 2009. Origins of strandline duricrusts around the Makgadikgadi Pans (Botswana Kalahari) as deduced from their chemical and isotope composition. Sed. Geol. 219 (1–4), 262–279.

Rose, L.A., Karwan, D.L. and Godsey, S.E., 2018. Concentration–discharge relationships describe solute and sediment mobilization, reaction, and transport at event and longer timescales. Hydrological processes, 32(18), pp.2829-2844.

Steudel, T., Göhmann, H., Flügel, W.A. and Helmschrot, J., 2013. Assessment of hydrological dynamics in the upper Okavango River Basins. Biodiversity and Ecology, 5, pp.247-262.

Tooth, S., 2000. Process, form and change in dryland rivers: a review of recent research. Earth Sci. Rev. 51 (1–4), 67–107.

Tramblay, Y., Rutkowska, A., Sauquet, E., Sefton, C., Laaha, G., Osuch, M., Albuquerque, T., Alves, M.H., Banasik, K., Beaufort, A. and Brocca, L., 2021. Trends in flow intermittence for European rivers. Hydrological Sciences Journal, 66(1), pp.37-49.

Wilson, B.H. and Dincer, T., 1976, August. An introduction to the hydrology and hydrography of the Okavango Delta. In Symposium on the Okavango Delta (pp. 33-48). Botswana Soc. Gaborone Botswana.

Wolski, P., Murray-Hudson, M., Savenije, H. and Gumbricht, T., 2005. Modeling of the hydrology of the Okavango Delta. Publication of the Water and Ecosystem Resources for Regional Development (WERRD) project, HOORC, Maun, Botswana.

Wolski, P., Savenije, H.H., Murray-Hudson, M. and Gumbricht, T., 2006. Modelling of the flooding in the Okavango Delta, Botswana, using a hybrid reservoir-GIS model. Journal of Hydrology, 331(1-2), pp.58-72.

Zarch, M.A.A., Sivakumar, B., Malekinezhad, H. and Sharma, A., 2017. Future aridity under conditions of global climate change. Journal of Hydrology, 554, pp.451-469.

Zeroual, A., Meddi, M.O.H.A.M.E.D. and Bensaad, S.A.F.I.A., 2013. The impact of climate change on river flow in arid and semi-arid rivers in Algeria. IAHS-AISH Proceedings and Reports, 359(July), pp.1-6.